CALCULATION OF MULTICOMPONENT CHEMICAL EQUILIBRIA IN GAS-SOLID-LIQUID SYSTEMS: CALCULATION METHODS, THERMOCHEMICAL DATA, AND APPLICATIONS TO STUDIES OF HIGH-TEMPERATURE VOLCANIC GASES WITH EXAMPLES FROM MOUNT ST. HELENS

ROBERT B. SYMONDS* and MARK H. REED**

ABSTRACT. This paper documents the numerical formulations, thermochemical data base, and possible applications of computer programs, SOLVGAS and GASWORKS, for calculating multicomponent chemical equilibria in gas-solid-liquid systems. SOLVGAS and GASWORKS compute simultaneous equilibria by solving simultaneously a set of mass balance and mass action equations written for all gas species and for all gas-solid or gas-liquid equilibria. The programs interface with a thermochemical data base, GASTHERM, which contains coefficients for retrieval of the equilibrium constants from 25° to 1200°C. The equilibrium constants are for derived-species and numerical equilibria written with a specific set of thermodynamic components. GASTHERM includes >1000 species of gases, solids, and liquids for a 42 element system.

The programs and data base model dynamic chemical processes in 30- to 40-component volcanic-gas systems. By linking a series of individual calculations with stepwise changes in temperature, pressure, and composition between steps, we can model gas evaporation from magma, mixing of magmatic and hydrothermal gases, precipitation of minerals during pressure and temperature decrease, mixing of volcanic gas with air, and reaction of gases with wall rock. We show examples of the gas-evaporation-from-magma and precipitation-with-cooling calculations for volcanic gases collected from Mount St. Helens in September 1981. Constraining the model with samples of gases, sublimates, and lavas from the volcano, we predict: (1) the amounts of trace elements volatilized from shallow magma, deep magma, and wall rock, and (2) the solids that precipitate from the gas upon cooling. We then test the model's predictions by comparing them with the measured trace-element concentrations in gases and the observed sublimate sequence. This study leads to the following conclusions: (1) most of the trace elements in the Mount St. Helens gases are volatilized from shallow magma as simple chlorides (CuCl, AgCl, CsCl, et cetera); some elements reside in various other types of gas species (H_2MoO_4, AuS, $Fe(OH)_2$, Hg, H_2Se, et cetera); (2) some elements (for example, Al, Ca) exist dominantly in rock aerosols, not gases, in the gas stream; (3) near-surface cooling of the gases triggers precipitation of oxides, sulfides, halides, tungstates, and native elements; and (4) equilibrium cooling of the gases to 100°C causes most trace elements, except for Hg, Sb, and Se, to precipitate from the gas.

* Department of Geological Engineering, Geology, and Geophysics, Michigan Technological University, Houghton, Michigan 49931. Present address: U.S. Geological Survey, Cascades Volcano Observatory, 5400 MacArthur Blvd., Vancouver, Washington 98661.
** Department of Geological Sciences, University of Oregon, Eugene, Oregon 97403.

INTRODUCTION

Degassing of volcanoes is a complex natural phenomenon. The process begins with the discharge of gases from magma. These magmatic volatiles are dominated by a few species (H_2O, CO_2, CO, SO_2, H_2S, H_2, HCl, HF, N_2, and rare gases; see for example, Gerlach and Nordlie, 1975; Giggenbach and Matsuo, 1991) that we will call the *major gas species*. The gases also contain a number of *trace elements* (Na, Cu, Pb, B, et cetera) and their species (NaCl, CuCl, PbS, H_2BO_3) (Symonds and others, 1987; Quisefit and others, 1989). As the gases rise through the fracture system, they may mix with hydrothermal vapor (Gerlach and Casadevall, 1986b), entrain rock *aerosols* (suspended insoluble particles in a gas; see Vie Le Sage, 1983), and react with the wall rock (Getahun, Reed, and Symonds, 1992). Upon nearing the fumarole orifice, the gases cool and mix with atmospheric gases (Stoiber and Rose, 1974). Cooling causes *sublimates* (solids precipitated from the gas) to form (Symonds and others, 1987). Some sublimates precipitate on the walls of the vent as *incrustations* (colorful deposits around volcanic fumaroles that include both sublimates and solids that form by other processes), but others remain in the gas stream as aerosols. Mixing with atmospheric gases causes cooling, dilution, and oxidation of volcanic gases, and the formation of hygroscopic sulfuric acid (Symonds, Reed, and Rose, 1992); these processes, along with reactions with the wall rock, produce most low-temperature fumarolic incrustations (Stoiber and Rose, 1974). Finally, the volcanic gas discharges into the atmosphere where it mixes further with atmospheric gases and cools to the ambient air temperature.

Samples of gases, *condensates* (condensed volcanic gas analyzed for trace elements), sublimates, incrustations, and aerosols provide the starting point for interpreting the natural processes. However, it is clear from this work and others (for example, Symonds and others, 1987; Quisefit and others, 1989) that thermochemical modeling can help unravel the complex origins of gas and condensate compositions and the types and amounts of solids (sublimates, incrustations, aerosols). Central to this approach are tests for equilibrium between the volcanic gases (major gases, condensates) and the magma, sublimates, incrustations, and aerosols. In accounting for agreements with and departures from equilibrium, one gains insight into the critical genetic processes.

The ideal thermochemical model would consider every possible reaction between gases, solids, and liquids in 30- to 60-component volcanic-gas systems. It is possible to approximate such a comprehensive model by compiling the large but finite amount of modern thermochemical data, including the most abundant or probable species of nearly every component under consideration. Many of the first thermochemical models of volcanic gases (Ellis, 1957; Heald, Naughton, and Barnes, 1963; Gerlach and Nordlie, 1975) only considered species in the C–O–H–S or C–O–H–S–Cl–F systems, the dominant elements in terrestrial volcanic gases. Early modeling studies, which did include more components

(Krauskopf, 1957, 1964; Naughton and others, 1974), can be improved using new thermochemical data and more sophisticated computer models.

Recent studies (Symonds and others, 1987; Le Guern, ms; Quisefit and others, 1989; Bernard, Symonds, and Rose, 1990; Symonds, Reed, and Rose, 1992) use more versatile models that consider hundreds of gas, solid, and liquid species in 30- to 40-component systems; they also take advantage of the vastly improved quality and quantity of recent thermochemical data. In most of these studies, thermochemical modeling was a small part of the overall project; hence, they excluded details of the modeling and documentation of the large thermochemical data bases. In this work, we redress this deficiency by addressing: (1) description of equations and formulations applied in computer programs, SOLVGAS and GASWORKS, used for these calculations, (2) documentation of the thermochemical data base, (3) description of the numerous applications of multicomponent thermochemical models to volcanic gases and related scientific disciplines, and (4) evaluation of the quality of our modeling results.

NUMERICAL MODELS

We have developed FORTRAN computer programs GASWORKS and SOLVGAS for computing multicomponent chemical equilibria in gas–solid–liquid systems. The numerical formulations used by the programs are described in app. 1. GASWORKS computes heterogeneous equilibria among gases, solids, and liquids during processes of cooling (or heating), pressure changes, gas-gas mixing, and gas-rock reaction. SOLVGAS calculates homogeneous equilibrium (distribution of species) in a gas phase. It also calculates saturation indices, log (Q/K) values, for solids and liquids (Reed and Spycher, 1984; Symonds and others, 1987). Both programs consider hundreds of gas, solid, and liquid species in systems of up to 42 components as a function of temperature and pressure using the basic formulations of equilibrium calculations of Reed (1982) modified for gases (app. 1). The programs provide for strict oxygen mass balance, allowing calculation of the oxygen fugacity (fO_2) at any pressure and temperature. Thermochemical data (below) constrain the calculations, which consist of solving simultaneously a series of mass balance and mass action equations using a Newton-Raphson method.

These programs were applied previously to samples of volcanic gases, condensates, and sublimates from Merapi Volcano, Indonesia (Symonds and others, 1987); the speciation of Cl and F in volcanic gases (Symonds, Rose, and Reed, 1988); the possible gas-phase transport of Hg, As, and Sb in geothermal systems (Spycher and Reed, 1989); the restoration of Augustine gas samples (Symonds and others, 1990; Kodosky, Motyka, and Symonds, 1991); the speciation of Mo, W, and Re in magmatic fluids (Bernard, Symonds, and Rose, 1990); the speciation and origin of trace elements in Augustine volcanic gases (Symonds, Reed, and

Rose, 1992); and to gas-phase alteration of wall rock in high temperature fumaroles at Augustine volcano (Getahun, Reed, and Symonds, 1992).

Applicability to natural systems.—The appropriateness of the modeling depends in part on whether volcanic gases approach chemical equilibrium. Thermodynamic evaluations of high-temperature ($> 500°C$) volcanic gases show that the major gas species are initially in equilibrium at or above the collection temperature (Gerlach, 1980a, b; Gerlach and Casadevall, 1986a). Furthermore, the relevance of equilibrium among trace-element species in high-temperature volcanic gases can also be evaluated by comparing numerical calculations with the observed fumarole sublimates and the measured contents of trace elements in volcanic gases (Symonds and others, 1987). A good match between the predicted solids and the observed sublimate sequence is evidence for the validity of the equilibrium model. Agreement between the calculated volatilities and the observed trace-element contents of the gases also supports the equilibrium degassing model. Such comparisons at Merapi volcano suggest that equilibrium calculations provide a means to understand the natural process, even though the calculations do not exactly reproduce the observed results (Symonds and others, 1987).

The utility of the modeling also depends on whether the quality and quantity of thermochemical data are sufficient to predict the gases, minerals, and liquids actually present in the natural system. Again, comparing numerical calculations with appropriate samples aids evaluation of thermochemical data. One reason for doing these calculations is to test these assumptions.

THERMOCHEMICAL DATA

The validity of numerical calculations from SOLVGAS and GASWORKS depends on the quality and quantity of the thermochemical data. Large errors or missing species in the thermochemical data base can lead to erroneous conclusions.

Reference states and conventions.—The standard states for the gases, solids, and liquids in our data base are the ideal gas at unit fugacity, the pure crystalline (or vitreous) solid, and the pure liquid, respectively, all at 298.15 K and 1 atm pressure. For each species, we obtained values for the standard enthalpy of formation from the elements, $\Delta_f H^0$, and the standard entropy, S^0, both at 298.15 K and 1 atm pressure; for some solid species (those from Robie, Hemingway, and Fisher, 1978; Helgeson and others, 1978; and Berman, 1988), we used the reported values at 298.15 K and 1 bar pressure. We also obtained a heat capacity equation, generally of the form:

$$C_P^0 = a + bT + cT^{-2}, \tag{1}$$

where, C_P^0 is the standard heat capacity at constant pressure, T is temperature (K), and a, b, and c are constants; for some species, eq (1) contains a fourth term, dT^2. Heat capacities for a number of solids (those

from Berman and Brown, 1985; Berman, 1988) are described by a different equation:

$$C_P^0 = k_0 + k_1 T^{-0.5} + k_2 T^{-2} + k_3 T^{-3}, \tag{2}$$

where k_0, k_1, k_2, and k_3 are constants. Where an appropriate heat capacity equation was not available, tabulated heat capacity data were fit to eq (1) using least-squares regression.

Thermochemical data for the elements are from Pankratz (1982). In general, we used the stable form (gas, solid, or liquid) of each element at 298.15 K and 1 atm pressure as the reference state; exceptions are S, Se, and Te for which we used the unconventional reference states of $S_2(g)$, $Se_2(g)$, and $Te_2(g)$ (Pankratz, 1982).

Finally, we calculated the standard Gibbs free energy of formation from the elements, $\Delta_f G^0$, at 298.15 K and 1 atm pressure using the equation:

$$\Delta_f G^0 = \Delta_f H^0 - T\Delta_f S^0, \tag{3}$$

where T is 298.15 K, and $\Delta_f S^0$ is the standard entropy of formation from the elements (S^0 data for the elements are from Pankratz, 1982).

Sources of data.—For each gas, liquid, and solid species included in the calculations, we chose what we believe to be the "best" available thermochemical data. Thermochemical data for gas, solid, and liquid species were obtained from the U.S. Bureau of Mines (DeKock, 1982; Pankratz, 1982, 1984; Pankratz, Stuve, and Gokcen, 1984; Pankratz, Mah, and Watson, 1987); the JANAF thermochemical tables (Stull and Prophet, 1971; Chase and others, 1974, 1975, 1978, 1982); Barin and Knacke (1973); Barin, Knacke, and Kubaschewski (1977); Berman and Brown (1985); Berman (1988); Robie, Hemingway, and Fisher (1978); Helgeson and others (1978); and Anovitz and others (1985). We list the specific source for each species in table 1 and app. 2.

Methods.—For each of the 42 elements included in the calculations, it is necessary to choose a component gas species. Theoretically, the choice of component gas species is arbitrary; regardless of the component species chosen, the final calculated distribution of species should be the same. With the numerical limitations of modern computers (for example, precision shortcomings, constraints on the size of exponents), however, the choice of component gas species makes a difference in the computer's ability to solve the equations with speed and accuracy. Therefore, we chose the dominant, or one of the more abundant, gas species of each element in high-temperature volcanic gases as the component species (table 1). Our component species (table 1) optimize computations involving reduced volcanic gases that contain some HCl and HF; equilibrium calculations involving extremely oxidized (> 1 percent O_2) or halogen-poor ($< 10^{-5}$ percent HCl or HF) gases might require different component species. To change component species, one simply combines the appropriate log K equations (below), although changing the component

TABLE 1

Component gas species presently used in GASTHERM. Listed in order of increasing atomic number

	Element	Component gas species	Reference
1	H	H_2	Pankratz (1982)
2	Li	LiCl	Pankratz (1984)
3	C	CO_2	Pankratz (1982)
4	N	N_2	Pankratz (1982)
5	O	H_2O	Pankratz (1982)
6	F	HF	Pankratz (1984)
7	Na	NaCl	Pankratz (1984)
8	Mg	$MgCl_2$	Pankratz (1984)
9	Al	AlF_3	Pankratz (1984)
10	Si	SiF_4	Pankratz (1984)
11	S	H_2S	Pankratz, Mah, and Watson (1987)
12	Cl	HCl	Pankratz (1984)
13	K	KCl	Pankratz (1984)
14	Ca	$CaCl_2$	Pankratz (1984)
15	Ti	TiF_4	Pankratz (1984)
16	V	VCl_4	Pankratz (1984)
17	Cr	$CrCl_4$	Pankratz (1984)
18	Mn	$MnCl_2$	Barin and Knacke (1973)
19	Fe	$FeCl_2$	Pankratz (1984)
20	Co	$CoCl_2$	Pankratz (1984)
21	Ni	$NiCl_2$	Pankratz (1984)
22	Cu	CuCl	Pankratz (1984)
23	Zn	$ZnCl_2$	Barin and Knacke (1973)
24	Ga	$GaCl_3$	Pankratz (1984)
25	As	$AsCl_3$	Pankratz (1984)
26	Se	H_2Se	Barin, Knacke, and Kubaschewski (1977)
27	Br	HBr	Pankratz (1984)
28	Rb	RbCl	Pankratz (1984)
29	Sr	$SrCl_2$	Pankratz (1984)
30	Mo	H_2MoO_4	Stull and Prophet (1971)
31	Ag	AgCl	Barin and Knacke (1973)
32	Cd	Cd	Pankratz (1982)
33	Sn	$SnCl_2$	Pankratz (1984)
34	Sb	$SbCl_3$	Pankratz (1984)
35	Te	H_2Te	Barin, Knacke, and Kubaschewski (1977)
36	Cs	CsCl	Pankratz (1984)
37	W	H_2WO_4	Stull and Prophet (1971)
38	Ir	Ir	Pankratz (1982)
39	Au	Au	Pankratz (1982)
40	Hg	Hg	Pankratz (1982)
41	Pb	$PbCl_2$	Pankratz (1984)
42	Bi	$BiCl_3$	Pankratz (1984)

species for H (H_2) and O (H_2O) requires additional modification of SOLVGAS and GASWORKS, since they fix fO_2 (app. 1).

For every component, we have included all the derived gas species for which we could find thermochemical data at the time of this compila-

tion. "Derived species" are any species formed by combinations of component species (app. 2). Our compilation of solid and liquid species is not comprehensive, as we have not included every possible species. The data base GASTHERM presently incorporates 627 gas species and 398 solids and liquids in the 42 component system (app. 2).

To calculate the distribution of gas, solid, and liquid species, we need the equilibrium constant, K, for the reaction between each derived species and its respective component species. First, we calculated the apparent standard Gibbs free energy of formation from the elements, $\Delta_a G^T$, of the ith species involved in each reaction at 1 atm pressure and at a given temperature, T(K), using the equation:

$$\Delta_a G^T = \Delta_f G^0 - (T - T_0)\Delta_f S^0 + \int_{T_0}^{T} C_p^0 dT - T \int_{T_0}^{T} \frac{C_p^0}{T} dT, \qquad (4)$$

where T_0 is 298.15 K, and C_p^0 is described using eq (1) or (2). Then, we calculated the standard Gibbs free energy for the reaction, $\Delta_r G^T$, at the same temperature, T, with the equation:

$$\Delta_r G^T = \sum_i \nu_i \Delta_a G^T, \qquad (5)$$

where $\Delta_a G^T$ is defined in eq (4), and ν_i is the stoichiometric coefficient of the ith species in the reaction. Finally, we calculated the logarithm of the equilibrium constant for the reaction, log K^T, at the temperature, T, with the equation:

$$\log K^T = -\Delta_r G^T/(2.303RT), \qquad (6)$$

where R (1.987 cal $\cdot$ K^{-1} $\cdot$ mole^{-1}) is the gas constant.

We store values for log K^T calculated at 298.15 K (25°C) and from 373.15 K (100°C) to 1473.15 K (1200°C) at 100 K increments in a data file, GASTHERM, for use by the programs. To obtain log K^T values at any arbitrary temperature over the range of data validity, it is most convenient to use a function for log K^T rather than calculating K's each time using eqs (4) through (6). Substituting eq (1), our dominant heat capacity equation, for C_p^0 in eq (4) and combining terms in eqs (4) through (6), results in an expression for log K^T of the form:

$$\log K^T = l_0 + l_1 T^{-1} + l_2 T + l_3 T^{-2} + l_4 \log (T), \qquad (7)$$

where l_0, l_1, l_2, l_3, and l_4 are constants. To fit the computed log K^T values to eq (7), we used least-squares regression. App. 2 contains the coefficients for eq (7), l_0, l_1, l_2, l_3, and l_4, for each derived species reaction in GASTHERM.

Errors.—The main errors in our thermochemical data base are as follows:

1. *Errors due to missing species.* If the data base does not contain species actually present in the volcanic gas, the calculations cannot possibly

reproduce the natural system with respect to those species. Missing species may make calculations for Au, Cd, Cr, Ir, and Si erroneous (this work; Symonds, Reed, and Rose, 1992).

2. *Errors in the $\Delta_f G^0$ values*. Poorly determined free energies can lead to large uncertainties in thermochemical calculations. Unfortunately, many of our references do not report uncertainties in $\Delta_f G^0$, making this source of error difficult to assess. However, JANAF (for example, Stull and Prophet, 1971) reports uncertainties in $\Delta_f G^0$ so we use their data to evaluate this source of error. The error in $\Delta_f G^0$ is generally between ± 0.1 and ± 2 kcal/mole. The error of ± 2 kcal/mole for $\Delta_f G^0$ of $(NaCl)_2$, the dominant sodium gas species when halite precipitates, leads to a $\pm 25°C$ error in the calculated precipitation temperature of halite (below). A similar if hypothetical error (the actual error is ± 0.2 kcal/mole) for $\Delta_f G^0$ of SiF_4, the dominant silicon gas species, leads to a ± 0.5 order of magnitude error in its calculated volatility (below). Since the uncertainties in $\Delta_f G^0$ are generally less than ± 2 kcal/mole, the errors in the calculated precipitation temperatures and volatilities are usually less than $\pm 25°C$ and ± 0.5 orders of magnitude, respectively. However, the uncertainty in $\Delta_f G^0$ for some species is much larger than ± 2 kcal/mole, and this may greatly affect the model calculations. For example, the error in $\Delta_f G^0$ for $PbCl_4$ and $PbBr_4$ is ± 21 kcal/mole, large enough to make the calculated precipitation temperature of galena very uncertain (see below).

3. *Errors due to inconsistencies between different sources of thermochemical data*. Since the thermochemical data come from several different sources, errors arise from discrepancies between the various sources. For example, there is a difference of 1.14 kcal/mole in the $\Delta_f G^0$ values for $(NaCl)_2$ reported by JANAF (Stull and Prophet, 1971) and Pankratz (1984) (the heat capacity data are the same). This translates to a $12°C$ difference in the precipitation temperature of halite. Since differences in $\Delta_f G^0$ values are generally less than 1 kcal/mole, the error from inconsistent $\Delta_f G^0$ values is generally less than for $(NaCl)_2$.

4. *Errors in the log K^T values owing to the use of eqs (1) through (5) to calculate $\Delta_r G^T$*. Pankratz (1982) states that calculating $\Delta_r G^T$ from tabular values of $\Delta_f G^T$ (reported in many compilations) is more precise than using eqs (1) through (5) because the tabulated $\Delta_f G^T$ values are derived from more accurate equations. However, the resulting errors in $\Delta_r G^T$ are generally less than 1 percent; a small sacrifice for the gain in convenience for computer assisted calculations.

5. *Errors in log K^T values due to the use of eq (7)*. The average absolute error in the log K^T value from using eq (7) is almost always much less than ± 0.1 percent, which translates to a maximum error of $\pm 1°C$ in the calculated condensation temperatures, for example. This is a small sacrifice in quality for a substantial increase in program efficiency.

At the present time, missing species and poorly determined values for $\Delta_f G^0$ are the greatest problems with the data base. These errors generally outweigh the discrepancies between different sources of ther-

mochemical data and errors from mathematical models used to fit data. The data in GASTHERM should suffice for modeling of volcanic gases as shown in this paper, except where noted here and below. However, we caution users not to use the compilation for precise work, such as to extract thermochemical data from phase equilibrium experiments.

APPLICATIONS TO MOUNT ST. HELENS

Programs SOLVGAS and GASWORKS model reactions in volcanic gases as they travel from the magma to the atmosphere. When constrained with appropriate samples, the modeling helps understanding of the natural processes, checking of the quality of the input gas analyses, and determining whether trace elements come from degassing magma or from some other source. All modeling of multicomponent chemical equilibria in volcanic gases requires data on the complete gas composition, including trace elements. In addition, we need (1) data on the mineralogy and composition of the magma to model the volatilization of metals from magma, (2) information on the composition and zoning of sublimates and incrustations to model cooling, oxidation, and wall rock interactions in fumaroles, and (3) data on the species and aerosols in volcanic plumes to model reactions that occur when volcanic gases mix with the atmosphere.

We chose data collected from July to September 1981 from Mount St. Helens, one of the best studied volcanos in the world. Since the cataclysmic eruption on 18 May 1980, numerous studies have produced a wealth of data on the Mount St. Helens gases. Research focused on the SO_2 emission rates (Casadevall and others, 1983), the major gases (Gerlach and Casadevall, 1986a, b), the trace elements in the gas (Le Guern, ms), volcanic aerosols (Rose, Chuan, and Woods, 1982; Thomas, Varekamp, and Buseck, 1982; Varekamp and others, 1986; Chuan, Rose, and Woods, 1987; Rose, 1987 and unpublished), and on incrustations and sublimates (Keith, Casadevall, and Johnston, 1981; Graeber, Gerlach, and Hlava, 1982; Bernard, ms; Bernard and Le Guern, 1986; Rose, 1987 and unpublished). One very complete, high-quality set was collected during the period July to September 1981. At that time, high-temperature fumaroles with minimal air contamination were easily accessible. Gases in excess of 600°C discharged along a northwest-striking fissure on the crater floor and from an active scarp on the northwest side of the lava dome (the radial and scarp fumaroles, respectively). The wide array of gas data collected during this period provides multiple constraints on our modeling results. For the Mount St. Helens case, we (1) calculate trace-element volatilities to test whether the observed trace-element contents of the gases can be explained by volatilization of shallow magma, deep magma, or the wall rock, or whether they come from some other source; (2) cool the analyzed gas numerically and compare the predicted solids with the observed fumarolic sublimates to test the quality of the input gas composition and the modeling results; and (3) revise the

input gas composition and repeat the cooling calculations to predict cooling reactions in the Mount St. Helens volcanic gases.

Geologic setting.—Mount St. Helens is a stratovolcano located in south-central Washington. Eruptions began about 40,000 yrs ago and have continued to the present (Mullineaux and Crandell, 1981). Recent eruptive activity commenced with the 18 May 1980 eruption that created the present amphitheater-shaped crater (Christiansen and Peterson, 1981; Voight, 1981). Following the 18 May eruption, the volcano erupted explosively on 25 May, 12 June, 22 July, 7 August, and 16 to 18 October 1980 (Christiansen and Peterson, 1981). A lava dome extruded from the crater floor at the end of the October 1980 eruption and grew until 1986 through a series of dome-building eruptions (Swanson and Holcomb, 1990). Degassing occurred during eruptions and, at a lower level, between eruptions; gas emission rates declined significantly over the 7-yr eruptive period (Casadevall and others, 1983).

Eruptive products.—The materials erupted from Mount St. Helens from 18 May 1980 through August 1982 are dacitic to andesitic in composition; silica concentration decreased during each of the first five explosive eruptions from a high of over 64 wt percent but has been almost constant at 62 to 63 wt percent since August 1980 (Cashman and Taggart, 1983). The dome lavas erupted in 1981 and 1982 contain about 32 percent plagioclase, 4.5 percent orthopyroxene, 1.5 percent hornblende, 2 percent magnetite and ilmenite, and < 0.5 percent clinopyroxene (Cashman and Taggart, 1983). The recent eruptive products also contain trace amounts of Fe–Cu sulfides (Rose and others, 1983).

Volcanic gas composition.—One typically collects volcanic gases in evacuated bottles, which are partly filled with a caustic soda solution that absorbs the acid gases (Giggenbach, 1975). In the laboratory, the headspaces of the bottles are analyzed by gas chromatography, and the solutions are analyzed by ion chromatography and wet chemical methods. It is also possible to analyze the gases completely at the collection site using an in situ field gas chromatograph (FGC) (Le Guern, Gerlach, and Nohl, 1982).

Testing whether the species were once in equilibrium is one way to evaluate analyses of volcanic gases (Gerlach, 1980a; Gerlach and Casadevall, 1986a). This approach is successful because high-temperature volcanic gases often approach a state of chemical equilibrium, although samples of them may be nonequilibrium mixtures due to secondary alterations such as disequilibrium atmospheric oxidation, sampling problems, or analytical errors (Gerlach 1980a, b, c, d; Gerlach and Casadevall, 1986a). If the fumarolic gases are in equilibrium, the highest quality samples are *quenched equilibrium compositions*, such as the 1979 FGC analysis from Merapi volcano (Le Guern, Gerlach, and Nohl, 1982). Such samples allow inference of the *last equilibrium temperature*. If the gases are nonequilibrium mixtures due to secondary alterations, they can be *restored* or returned to their equilibrium state if the analyses are reason-

ably complete and of high quality (Gerlach and Casadevall, 1986a). Restored compositions allow determination of the last equilibrium temperature and are almost as good as quenched equilibrium compositions. *Apparent compositions* are based on incomplete analyses and the hypothesis that the gases initially approached a state of chemical equilibrium (Gerlach and Casadevall, 1986a). They must be complete enough, however, to deduce the last equilibrium temperature and the concentrations of the undetermined species. Apparent compositions are less reliable than restored compositions. *Estimated' compositions* are based on incomplete analyses and the hypothesis that the gases initially approached a state of chemical equilibrium (Gerlach and Casadevall, 1986a). However, for estimated compositions it is necessary to assume that the gases were in equilibrium at the collection temperature since they are not complete enough to allow simultaneous determination of both the last equilibrium temperature and concentrations of the undetermined species. Estimated compositions are highly unreliable.

Of the 50 gas samples collected by various workers at Mount St. Helens between September 1980 and December 1981, Gerlach and Casadevall (1986a) could restore only two. For our modeling, we chose the restored FGC analysis from the radial fumaroles on 17 September 1981 collected by F. Le Guern. The other restorable gas sample was collected from the radial fumaroles one day earlier in a caustic soda bottle and is not significantly different from the FGC composition (Gerlach and Casadevall, 1986a). Additional caustic soda gas samples provide the HCl and HF contents of the September 1981 gas (Bernard, ms).

To estimate the concentrations of trace elements in the volcanic gas, we used an analysis of a gas condensate sample collected in an ether condenser on 17 September 1981 (Le Guern, ms). Since this condensate was collected by pumping the volcanic gas mixture, including any rock aerosols, through a cold trap, it provides an estimate of the bulk concentrations of trace elements in the volcanic gas, solid contaminants included. To estimate the bulk concentration of a trace element in the volcanic gas, we use the equation:

$$C_i = R_i M_w, \tag{8}$$

where C_i is the mole percent of the trace component, i, in the volcanic gas; R_i is the molar ratio of i to H_2O in the condensate analysis; and M_w is the mole percent of H_2O in the major-gas analysis. Table 2 shows the complete September 1981 gas composition, including trace elements.

Sublimates.—Knowledge of sublimates and their zoning sequence around volcanic fumaroles aids interpretation of the cooling calculations and the quality of the analyzed gas composition as discussed below. Unfortunately, incrustations include both sublimates and solids that form by complex reactions involving volcanic gases, wall rock, liquid species, and atmospheric gases (Stoiber and Rose, 1974; Getahun, Reed, and Symonds, 1992). To isolate sublimates from other types of incrustations, Le Guern and Bernard (1982) developed the silica-tube collection method.

TABLE 2

Complete Mount St. Helens gas composition for 17 September 1981. The major gas composition is from a field gas chromatograph analysis by Le Guern (unpublished), restored by Gerlach and Casadevall (1986a). Data for HCl, HF, and trace elements are from Bernard (ms) and Le Guern (ms). N_2, O_2, and Ar, which are mostly air contaminants, are excluded from the composition as discussed by Gerlach and Casadevall (1986a)

Major Gas Species (mole %)

H_2O	98.6
CO_2	0.886
H_2	0.39
H_2S	0.099
SO_2	0.067
HCl	0.076
HF	0.03
CO	0.0023
log fO_2	-15.77
T_{eq}	710

Trace Elements (mole %)

Na	4.1×10^{-4}	Sb	1.2×10^{-7}
K	1.8×10^{-4}	Rb	1.0×10^{-7}
Al	1.6×10^{-4}	Mn	1.0×10^{-7}
As	3.3×10^{-5}	Ta	7.8×10^{-8}
Sr	1.5×10^{-5}	U	4.5×10^{-8}
Fe	6.4×10^{-6}	Hf	4.2×10^{-8}
Pb	4.7×10^{-6}	W	2.9×10^{-8}
Mo	1.8×10^{-6}	Cs	2.7×10^{-8}
Cu	1.5×10^{-6}	Co	1.2×10^{-8}
Bi	1.0×10^{-6}	I	9.0×10^{-9}
Se	6.8×10^{-7}	La	3.8×10^{-9}
Br	6.7×10^{-7}	Ba	2.6×10^{-9}
Cd	6.6×10^{-7}	Dy	2.3×10^{-9}
Zn	5.4×10^{-7}	Th	5.4×10^{-10}
Ca	4.9×10^{-7}	Au	3.0×10^{-10}
Cr	4.1×10^{-7}	Ag	2.5×10^{-10}
Sc	2.4×10^{-7}	Lu	7.5×10^{-11}
Hg	1.8×10^{-7}	Eu	4.7×10^{-11}
V	1.7×10^{-7}	Ir	1.9×10^{-11}
Te	1.3×10^{-7}		

One inserts a silica tube into a fumarole, and sublimates form as the volcanic gas cools in the tube.

Bernard (Bernard, ms; Bernard and Le Guern, 1986) and Graeber, Gerlach, and Hlava (1982) collected sublimates from the radial fumaroles at Mount St. Helens in September 1981 using the silica-tube method. Table 3 gives Bernard's results. Graeber, Gerlach, and Hlava (1982) report generally similar findings, but they also discovered trace amounts of $FeS_x(s)$, $Ni_xS_y(s)$, and $(Na, K)_4CdCl_6(s)$, in their silica tubes.

Incrustations.—Study of both silica-tube sublimates and natural incrustations can help determine which minerals precipitate directly from the gas and which phases form by reactions of volcanic gases with the wall

TABLE 3

Sublimates collected from 675° to 650°C vents in the radial and scarp fumarole fields at Mount St. Helens in September 1981 using the silica tube method as reported by Bernard (ms) and Bernard and Le Guern (1986). Small amounts of eroded rock fragments were also observed throughout the silica tubes (Bernard, personal communication, 1990)

Mineral or Phase*	Minor Elements**	Temperature (°C)
magnetite (Fe_3O_4)		> 570
alpha-cristobalite (SiO_2)		> 570
molybdenite (MoS_2)	Fe, Re	570–480
ferberite ($FeWO_4$)	Mn	570–500
halite (NaCl)		550–450
sylvite (KCl)		550–450
greenockite (CdS)	Cu, Zn, Fe	520–450
galena (PbS)	Bi, Sn	480–400
$Pb_3Bi_2S_6$ (?)	Sn	450–400
AsS (?)	Te	<400

* All phases except $Pb_3Bi_2S_6$ and AsS were confirmed by X-ray diffraction; $Pb_3Bi_2S_6$ and AsS were tentatively identified by energy dispersive X-ray spectrometry (Bernard, ms; Bernard and Le Guern, 1986).
** Concentrations of these elements are greater than 1 wt percent in the mineral as determined by energy dispersive X-ray spectrometry.

rock or atmospheric gases. High-temperature (>300°C) incrustations were collected from the radial fumarole field in August 1981 (Rose, 1987 and unpublished) and in September 1981 (Bernard, ms; Bernard and Le Guern, 1986) (table 4). Although there are many similarities in the minerals reported by these studies, there are important differences: only Rose (1987 and unpublished) found thenardite, pentlandite, tetrahedrite, plattnerite, and ilsemannite, whereas only Bernard (Bernard, ms; Bernard and Le Guern, 1986) reported halite, sylvite, molybdenite, W-rich powellite, greenockite, hematite, and galena. Rose (unpublished) also identified cubanite but perhaps that is the unidentified Cu–Fe–S phase reported by Bernard (ms) and Bernard and Le Guern (1986). Many of the differences between the two studies arise from different sampling strategies: Bernard (Bernard, ms; Bernard and Le Guern, 1986) only sampled incrustations from reduced zones in the fumaroles, 5 to 15 cm below the surface, whereas Rose (1987 and unpublished) sampled oxidized incrustations surrounding the fumaroles as well as the reduced incrustations.

Volcanic aerosols.—Aerosols can be collected on filters or with a quartz-crystal-microbalance (QCM) cascade impactor (Vie Le Sage, 1983); in either case, scanning electron microscopy (SEM) can help identify their constituent phases. Aerosols were collected at Mount St. Helens from the radial fumaroles and in the plume during July 1981 using Nuclepore

TABLE 4

Incrustation minerals collected from fumaroles at Mount St. Helens in 1980 and 1981. High-temperature (> 300°C) incrustations were collected from the radial fumaroles in August 1981 (Rose, 1987 and unpublished) and September 1981 (Bernard, ms; Bernard and Le Guern, 1986). Low-temperature (< 250°C) incrustations were collected in the summer of 1980 from various fumaroles in the crater and on the pyroclastic flows (Keith, Casadevall, and Johnston, 1981). Phases were identified by X-ray diffraction and SEM

White crusts (>550°C)

thenardite	Na_2SO_4
halite	$NaCl$
sylvite	KCl
molybdenite	MoS_2
W-rich powellite	$Ca(W,Mo)O_4$
greenockite	CdS
hematite	Fe_2O_3

Black crusts (450-550°C)

lillianite	$Pb_3Bi_2S_6$
bismuthinite	Bi_2S_3
cannizzarite	$Pb_4Bi_2S_6$
galena	PbS
pentlandite	$(Fe,Ni)_9S_8$
cubanite	$CuFe_2S_3$
tetrahedrite	$(Cu,Ag,Fe)_{12}SbS_{13}$
plattnerite	PbO_2

Blue crusts (300-350°C)

ilsemannite	$Mo_3O_8 \cdot nH_2O$ (?)

Red, orange, yellow, and white crusts (<250°C)

sulfur	S
gypsum	$CaSO_4 \cdot 2H_2O$
anhydrite	$CaSO_4$
thenardite	Na_2SO_4
melanterite	$Fe_2SO_4 \cdot 7H_2O$
glauberite	$Na_2Ca(SO_4)_2$
natroalunite	$(Na,K)Al_3(SO_4)_2(OH)_6$
hematite	Fe_2O_3
Fe hydroxides	
halotrichite	$FeAl_2(SO_4)_4 \cdot 22H_2O$
Unnamed (ASTM 23-128)	$CaSO_4 \cdot 15H_2O$
halite	$NaCl$
sal ammoniac	NH_4Cl

filters (Varekamp and others, 1986) and in August 1981 using the QCM (Rose, 1987 and unpublished; Chuan, Rose, and Woods, 1987). The results (table 5) show that water, sulfuric acid (H_2SO_4) silicate rock aerosols, and various chlorides and sulfates are the dominant fumarole

Aerosols identified or inferred in the radial fumaroles and in the plume at Mount St. Helens in July and August 1981. Phases were identified tentatively by semiquantitative (standardless) energy dispersive X-ray spectrometry and morphology

Phase	Site	Reference
$H_2O(l)$	plume, fumarole	2
silicate rock aerosols	plume, fumarole	1,2
$H_2SO_4(l)$	plume, fumarole	1,2
NaCl or (Na,K)Cl	plume, fumarole	1,2
sulfate aerosols*	plume, fumarole	1,2
Fe oxides	fumarole	1
As_2S_3	fumarole	2
KNO_3 (?)	fumarole	2
SnO_2 (?)	fumarole	2
$(Sn,Pb)O_2$ (?)	fumarole	2

* The sulfate phases are complex and occur as overgrowths on ash or as individual grains. Sulfates contain various amounts of Ca, K, Na, Al, and Mg, and some grains also contain minor Zn, Cu, and Fe.

1 July 1981 (Varekamp and others, 1986)
2 August 1981 (Rose, 1987 and unpublished; Chuan, Rose, and Woods, 1987)

and plume aerosols, although the fumarole aerosols also include $As_2S_3(s)$, $KNO_3(s)$, and oxides of Fe, Sn, and Pb. Although the findings of the two studies are similar, there are some differences: (1) Rose (unpublished) detected minor amounts of Cl (using EDS) in $H_2SO_4(l)$, but Cl was below detection (also using EDS) in the $H_2SO_4(l)$ analyzed by Varekamp and others (1986); (2) Varekamp and others (1986) report Fe oxides and various Na-, Ca-, and Mg-bearing sulfates, which were not found in August 1981 (Rose, 1987 and unpublished; Chuan, Rose, and Woods, 1987); and (3) Rose (unpublished) found $As_2S_3(s)$, $K_2SO_4(s)$, and oxides of Pb and Sn, all unreported by Varekamp and others (1986). In addition, Varekamp and others (1986) collected various anthropogenic aerosols in the plume such as fertilizer grains (containing K and P) and Cr-rich spheres. Chuan, Rose, and Woods (1987, p. 173) and Rose (1987, p. 157) also report abundant acanthite (Ag_2S) crystals, which were not found by Varekamp and others (1986); they may be sublimates or, as suggested by R. Andres (personal communication, 1990), artificial products of a reaction between $H_2SO_4(l)$ and the Ag-bearing impactor plates of the QCM. Some of the sulfates reported by Varekamp and others (1986) probably formed by reactions between $H_2SO_4(l)$ and grains of ash.

GEOLOGIC MODEL

Figure 1 shows our geologic model of the radial fumaroles. Gerlach and Casadevall (1986b) argue that the major volcanic gases discharged from the September 1981 fumaroles are mixtures of magmatic gases and
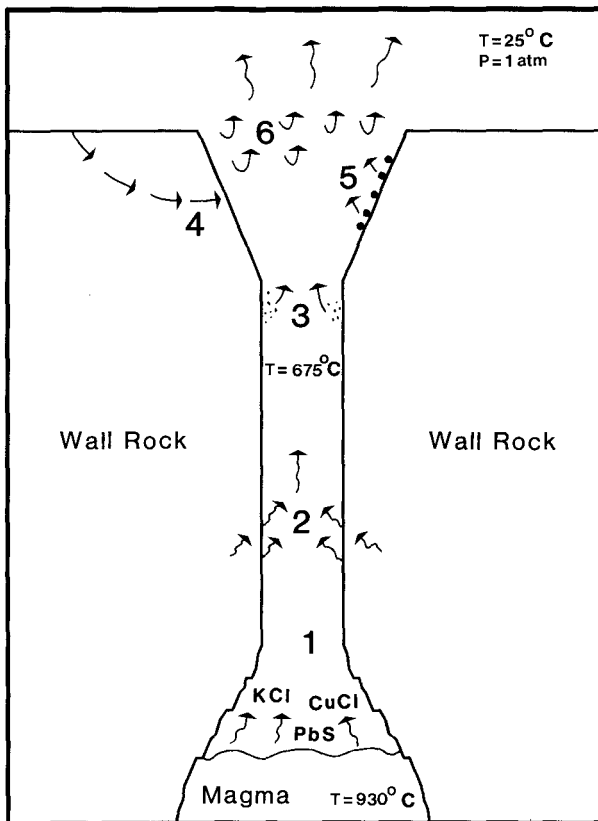
Fig. 1. Schematic diagram showing possible chemical and physical processes affecting the origin, abundance, and reactions of trace elements in the Mount St. Helens volcanic gases, depicted specifically for the radial fumaroles in September 1981. The deepest possible source of trace elements is volatilization of 930°C magma or hot wall rock at some unknown depth in the edifice of the volcano (process 1). As the magmatic gases rise toward the surface they mix with hydrothermal vapor, which dilutes and cools the magmatic gases (process 2). Additional contamination of the magmatic gases may come from rock aerosols eroded from the wall rock by the gas stream (process 3). In the fumarole the gas may be affected by boiling of near-surface acidic water into the volcanic gas (process 4); reaction of condensed acid droplets with the wall rock or rock aerosols in the gas stream (process 5); and mixing with atmospheric gases (process 6). In response to cooling of the volcanic gases by processes 2, 4, and 6, sublimates may form on the wall rock or as aerosols in the gas stream; additional incrustations may result from reactions between the volcanic gas and the wall rock, triggered in part by processes 5 and 6.

hydrothermal vapor. Using Fe-Ti oxide estimates, the temperature of the magma ranges from 868° to 1000°C (Melson and Hopson, 1981; Scheidegger, Federman, and Tallman, 1982; Rutherford and others, 1985). We use the most recent and intermediate magma temperature estimate of 930° ± 10°C (Rutherford and others, 1985). The depth and therefore

pressure of the degassing magma is less certain; degassing may occur from near-surface magma in the lava dome or from a magma chamber, perhaps 7 km below the surface (Rutherford and others, 1985). Therefore, it is possible that trace elements in the September 1981 gases were volatilized from 930°C dacite magma located near the surface or at considerable depth. It is also possible that the trace elements were volatilized from <930°C dacite wall rock; this might occur after the magmatic gases mixed with hydrothermal vapor. In any case, the volatilization process involves a reaction between volcanic gas and dacite at some high temperature. The volcanic gas then ascends rapidly to the surface through fractures; the gas stream may erode the wall rock and entrain rock fragments. As this gas-ash mixture vents through fumaroles, it starts to mix and react with cold (25°C) atmospheric gases, which cause cooling and precipitation of solids. When the volcanic gas cools below 200°C, in low-temperature zones around fumaroles, sulfuric acid species may condense on the wall rock, triggering liquid-rock reactions (Symonds, Reed, and Rose, 1992). Finally, the gas mixture discharges into the atmosphere where a series of complex reactions may occur between the volcanic gas, the atmosphere, and entrained ash, resulting in additional aerosol formation.

VOLATILITY MODELING

Trace elements in the Mount St. Helens condensates may have come from volatilization of magma or wall rock, or from eroded rock particles that dissolved in the samples. To discriminate between volatilization from magma or wall rock and other sources of trace elements in the volcanic gas, we have developed a numerical method using GASWORKS to test the volatilization hypothesis. To calculate volatilities of trace elements in the gas, we fix the fugacities of the major gases (HBr included because of the intrinsic volatility of metal bromides) and fO_2 at a specified temperature and pressure and equilibrate the gas mixture with an appropriate mineral assemblage for the source magma. The mineral assemblage must contain components for the trace elements of interest. We also must estimate the activity of each endmember mineral species. There are two approaches: (1) use analyses of minerals in rocks to calculate activities of endmember mineral species, or (2) compute mineral compositions using a gas-rock titration procedure. In the first method, one must decide which minerals equilibrated with the gas and obtain the appropriate compositional data for all such minerals. In the second case, one needs the magma composition and the known or assumed solid solutions in minerals; GASWORKS uses these assumptions to compute the equilibrium compositions of minerals as rock is titrated into the gas. We prefer the second method, gas-rock titration, because: (A) it involves fewer a priori assumptions about the buffering mineral assemblage; (B) we know the bulk magma composition better than the specific compositions of minerals; and (C) it allows for possible gas-phase alteration of phenocryst assemblages in fumaroles.

Comparison of computed volatilities with the trace element contents of gas samples provides a means to test whether the trace elements are volatilized from magma or wall rock and, if so, the minimum amount of magma or wall rock necessary to buffer each trace element. The numerical simulations also help assess the role of erosion, leaching, or acid attack when they fail to explain the observed trace-element concentrations.

We do not know whether trace elements are volatilized from shallow magma, deep magma, or from cooler wall rock in fumarolic pathways, or whether they come from some other source. To help discriminate between these sources, we do several calculations. First, we calculate a gas/rock titration at 930°C and 1 atm to simulate degassing of near-surface magma. Second, we do a gas/rock titration at 930°C and 100 atm to examine magma degassing at depth. Finally, we do a gas/rock titration at 710°C and 1 atm to model volatilization from fumarole wall rock.

The titration proceeds by adding rock to the gas. For each incremental addition of rock to the gas, GASWORKS calculates the equilibrium mineral assemblage for that bulk composition. The reaction progress is described by a weight ratio of gas to rock, the gas/rock (G/R) ratio. We calculate over a range of G/R ratios to test whether elements are volatilized from the magma where the G/R ratio is low or from altered wall rock where the G/R ratio is high.

Assumptions for the 930°C and 1 atm gas/rock titration.—For each gas-rock titration, GASWORKS needs the following information: (1) the fugacities of the major gases, (2) the magma composition, (3) the observed solid solutions in the magmatic minerals, (4) the temperature and pressure (930°C and 1 atm in this case), and (5) the fO_2. We have no independent way to estimate the major gases discharged from the Mount St. Helens magma. For the purposes of these volatility calculations, we assume that H_2O, CO_2, SO_2, H_2S, H_2, HCl, HF, CO, and HBr in the September 1981 gas analysis (table 2) came from the magma, or, at least, that the volatilization process did not alter them significantly. In accordance with these assumptions, we estimate these fugacities by recalculating the September 1981 gas analysis at the assumed magmatic conditions (930°C; 1 atm; $fO_2 = -11.39$, see below) and then hold them constant during the course of the titrations.

We assume that the lava extruded in October 1981 best represents the magma composition during discharge of the September 1981 gases. Hence, we use an average composition of the October 1981 lava (Cashman and Taggart, 1983) for the contents of SiO_2, Al_2O_3, CaO, Fe_2O_3, Na_2O, MgO, K_2O, TiO_2, and MnO_2 in the magma (table 6). Since Cashman and Taggart (1983) did not analyze for Cu, we use an analysis of a pumice block erupted in 18 May 1980 (Halliday and others, 1983) to approximate the Cu concentration in the September 1981 magma (table 6).

The recent eruptive products from Mount St. Helens contain K-bearing plagioclase (An_{40}-An_{60}); hypersthene (34 mole percent orthoferrosilite) with minor amounts of Ca, Al, and Mn; Ti-bearing magnetite;

TABLE 6

Assumed composition of the Mount St. Helens dacite for modeling in this paper. Only data that are used in the calculations are reported

Major Elements (wt %)		Source
SiO_2	61.60	1
Al_2O_3	18.20	1
CaO	5.33	1
Fe_2O_3	5.13	1
Na_2O	4.48	1
MgO	2.29	1
K_2O	1.25	1
TiO_2	0.67	1
MnO	0.08	1
Trace Elements (ppm)		
Cu	45	2

[1] October 1981 dacite lava from Cashman and Taggart (1983)
[2] May 1980 pumice block from Halliday and others (1983)

Mg-bearing ilmenite-hematite; and augite (Scheidegger, Federman, and Tallman, 1982). To model these solid solutions, we assume ideal, multisite mixing between: (1) anorthite ($CaAl_2Si_2O_8$), high-albite ($NaAlSi_3O_8$), and sanidine ($KAlSi_3O_8$); (2) orthoenstatite ($MgSiO_3$), orthoferrosilite ($FeSiO_3$), Ca–Al pyroxene ($Ca_{0.5}AlSi_{0.5}O_3$), and rhodonite ($MnSiO_3$); (3) magnetite (Fe_3O_4) and ulvöspinel (Fe_2TiO_4); (4) ilmenite ($FeTiO_3$), hematite (Fe_2O_3), and $MgTiO_3$; and (5) diopside ($CaMgSi_2O_6$), hedenbergite ($CaFeSi_2O_6$), and jadeite ($NaAlSi_2O_6$).

Finally, we need to know the fO_2 of the volcanic gas under the assumed magmatic conditions. The first option assumes that the September 1981 volcanic gases were buffered initially by the magma at 930°C and 1 atm and then cooled as a closed system; in this case, we calculate (app. 1) the equilibrium fO_2 using the mass balances from the restored September 1981 sample (table 2). Alternatively, we could use Fe–Ti oxide fO_2 estimates to approximate the fO_2 of the gases expelled from the magma. To test the first hypothesis, we heat the restored gas composition to 930°C at 1 atm as a closed system. The resulting fO_2 trend agrees well with the temperature-fO_2 relationships of eight restored and apparent gas samples (Gerlach and Casadevall, 1986a) collected from Mount St. Helens in 1980 and 1981 (fig. 2). Therefore, we use the calculated fO_2 of
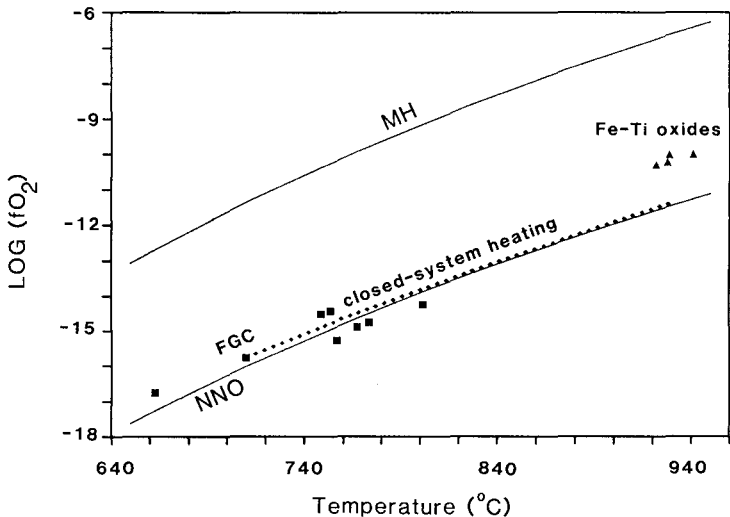
Fig. 2. The dotted line shows the calculated fO_2 for closed-system heating of the restored September 1981 field gas chromatograph (FGC) gas composition (table 2) from 710°C, the last equilibrium temperature (marked FGC), to 930°C, the assumed magma temperature. The squares show the fO_2 and last equilibrium temperatures of the restored and apparent Mount St. Helens gas compositions (Gerlach and Casadevall, 1986a). Triangles mark several estimates of the temperature and fO_2 of the magma, as determined from Fe-Ti oxide pairs in pumice erupted on 18 May 1980 (sample SH-084) (Rutherford and others, 1985). The Ni-NiO (NNO) and magnetite-hematite (MH) fO_2 buffers are shown for reference.

-11.39 at 930°C and 1 atm rather than the somewhat higher fO_2 values obtained from Fe–Ti oxide data (Rutherford and others, 1985).

Gas-rock titration at 930°C and 1 atm.—We start at a log gas/rock (LG/R) ratio of 6.0 and proceed toward lower LG/R ratios to study gas-rock interactions in fumaroles. We terminate the calculations at a LG/R ratio of -2.0 to simulate the small amounts of volatiles (1-4 wt percent H_2O, Merzbacher and Eggler, 1984) in the Mount St. Helens magma.

Figure 3 shows the results of the titrations from a LG/R ratio of 6.0 to a LG/R ratio of 0.0. We only show the results to a LG/R of 0.0, because lower G/R ratios do not cause significant changes in the buffering mineral assemblages. At an LG/R ratio of 6.0, the computed equilibrium mineral assemblage consists of beta-tridymite (SiO_2), anorthite (anorthite, high-albite, sanidine), cordierite ($Mg_2Al_4Si_5O_{18}$), sillimanite (Al_2SiO_5), and rutile (TiO_2). These minerals control the concentrations of trace elements in the gas phase. The assemblage tridymite–rutile–sillimanite–cordierite buffers SiF_4, TiF_3, AlF_2O, and $Mg(OH)_2$, the main gas species of Si, Ti, Al, and Mg. The assemblage anorthite–albite–sanidine–sillimanite–tridymite controls NaCl, KCl, and $CaCl_2$, the dominant species of Na, K,
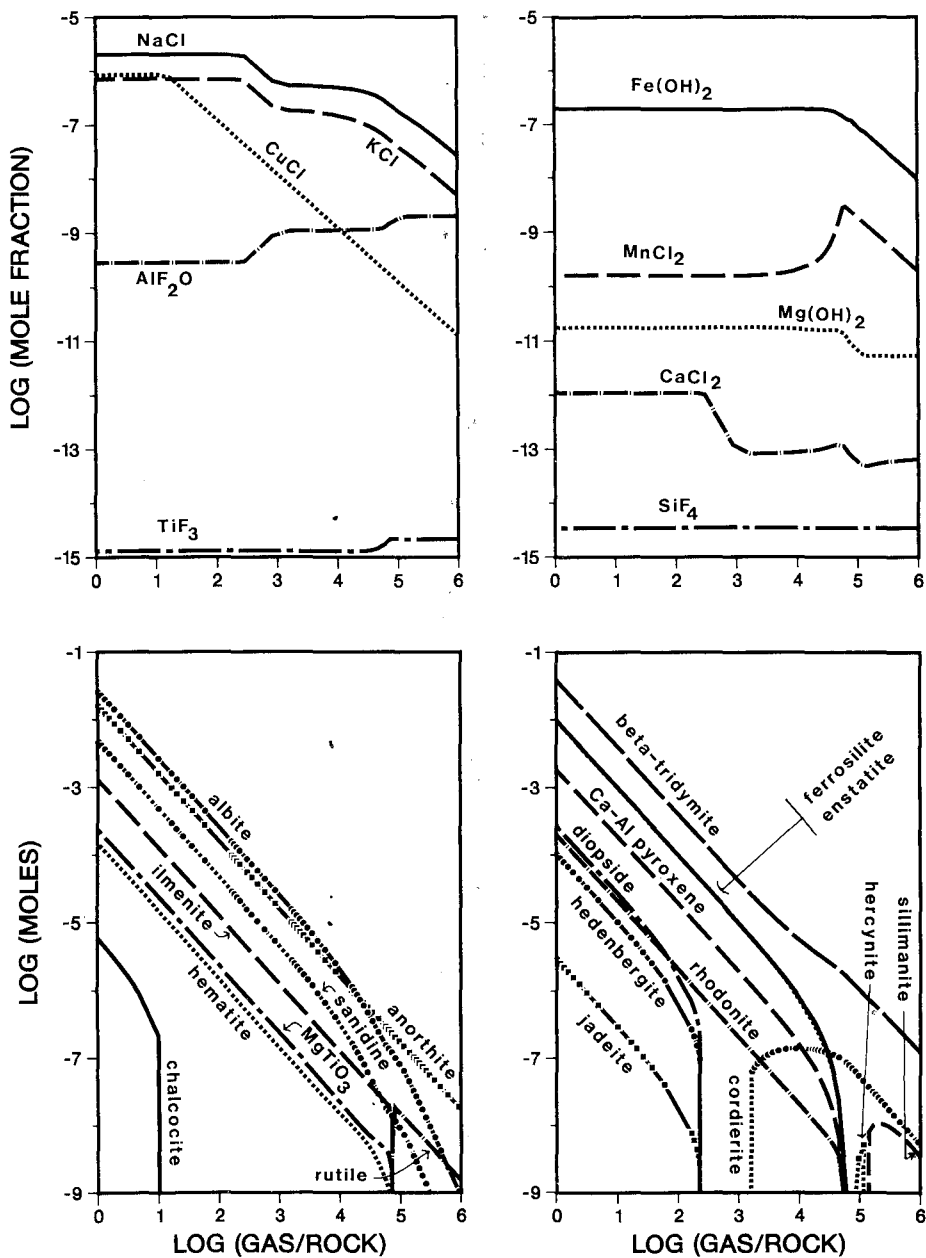
Fig. 3. Calculated results of the volcanic gas-dacite reaction at 930°C and 1 atm pressure for the Mount St. Helens case. The upper part of figure shows the most abundant gas species of trace elements; the lower half shows the distribution of mineral species, solid solutions included. Fugacities of the major gas species (H_2O, CO_2, H_2, H_2S, SO_2, HCl, HF, CO) and HBr were fixed using the restored September 1981 gas composition (table 2), recalculated at 930°C and 1 atm pressure.

and Ca. As additional rock is titrated into the gas, NaCl and KCl increase, and CaCl$_2$ decreases (slightly) because plagioclase becomes richer in Na and K and poorer in Ca.

At a LG/R ratio of 5.1, sillimanite evaporates into the gas and hercynite (FeAl$_2$O$_4$) forms. The disappearance of sillimanite destroys the sillimanite-tridymite AlF$_2$O buffer, and, with addition of more rock, AlF$_2$O decreases slightly. Sillimanite evaporation also destroys the cordierite–sillimanite–tridymite Mg(OH)$_2$ buffer and the anorthite–sillimanite–tridymite CaCl$_2$ buffer; both species increase as more rock is added. Hercynite evaporates into the gas at a LG/R ratio of 4.9.

Ilmenite (ilmenite, MgTiO$_3$, hematite) replaces rutile at a LG/R ratio of 4.9, and ilmenite-hematite becomes the new buffer for TiF$_3$. At a LG/R ratio of 4.8, ferrohypersthene (orthoferrosilite, orthoenstatite, Ca–Al pyroxene, rhodonite) forms. The assemblage cordierite–orthoferrosilite–orthoenstatite–rhodonite–tridymite fixes the mole fractions of AlF$_2$O, Fe(OH)$_2$, Mg(OH)$_2$, and MnCl$_2$, the dominant species of Al, Fe, Mg, and Mn, although the abundance of MnCl$_2$ decreases, until the mole fraction of rhodonite in ferrohypersthene stabilizes at lower G/R ratios.

When more rock is titrated into the gas, cordierite becomes increasingly unstable and finally evaporates into the gas at a LG/R ratio of 3.2. This disables the individual buffers for AlF$_2$O and CaCl$_2$, and, as we add more rock, they decrease and increase, respectively. Salite (diopside, hedenbergite, jadeite) forms at a LG/R ratio of 2.4. Precipitation of salite establishes the diopside–orthoenstatite–anorthite–tridymite assemblage that buffers CaCl$_2$ and AlF$_2$O. It also fixes the assemblage albite–sanidine–anorthite–diopside–orthoenstatite–tridymite that buffers NaCl and KCl. Finally, at a LG/R ratio of 1.0, chalcocite (Cu$_2$S) forms; it buffers CuCl, the dominant gas species of Cu, which increases steadily as the LG/R decreases from 6.0 to 1.0. Chalcocite is the last phase to form in the final equilibrium mineral assemblage, which consists of beta-tridymite, andesine, ferrohypersthene, salite, ilmenite, and chalcocite. This is the computed magmatic mineral assemblage as it does not change as we add more rock, at least up to a LG/R of −2.0 where we terminate the calculations. Consequently, the mole fractions of NaCl, CuCl, KCl, Fe(OH)$_2$, AlF$_2$O, MnCl$_2$, MgCl$_2$, CaCl$_2$, SiF$_4$, and TiF$_3$ are effectively buffered at LG/R ratios below 1.0, and all but CuCl are buffered at LG/R below 2.4.

Since the mineral assemblage at a LG/R ratio of ≤ 1.0 is the effective magma buffer, the changes that occur to this assemblage at higher G/R ratios reflect various stages of gas-phase alteration of the wall rock that potentially occurs in high-temperature fractures or fumaroles through which volcanic gases flow. Gas alteration of rock proceeds from left to right in figure 3. In a fumarole, the most altered rock forms the vent walls, and the degree of alteration decreases away from the vent. Therefore, the alteration assemblages closest to the vent would form at higher G/R ratios than ones farther from the vent.

Calculated versus observed mineral assemblage.—We evaluate the gas-rock titrations by comparing the computed mineral assemblage with that

observed in the Mount St. Helens lavas. The final equilibrium mineral assemblage (LG/R ratio of ≤ 1.0) consists of beta-tridymite, andesine, ferrohypersthene, salite, ilmenite, and chalcocite. This agrees well with the observed mineral assemblage in the dome lavas erupted from Mount St. Helens in the 1980's, which consists of andesine to labradorite plagioclase, hypersthene, hornblende, magnetite, ilmenite, augite, and Fe–Cu sulfides. There are, however, three major differences: (1) the dome lavas are 40 to 45 percent crystalline, including microphenocrysts in the groundmass (Cashman and Taggart, 1983), whereas the calculated mineral assemblage is 100 percent crystalline; (2) the calculated mineral assemblage contains beta-tridymite, which is not present in the dome lavas; and (3) the dome lavas contain hornblende and magnetite, which are not in the computed mineral assemblage. Incomplete crystallization of the dome lavas is the result of their rapid cooling, a departure from the equilibrium assumption of our model. Furthermore, our data base does not provide for silicate liquids, so they cannot possibly form in our model. Nonetheless, the overall agreement of the computed mineral assemblage with the phenocrysts observed in the lavas suggests that the calculated mineral buffers are a reasonable approximation of the actual buffers in the magma. The lack of beta-tridymite in the dome lavas is a departure from the computed mineral assemblages, possibly a consequence of the rapid cooling of the dome lavas, since the SiO_2 polymorphs are among the last phases to crystallize from an igneous melt. In contrast, the absence of magnetite may result from our incomplete solid-solution model of magnetite, which would be more likely to precipitate if our mixing model incorporated Al, Mg, and Mn, minor elements in the Mount St. Helens magnetites (Melson and Hopson, 1981). We expect the absence of hornblende in the computed mineral assemblage, since hornblende has not been added to our thermochemical data base.

The overall agreement between the computed and observed magmatic mineral assemblages lends credence to the model's calculations and the computed volatilities (below). It also provides evidence that the thermochemical data used in the above calculations are generally of sufficient quantity and quality, which lends confidence to the computed gas species.

Gas-rock titration at 930°C and 100 atm.—To study the effect of a pressure increase on the gas/rock titrations, we repeated the above calculations at 930°C and 100 atm. We used the same assumptions as outlined above, except that we recalculated fugacities of the major gases and fO_2 at 930°C and 100 atm. The final equilibrium mineral assemblage (LG/R ratio of ≤ 1.0) is virtually identical to the 930°C and 1 atm case. However, the quantity of orthoferrosilite (the site for Fe^{II}) decreases, and the quantity of hematite (the site for Fe^{III}) increases, reflecting the higher fO_2 (-10.99) at 100 atm. Although the mole fractions of $CaCl_2$, $Fe(OH)_2$, $Mg(OH)_2$, and $MnCl_2$ do not change with the pressure increase, higher pressure causes the mole fractions of $CuCl$, KCl, and $NaCl$ to decrease, whereas the mole fractions of AlF_2O, SiF_4, and TiF_3 increase. Such trends

are the result of entropy effects wherein higher pressures favor the reactant or product side of reactions, depending on which has fewer moles of gas; neither side is favored if both have the same number of moles of gas. For instance, the reaction:

$$\underset{\text{(beta-tridymite)}}{SiO_2} + 4HF \rightarrow SiF_4 + 2H_2O, \qquad (9)$$
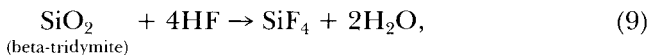
is driven to the right by a pressure increase because the product side of the reaction has fewer moles of gas. (The arrow in reaction 9 and in many of the following reactions indicates a process driven by change in pressure, temperature, or composition. An equal sign is used for equilibria at constant pressure, temperature, and composition.)

Gas-rock titration at 710°C and 1 atm.—To test whether trace elements could be volatilized from fumarole wall rock, we also repeated the volatility calculations at 710°C (the last equilibrium temperature of the September 1981 gas analysis) and 1 atm We used the same assumptions as for the 930°C and 1 atm case, except that we fixed the major-gas fugacities and fO_2 at 710°C and 1 atm (table 2). The major differences in the final equilibrium mineral assemblage (LG/R ratio of ≤ 3.0), as compared with the 930°C and 1 atm case, are that beta-quartz and bornite replace beta-tridymite and chalcocite, respectively. The concentrations of trace element species (AlF_2O, $CaCl_2$, $CuCl$, $Fe(OH)_2$, KCl, $Mg(OH)_2$, $MnCl_2$, $NaCl$, TiF_3) are generally 1 to 2 orders of magnitude lower than the 930°C and 1 atm case, reflecting the temperature decrease. One exception is SiF_4, which is an order of magnitude more abundant at 710°C than at 930°C; this is due to the retrograde volatility of SiF_4 (Symonds, Reed, and Rose, 1992).

Calculated versus observed trace element concentrations.—One way to test whether the trace elements in the Mount St. Helens volcanic gas are volatilized from magma or wall rock is to compare their computed volatilities with their observed concentrations. Elements whose volatilities equal their observed concentrations in the volcanic gas or exceed them ("excess volatility" condition, below) are more likely to be volatilized from magma or wall rock than elements whose volatilities are far less than their abundance in gas samples. An excess volatility may also indicate that a portion of that element precipitated en route to the surface or that the computed (or assumed) activity of the buffering mineral(s) is too high. On the other hand, trace elements with deficient volatilities compared to the gas samples may be contaminants in the samples, or the volatilities may be low because of missing gas species in the thermochemical data base.

As mentioned above, the trace elements may be volatilized from shallow magma, deep magma, or from altered wall rock in the fumarole. To test whether trace elements come from shallow magma, we compare the observed concentrations of trace elements to the calculated volatilities at 930°C, 1 atm, and at a LG/R ratio of -2.0 (table 7). We use a LG/R ratio of -2.0 to approximate the relatively low volatile content of the magma, although the same volatilities are calculated (table 7) at a LG/R

TABLE 7

Calculated volatilities of trace elements in the September 1981 Mount St. Helens volcanic gas using gas-rock titrations. Concentrations are given in mole percent

	Calculated	Calculated	Calculated	Calculated	Observed (raw data)
T°C	710	930	930	930	710
P (atm)	1.0	1.0	1.0	100.	1.0
fo_2	−15.77	−11.39	−11.39	−10.99	−15.77
G/R	1000.	1.0	0.01	0.01	?
LG/R	3.0	0.0	−2.0	−2.0	?
Na	6.9×10^{-6}	2.0×10^{-4}	2.0×10^{-4}	2.1×10^{-5}	4.1×10^{-4}
Cu	2.2×10^{-7}	8.7×10^{-5}	8.7×10^{-5}	2.5×10^{-6}	1.5×10^{-6}
K	2.3×10^{-6}	7.1×10^{-5}	7.1×10^{-5}	7.1×10^{-6}	1.8×10^{-4}
Fe	7.5×10^{-7}	2.2×10^{-5}	2.2×10^{-5}	2.2×10^{-5}	6.4×10^{-6}
Mn	2.8×10^{-9}	1.6×10^{-8}	1.6×10^{-8}	1.6×10^{-8}	1.0×10^{-7}
Al	1.4×10^{-9}	2.9×10^{-8}	2.9×10^{-8}	3.6×10^{-8}	1.6×10^{-4}
Mg	1.1×10^{-11}	2.2×10^{-9}	2.2×10^{-9}	2.3×10^{-9}	---
Ca	1.1×10^{-12}	1.3×10^{-10}	1.3×10^{-10}	1.3×10^{-10}	4.9×10^{-7}
Si	3.7×10^{-12}	5.9×10^{-13}	5.9×10^{-13}	3.5×10^{-11}	---
Ti	1.7×10^{-14}	1.3×10^{-13}	1.3×10^{-13}	9.9×10^{-13}	---

G/R = gas/rock ratio; LG/R = log gas/rock ratio; --- = not determined

ratio of 0.0, since the same mineral assemblage buffers the gas. Then we compare the observed trace element concentrations with the calculated volatilities at 930°C, 100 atm, and at a LG/R ratio of −2.0 to see if trace elements are volatilized from deeper magma (table 7). Finally, we compare the actual concentrations of trace elements with the calculated volatilities at 710°C, 1 atm, and at a LG/R ratio of 3.0 to test whether trace elements are volatilized from altered wall rock in the vent (table 7). Figure 4 shows that the computed volatilities at 930°C, 1 atm, and at a LG/R ratio of −2.0 provide the best overall agreement between the calculated and observed concentrations of trace elements. Thus, the trace elements in the September 1981 gases are more likely to be volatilized from shallow magma than from deep magma or altered wall rock.

Table 7 shows a detailed comparison of the observed trace element concentrations and the calculated volatilities at 930°C, 1 atm, and at a LG/R ratio of −2.0. The volatilities of Cu and Fe exceed their observed concentrations, suggesting that: (1) Cu and Fe come entirely from degassing magma, (2) using pure chalcocite to model the Fe–Cu sulfides in the magma causes the Cu volatilities to be too high, (3) subsurface precipitation of magnetite may remove some Fe from the gas before it reaches the fumarole, and (4) the magmatic gases might be diluted by hydrothermal vapor as suggested by Gerlach and Casadevall (1986b). The computed volatilities of Na, K, and Mn are deficient; volatilization from magma accounts for 50 percent of the Na, 39 percent of the K, and 16 percent of the Mn; the rest probably comes from wall rock erosion.
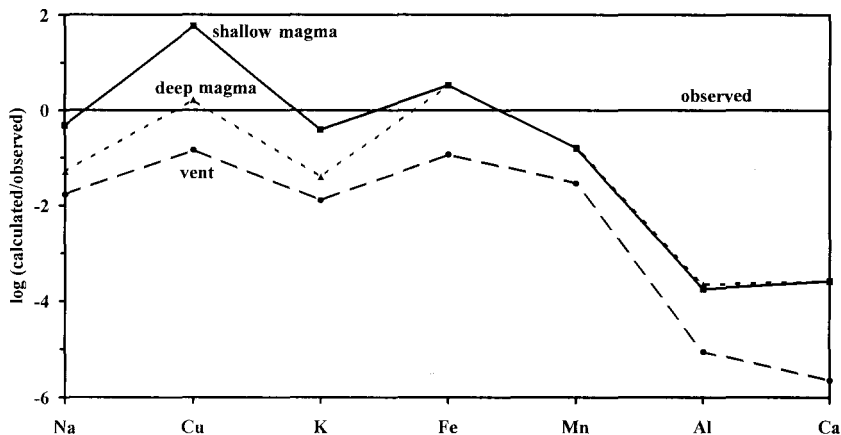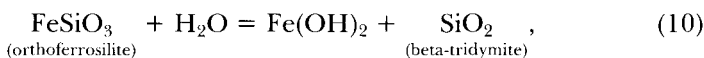
Fig. 4. Plot of calculated versus observed concentrations of Na, Cu, K, Fe, Mn, Al, and Ca in the Mount St. Helens volcanic gas. Calculated cases are for volatilization from deep magma (930°C, 100 atm, LG/R = −2.0), shallow magma (930°C, 1 atm, LG/R = −2.0), and from hot wall rock (710°C, 1 atm, LG/R = 3.0). All data are from table 7.

However, the computed volatilities of Al and Ca are over three orders of magnitude smaller than their observed concentrations, suggesting that they probably come entirely from wall rock erosion (see below).

   Comparison of the computed volatilities with trace element contents of the gas suggests that all of the Cu and Fe and some of the Na, K, and Mn probably volatilized from shallow magma at about 930°C. Furthermore, comparison between the computed mineral assemblage and that observed in the dome lavas allows speculation on which phases buffer the concentrations of these trace elements. Using the above criteria, we propose that the following magma-gas equilibria buffer the concentrations of gaseous Fe, Mn, Na, K, and Cu:

$$FeSiO_3 + H_2O = Fe(OH)_2 + SiO_2 \quad , \qquad (10)$$
$$\text{(orthoferrosilite)} \qquad\qquad \text{(beta-tridymite)}$$

$$MnSiO_3 + 2HCl = MnCl_2 + H_2O + SiO_2 \quad , \qquad (11)$$
$$\text{(rhodonite)} \qquad\qquad\qquad \text{(beta-tridymite)}$$

$$2NaAlSi_3O_8 + 2HCL + CaMgSi_2O_6$$
$$\text{(albite)} \qquad\qquad \text{(diopside)}$$
$$= MgSiO_3 + H_2O + CaAl_2Si_2O_8 + 2NaCl + 5SiO_2 \quad , \quad (12)$$
$$\text{(orthoenstatite)} \qquad \text{(anorthite)} \qquad\qquad \text{(beta-tridymite)}$$

$$2KAlSi_3O_8 + 2HCL + CaMgSi_2O_6$$
$$\text{(sanidine)} \qquad\qquad \text{(diopside)}$$
$$= MgSiO_3 + H_2O + CaAl_2Si_2O_8 + 2KCl + 5SiO_2 \quad , \quad (13)$$
$$\text{(orthoenstatite)} \qquad \text{(anorthite)} \qquad\qquad \text{(beta-tridymite)}$$

$$Cu_2S + 2HCl = 2CuCl + H_2S, \qquad (14)$$
$$\text{(chalcocite)}$$

We write these reactions using the dominant gases and minerals as calculated by GASWORKS (fig. 3). Orthoferrosilite, orthoenstatite, and rhodonite are the Fe, Mg, and Mn components of ferrohypersthene; albite, anorthite, and sanidine are the Na, Ca, and K components of andesine; and diopside is the Ca–Mg endmember in salite. Chalcocite approximates the Cu component of the Fe–Cu sulfides in the magma.

The anomalous condensate concentrations of Al and Ca could mean that they came from some other source or that the model's predictions are incorrect. We suggest that Al and Ca are contaminants in the condensates from wall rock erosion because (1) Bernard (ms), Bernard and Le Guern (1986), and Graeber, Gerlach, and Hlava (1982) did not find any Al- or Ca-bearing sublimates at Mount St. Helens, suggesting a dearth of volatile Al and Ca in the gas phase; (2) the volcanic aerosols (table 5) and silica-tube sublimates (table 3) contain silicate rock fragments; (3) GASTHERM includes 33 gas species of Al and 31 of Ca including chlorides, fluorides, bromides, hydroxide, elemental, and other gas species (app. 2) so presumably it incorporates the main species; and (4) wall rock erosion is the most plausible source of refractory elements in high-temperature volcanic gases (Symonds, Reed, and Rose, 1992). Of course, if rock aerosols are the source of Al and Ca, they must also supply other rock-forming elements (for example, Na, K, and Mn). However, the erosion component is only noticeable when it exceeds the volatile source.

HETEROGENEOUS EQUILIBRIUM COOLING OF RAW GAS COMPOSITIONS

One of the best ways to check the quality of volcanic gas data and the validity of equilibrium calculations is to cool the analyzed gases numerically and compare the predicted solids to the fumarolic sublimates. If the computations match the observed sublimate sequence, that suggests the analytical (gases, condensates, sublimates) and thermochemical data are of good quality and that the computed equilibria may occur in cooling volcanic gases. On the other hand, poor agreement may indicate complications: (1) problems with the input gas-phase composition due to contaminated condensates, unanalyzed elements, or inadequate collection or analytical procedures; (2) the solids collected with silica tubes or from the walls of fumaroles did not form by simple cooling of volcanic gases but formed instead by more complex reactions involving volcanic gases, atmospheric gases, the silica collection tubes, and/or the wall rock; (3) the model's predictions are incorrect owing to missing gas species or errors in the thermochemical data; or (4) nonequilibrium conditions.

Assumptions and reaction steps.—For heterogeneous equilibrium cooling calculations, GASWORKS needs the following information: (1) the initial gas composition; (2) the starting and stopping temperatures, and the size of the temperature increment between each calculation; (3) whether or not solids (and liquids) fractionate from the bulk composition after each temperature step; and (4) the observed solid solutions in sublimates. The main purpose of the first cooling calculation is to check

the quality of the condensate data by comparing the predicted solids with the observed sublimates so we can revise the gas composition for a more realistic computation (below). Accordingly, we test for unexpected solids, especially those saturating above the magma temperature, and for anomalous saturation temperatures for the observed solids; both conditions suggest that either the input gas-phase concentrations of the respective trace elements are too high or that the model's predictions are incorrect. We use the analyzed September 1981 gas (table 2) as our starting composition. The calculations begin at 1200°C, which is unquestionably hotter than the magma. We repeat them at 10°C decrements to obtain detailed results of the cooling. We only narrate the calculations to 500°C, as the computations at lower temperatures are not significantly different from the revised cooling calculations (below).

We assume that in the natural setting, once sublimates form, they do not back-react significantly with the gas stream, except at very low temperatures where they might come in contact with droplets of sulfuric acid or water. Accordingly, we fractionate solids from the bulk gas after the calculations converge at each temperature step.

Since most volcanic sublimates are compositionally simple, we model them accurately as pure endmember solids with unit activity. However, some sublimates contain significant amounts of minor elements, and it is more realistic to model them as solid solutions. In the Mount St. Helens sublimates, feberite contains minor amounts of Mn, and greenockite has minor amounts of Zn (table 3), so we assume ideal mixing exists between $FeWO_4(s)$ and $MnWO_4(s)$ and between greenockite and the isostructural ZnS solid, wurtzite. We do not include other observed solid solutions (table 3) in our model, either because we do not know the gas-phase concentrations of the respective trace elements (Re and Sn), or because those solid solutions (CuS and FeS in greenockite, Bi_2S_3 in galena, FeS_2 in molybdenite) are presumably not ideal.

Discrepancies between the calculated and observed sublimate assemblages.— Figure 5 shows the calculated results for cooling of the analyzed September 1981 gas composition from 1200° to 500°C. We only show the results for Na, K, Al, Sr, Fe, Ca, Cr, V, Mn, W, and Ir because, as demonstrated below, the predicted solids containing these elements are not in perfect agreement with the observed sublimate sequence. Furthermore, the results for additional elements are not significantly different from the revised cooling calculations that we show below.

The first apparent problem with the modeling is that corundum (Al_2O_3), $Cr_2O_3(s)$, $Ir(s)$, and $V_2O_3(s)$ start to precipitate between 1200° and 1100°C, 170° to 270°C hotter than the magma. If these elements actually degassed from magma, they should exist as gases, not solids, above the magma temperature. Other inconsistencies include: (A) halite and sylvite start to precipitate at 610° and 580°C, respectively, 50° to 60°C hotter than where they are first observed in the silica tubes; (B) the predicted Mn-bearing ferberite contains 37 to 72 mole percent $MnWO_4(s)$, at least an order of magnitude more than actually observed by Bernard
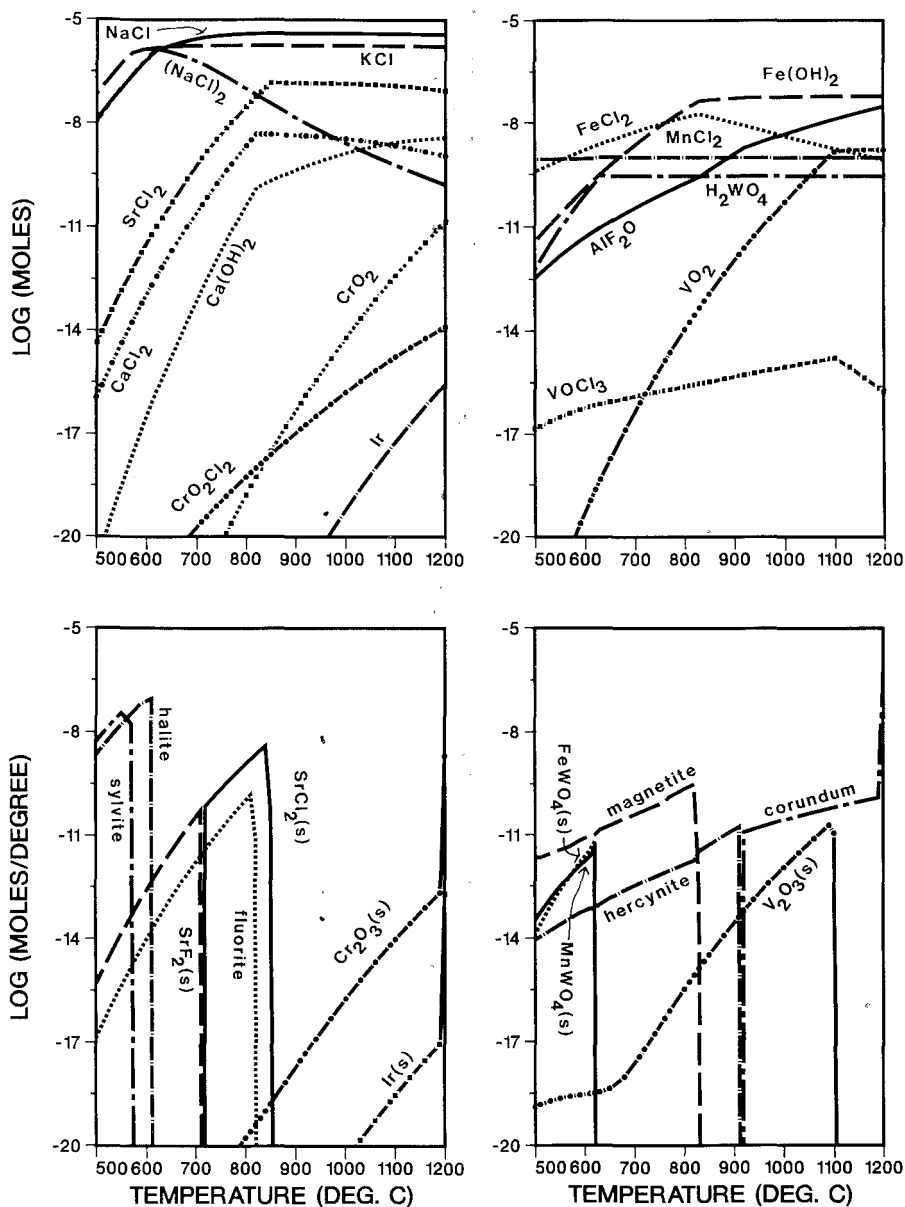
Fig. 5. Cooling of the Mount St. Helens volcanic gas from 1200° to 500°C with fractionation of solids and without any modification of the analyzed gas composition (table 2). We show the computed solids (lower) and most abundant gas species (upper) for Na, K, Al, Sr, Fe, Ca, Cr, V, Mn, W, and Ir. Gas species are plotted as log (moles) per 1 mole of gas initially introduced. Rate of mineral precipitation is moles per degree of temperature changes, per 1 mole of gas initially introduced.

(ms); and (C) the model predicts large amounts of $SrCl_2(s)$, fluorite, and $SrF_2(s)$ to precipitate between $850°$ and $610°C$, solids that are not observed in the Mount St. Helens sublimates or incrustations (Graeber, Gerlach, and Hlava, 1982; Bernard, ms; Bernard and Le Guern, 1986; Rose, 1987, unpublished).

Saturation of Al, Cr, Ir, and V solids above the magma temperature suggests that (1) the input gas-phase concentrations of these elements are too high, or (2) the GASTHERM data base may be missing the main gas species of Al, Cr, Ir, and V. Contaminated condensates may also account for the high saturation temperatures for halite and sylvite and the large Mn contents of the computed ferberite, although kinetically retarded reactions could also cause these effects. The inconsistent results related to Sr and Ca solids may arise from contaminated condensates, "missing" gas species, or kinetic effects, but it is also possible that the predicted solids actually formed and precipitated from the gas stream at higher temperatures ($>650°C$) than the collection vents.

As discussed above, we suggest that rock aerosol contamination accounts for all the Al and Ca in the condensates and some of the Na, K, and Mn. Since Cr and V solids are not found in the Mount St. Helens sublimates (table 3), they too may be contaminants, perhaps from wall rock erosion. Alternatively, there may be missing gas species of Cr and V such as oxyacids (for example, H_2CrO_4, Symonds, Reed, and Rose, 1992), which are the main species for related transition metals like Mo and W.

The results for Sr are ambiguous because we exclude Si, for which we lack analytical data, from our model calculations. Si is an abundant trace element in most volcanic condensates (Gemmell, 1987) and removing it from the calculations means that we do not check for supersaturated Sr silicates at magmatic conditions. To clarify the origin of Sr, we added trial amounts of Si to the gas and repeated the cooling calculations. Surprisingly, only small amounts of Si (10^{-12} mole percent) are required to cause $SrSiO_3(s)$ to saturate at the magma temperature of $930°C$; this supports an erosion source for Sr. We discount the possibility of missing the principal Sr gas species because GASTHERM has 12 Sr gas species (app. 2), including the most abundant species (hydroxides, chlorides, fluorides, bromides) for other alkaline earth elements (Ca and Mg).

However, we do not favor an erosion source for Ir but suggest instead that our model is missing the main Ir gas species for two reasons: (1) assuming the Ir content of the Mount St. Helens dacite is no more than 0.3 ppb, typical for basalts (Govindaraju, 1984) whose Ir concentrations are higher than dacites, the Ir/Al wt ratio in the condensate is at least 270 times higher than the same ratio in the lava, suggesting that Ir is volatilized from magma; and (2) our model only includes two gas species of iridium, Ir and IrF_6, making it probable that GASTHERM lacks the dominant gas species and, therefore, that the computed saturation temperature of Ir(s) is too high.

If the input gas-phase concentrations of Al, Ca, Cr, K, Mn, Na, Sr, and V are too high owing to rock-contaminated condensates, and the

data base is missing the main gas species of Ir, how will this affect the ensuing calculations? In the model calculations, corundum, $Cr_2O_3(s)$, fluorite, $MnWO_4(S)$, $SrF_2(s)$, and $V_2O_3(s)$ precipitate from the gas upon cooling by the reactions:

$$2AlF_2O + H_2O + H_2 \rightarrow \underset{(corundum)}{Al_2O_3} + 4HF, \qquad (15)$$

$$2CrO_2 + H_2 \rightarrow Cr_2O_3(s) + H_2O, \qquad (16)$$

$$CaCl_2 + 2HF \rightarrow \underset{(fluorite)}{CaF_2} + 2HCl, \qquad (17)$$

$$MnCl_2 + H_2WO_4 \rightarrow MnWO_4(s) + 2HCl, \qquad (18)$$

$$SrCl_2 + 2HF \rightarrow SrF_2(s) + 2HCl, \qquad (19)$$

$$2VO_2 + H_2 \rightarrow V_2O_3(s) + H_2O. \qquad (20)$$
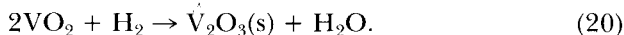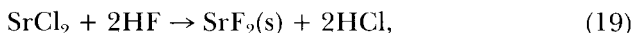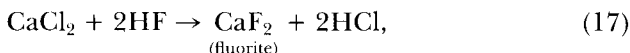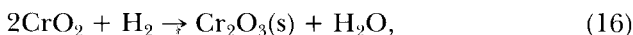
In contrast, halite, sylvite, $SrCl_2(s)$, and $Ir(s)$ crystallize from gas species of the same molecular formula. The main problem with using rock-contaminated condensates is that the predicted solids may be incorrect or their saturation temperatures too high. However, the extent to which these reactions modify the major components is trivial, because the concentrations of the relevant trace elements are several orders of magnitude smaller than HF, the least abundant major gas.

The above discussion illustrates how using rock-contaminated condensates will distort the cooling calculations. The modeling also produces spurious results if we exclude some elements, such as Si, from the calculations. We recommend repeating the modeling after correcting for such problems, especially if there are significant contaminants or critical unanalyzed elements.

HETEROGENEOUS EQUILIBRIUM COOLING OF REVISED GAS COMPOSITIONS

As demonstrated above, using the unmodified gas analysis for cooling calculations has problems: (1) some predicted solids may be distorted if the gas composition includes rock-aerosol contaminants; (2) excluding key elements, such as Si, from the cooling calculations may cause erroneous solids to precipitate; and (3) if we exclude the main gas species for an element, any solid containing that element will have an anomalously high saturation temperature. For the Mount St. Helens case, these inaccuracies affect significantly the outcome for only the specific trace elements involved; the resulting errors (from rock aerosol contamination) in computing the mass balances of major components are negligible. Nonetheless, it is worthwhile to correct for such flaws to improve our numerical simulation of the cooling process. An accurate model of cooling can help identify reactions in volcanic gases and provide insight on the origin of volcanic sublimates.

Assumptions and reaction steps.—We use the same assumptions as for the unrevised cooling calculations (above) with the following modifica=

tions: (1) we correct the input gas composition for rock contamination, unanalyzed components, and elements with inadequate thermochemical data; (2) we start at the magma temperature of 930°C; and (3) we stop at 110°C to compute low-temperature equilibria with the revised input gas. The unrevised cooling calculations (above) demonstrate that the input gas-phase concentrations of Al, Ca, Cr, K, Mn, Na, Sr, and V are too high, probably due to rock-contaminated condensates. Therefore, we use the computed magmatic (930°C, 1 atm, LG/R = −2.0) volatilities (table 7) to approximate the contents of Al, Ca, K, Mn, and Na in the gas escaping from the Mount St. Helens magma. Because the measured Fe content might be too low due to subsurface precipitation of magnetite (see above), we use the slightly higher magmatic volatility of Fe (table 7) for its input concentration. To compensate partly for unanalyzed components, we add Mg and Si to the gas using their respective magmatic volatilities (table 7). We exclude Cr, Sr, and V from the subsequent calculations, as we have no independent way to estimate their lower, gas-phase concentrations. We also omit Ir because our data base probably lacks the main Ir gas species (above).

As suggested by T. Gerlach, we also try correcting for rock-contaminated condensates by subtracting rock from the gas until the problems with Al, Ca, K, Na, and Mn go away. We accomplish this by removing all the Al, the most abundant rock contaminant, from the gas; Ca, K, Na, and Mn are removed in proportion to their whole rock abundances relative to Al (table 6). This removes from the gas 100 percent of the Al, 200 percent of the Mn, and 8600 percent of the Ca. It also eliminates 6 and 15 percent of the K and Na, respectively. These results are consistent with the relatively low volatilities of Al, Ca, K, Na, and Mn as compared to their observed concentrations (table 7) and suggest that rock subtraction is a tolerable way to correct for wall rock contaminants, although the corrections yield unsatisfactory results for Ca. The discrepancy in the Ca correction suggests that the condensate dissolved particles with a much lower Ca/Al ratio than the fresh dacite (for example, altered rock) or that the Ca content of the condensate was grossly underestimated. We do not discuss the cooling of the rock-subtracted gas as it is not significantly different from the results below, except that Al, Ca, and Mn are absent, and halite and sylvite precipitate at a slightly higher temperature.

Evolution of the cooling gas.—For the modified cooling calculations, we include all possible gas species for the 32 component system (app. 2), a total of 478 gases. Equilibrating with these gases are 33 solids, including silicates, oxides, halides, sulfides, tungstates, tellurides, and native elements; these were selected by the program, using a saturation index procedure (app 1) from 300 possible solids and liquids for this 32 component system (app. 2). Figures 6 to 10 show the distribution of the most abundant gas species for each component included in these calculations. Figure 11 shows the precipitation rates (with respect to tempera-
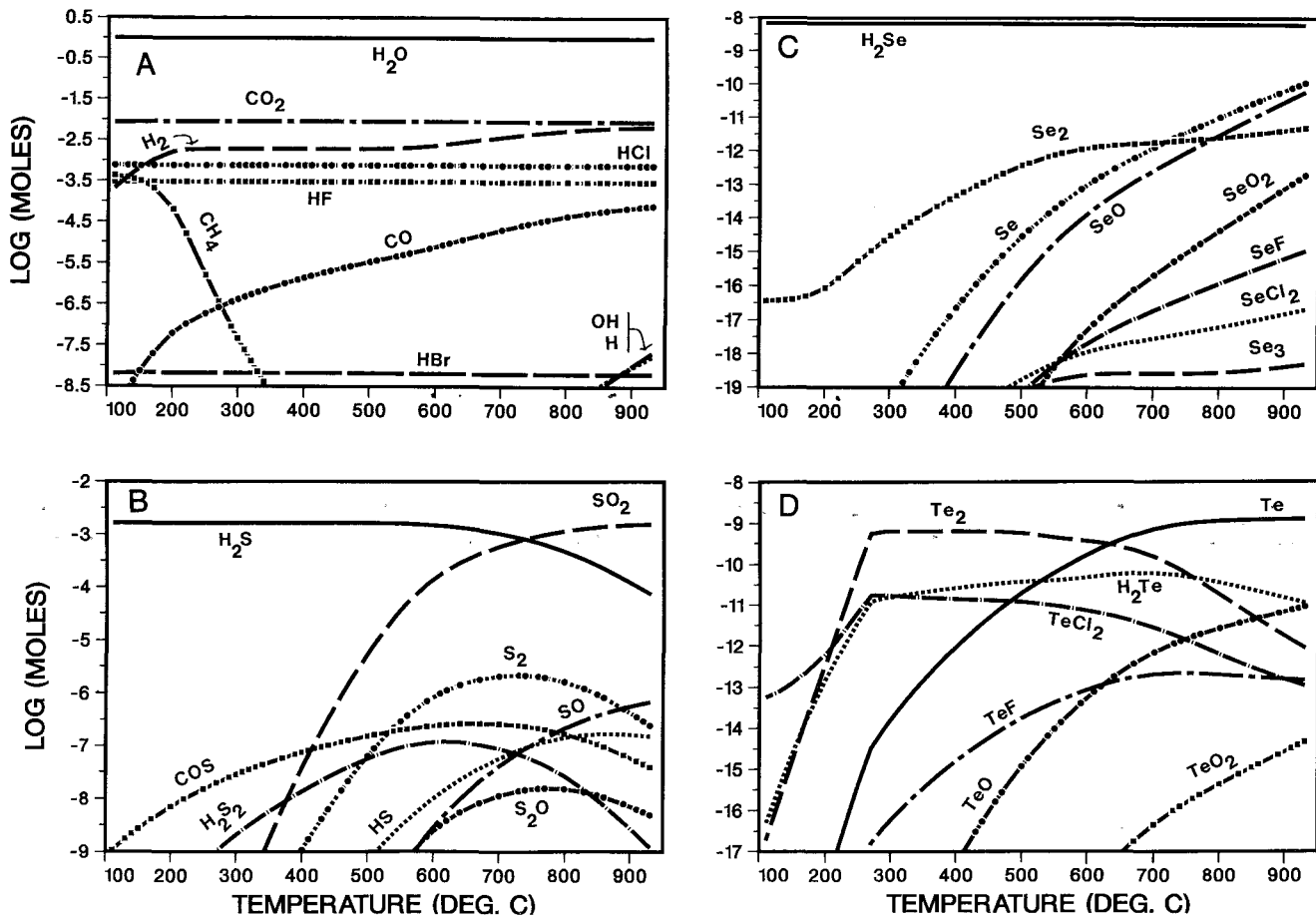
Fig. 6. Most abundant gas species of (A), H, C, and O; (B) S; (C) Se; and (D) Te for cooling of a modified Mount St. Helens volcanic gas. Calculations were performed from 930° to 110° at 10°C decrements, using the analyzed gas composition with modifications (see text). Supersaturated solids were fractionated from the bulk gas after each temperature step. Gas species are plotted as log (moles) per 1 mole of gas initially introduced (at 930°C).
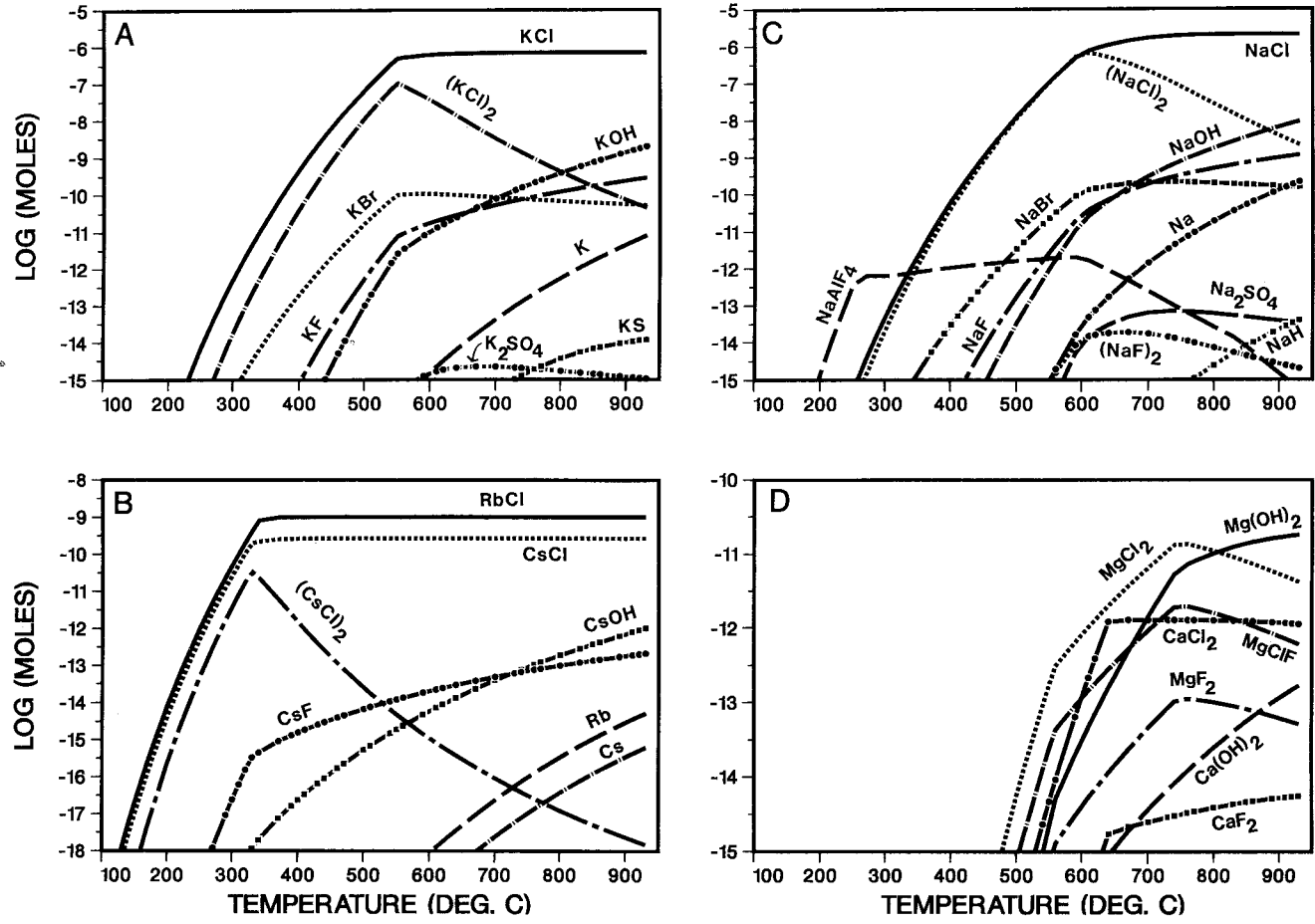
Fig. 7. Most abundant gas species of (A) K; (B) Rb and Cs; (C) Na; and (D) Mg and Ca for cooling of a modified Mount St. Helens volcanic gas. See caption for figure 6.
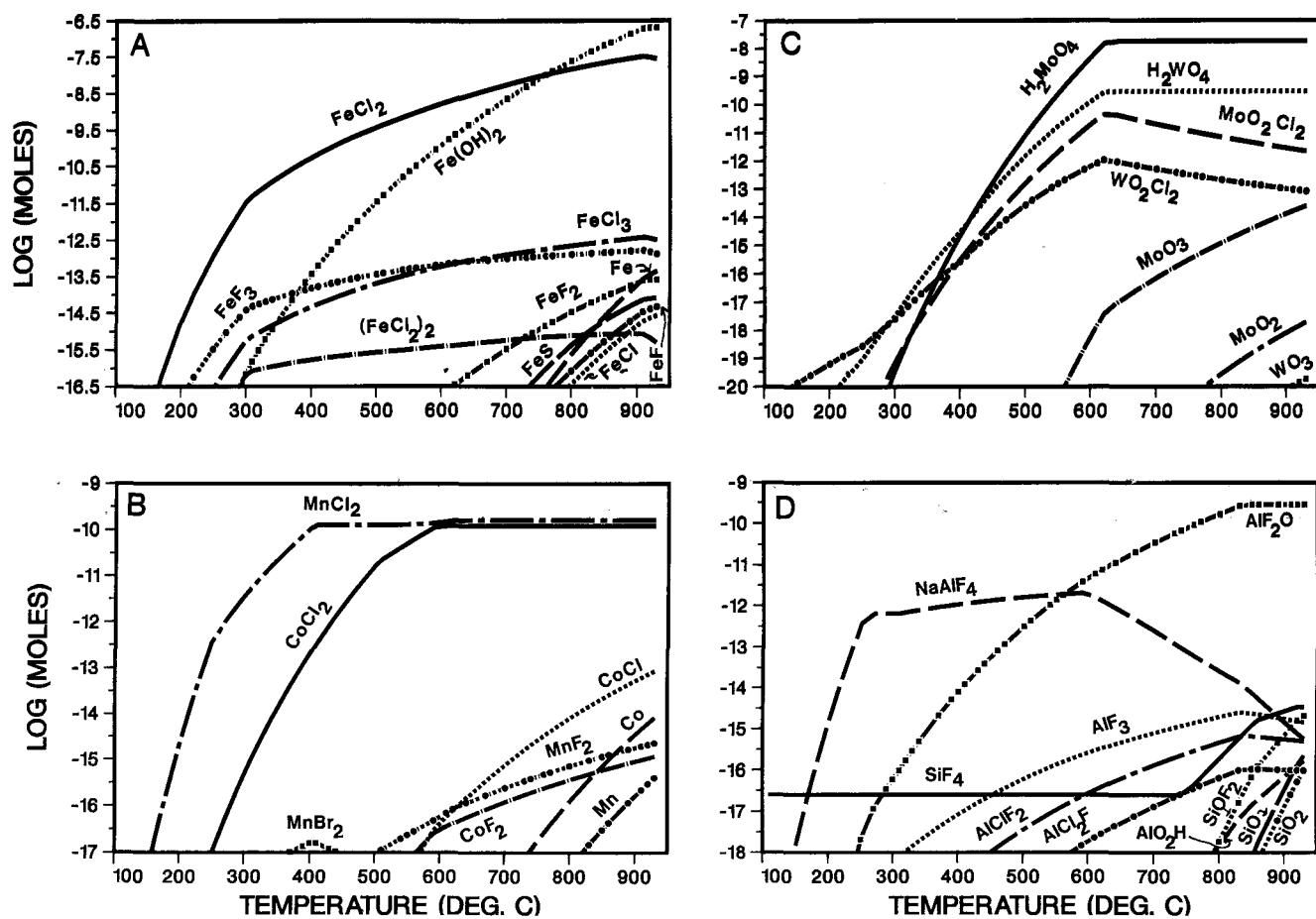
Fig. 8. Most abundant gas species of (A) Fe; (B) Mn and Co; (C) Mo and W; and (D) Al and Si for cooling of a modified Mount St. Helens volcanic gas. See caption for figure 6.
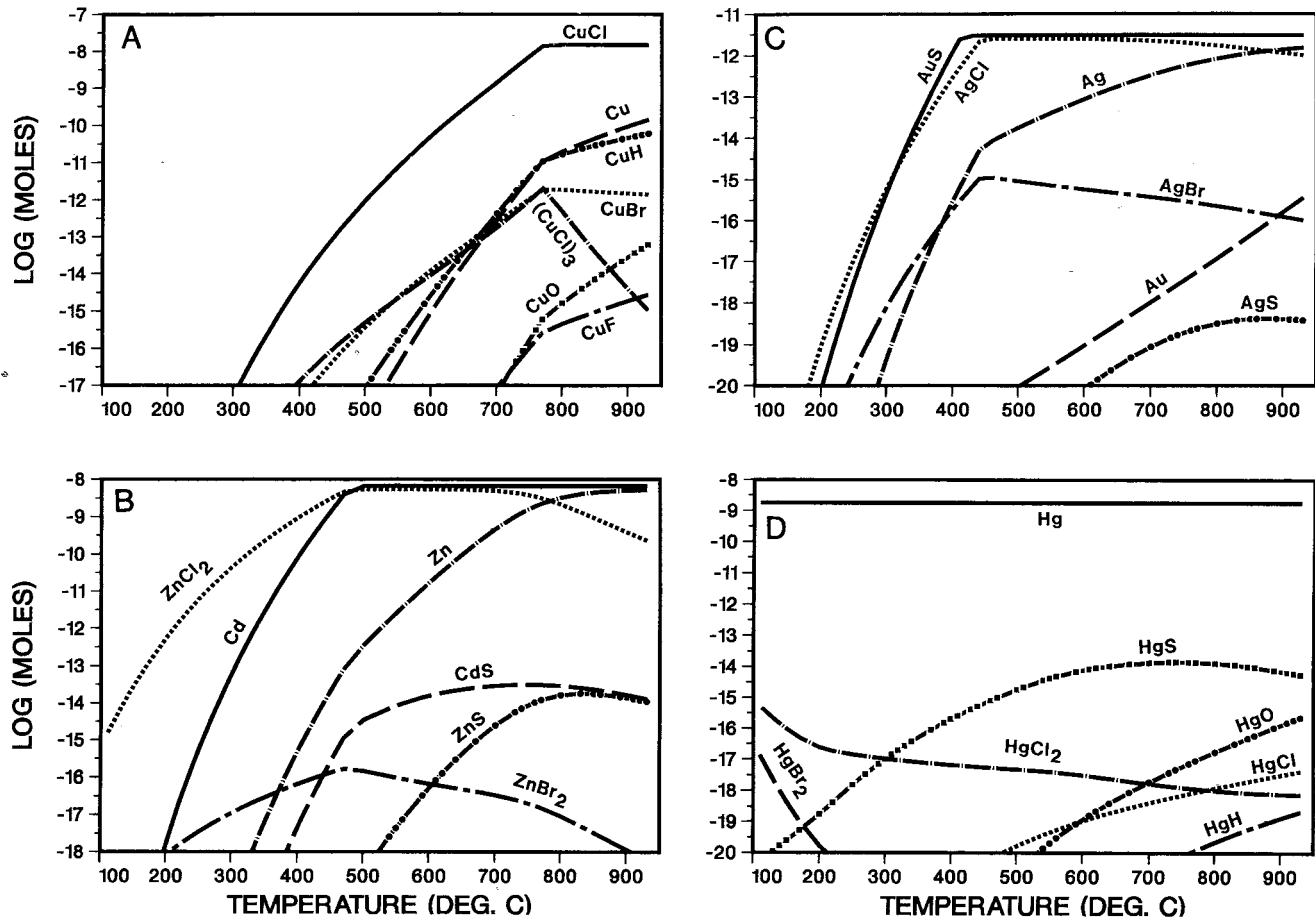
Fig. 9. Most abundant gas species of (A) Cu; (B) Zn and Cd; (C) Au and Ag; and (D) Hg for cooling of a modified Mount St. Helens volcanic gas. See caption for figure 6.
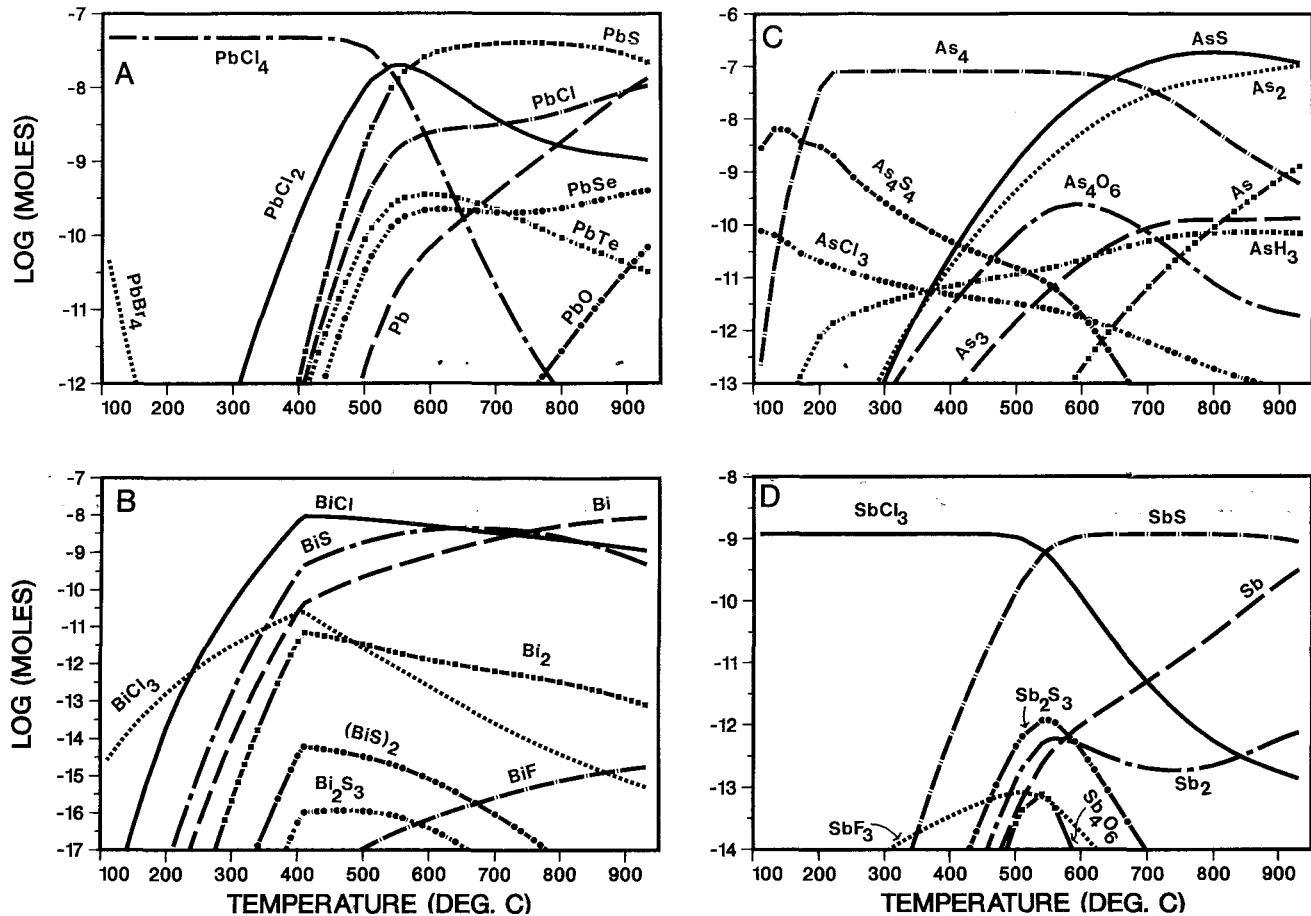
Fig. 10.   Most abundant gas species of (A) Pb; (B) Bi; (C) As; and (D) Sb for cooling of a modified Mount St. Helens volcanic gas. See caption for figure 6.
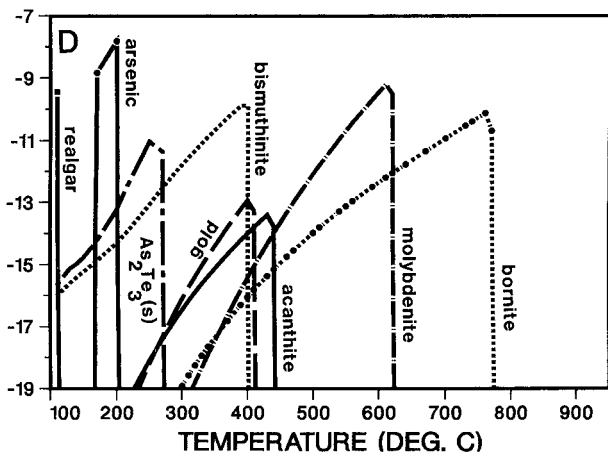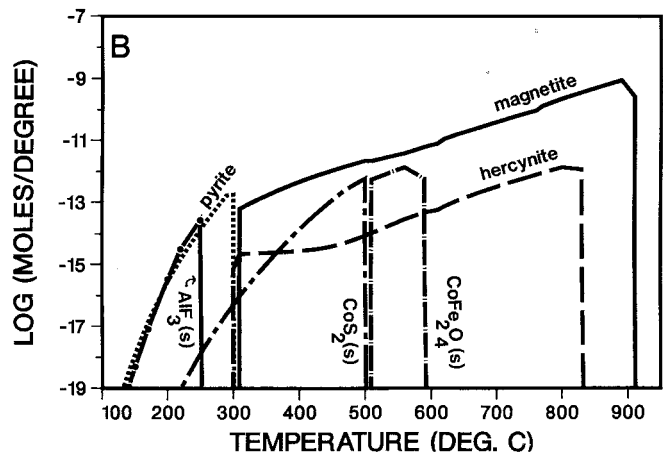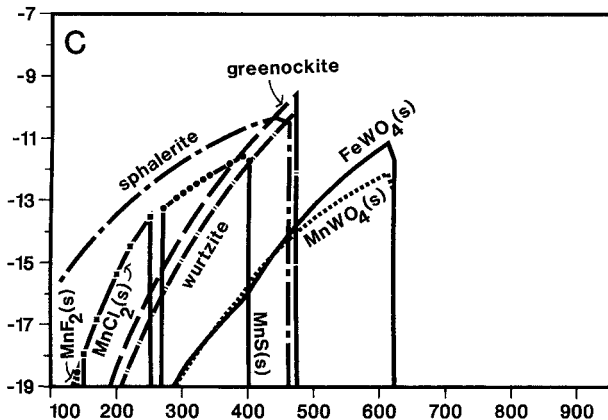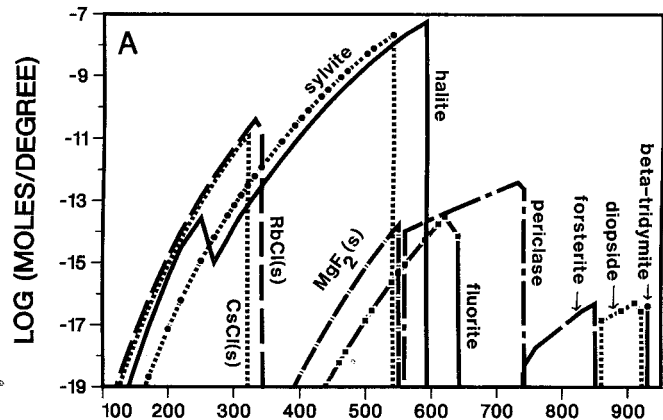
Fig. 11. Precipitation rates for solids of (A) Ca, Cs, K, Mg, Na, Rb, and Si; (B) Al, Co, and Fe; (C) Cd, Mn, W, and Zn; and (D) Ag, As, Au, Bi, Cu, Mo, and Te for cooling of a modified Mount St. Helens volcanic gas. Rate of precipitation is moles per degree of temperature change, per 1 mole of gas initially introduced. See caption for figure 6.

ture change) for the supersaturated solids, which fractionate from the gas in each 10°C temperature step.

Figure 6A-B shows gases in the H–O–C–S–Cl–F–Br system. At the magma temperature of 930°C, H_2O, CO_2, SO_2, HCl, HF, and HBr are the main species of H, O, C, S, Cl, F, and Br, while H_2, H_2S, and CO are abundant minor species. With falling temperatures, H_2S replaces SO_2 as the main sulfur species, the abundances of CO and H_2 decrease, and, below 300°C, CH_4 becomes a significant minor species of carbon. These cooling trends are caused by entropy effects, whereby lower temperatures favor fewer moles of gas on the product sides of the following reactions with negative $\Delta_r S'$s:

$$SO_2 + 3H_2 \rightarrow H_2S + 2H_2O, \tag{21}$$

$$CO + 3H_2 \rightarrow H_2O + CH_4. \tag{22}$$
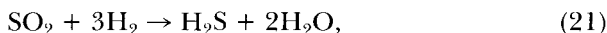
The speciation of other sulfur group elements, Se and Te, are shown in figures 6C and D, respectively. In contrast to sulfur (fig. 6B), selenium and tellurium are not transported as dioxides but as H_2Se and Te, respectively, at 930°C and 1 atm. At lower temperatures, however, the main gases of sulfur and selenium, H_2S and H_2Se, are chemically similar but tellurium is different; Te_2 replaces Te 610°C and $TeCl_2$ supersedes Te_2 at 200°C. Below 270°C, tellurium is removed from the gas by precipitation of $As_2Te_3(s)$ (fig. 11D), principally by the reaction:

$$1/2As_4 + 3/2Te_2 \rightarrow As_2Te_3(s). \tag{23}$$

At 930°C, the alkali metals are transported predominantly as monomeric chlorides, NaCl, KCl, RbCl, and CsCl (fig. 7A-C). The principal secondary species include hydroxides (NaOH, KOH, CsOH), fluorides (NaF, KF, CsF), dimeric chlorides ($(NaCl)_2$, $(KCl)_2$, $(CsCl)_2$), bromides (NaBr, KBr), and elemental species (Na, K, Rb, Cs). With cooling, the mole fractions of most minor species decrease, but dimers, $(NaCl)_2$, $(KCl)_2$, and $(CsCl)_2$, increase, sometimes enough to become the dominant species, as in the case of $(NaCl)_2$ between 590° and 560°C. Dimers replace monomers upon cooling because decreasing temperature favors the low-entropy sides of reactions such as the following:

$$2NaCl \rightarrow (NaCl)_2. \tag{24}$$
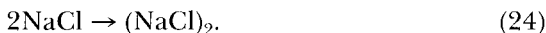
Cooling also favors the mixed-cation halide, $NaAlF_4$; it becomes the dominant Na gas at 330°C, again due to entropy effects.

The bulk gas concentrations of Na, K, Rb, and Cs decrease at lower temperatures (fig. 7A-C) as halite (NaCl), sylvite (KCl), RbCl(s), and CsCl(s) start to precipitate at 590°, 540°, 340°, and 320°C, respectively (fig. 11A). These alkali metal chlorides precipitate quantitatively from the gas by reactions such as:

$$KCl \rightarrow \underset{\text{(sylvite)}}{KCl}, \tag{25}$$

although halite precipitates from the dimer, $(NaCl)_2$. Halite, sylvite, RbCl(s), and CsCl(s) precipitate in order of increasing atomic number (fig. 11A); this is apparently a consequence of weaker ionic bonds in the solids with increasing atomic radius, a trend that causes the vapor pressures of alkali metal chlorides to rise with atomic number.

$Mg(OH)_2$ and $CaCl_2$ are the most abundant species of alkaline earth elements, Mg and Ca, at 930°C, but other significant species include $MgCl_2$, $MgClF$, $Ca(OH)_2$, MgF_2, and CaF_2 (fig. 7D). Upon cooling, $MgCl_2$ increases and supersedes $Mg(OH)_2$ as the dominant Mg species, but the abundances of other secondary Mg and Ca gases decline. Cooling also triggers the precipitation of Mg- and Ca-bearing solids, diopside ($CaMgSi_2O_6$) between 920° and 860°C, forsterite (Mg_2SiO_4) from 850° to 740°C, periclase (MgO) between 740° and 560°C, fluorite (CaF_2) at ≤ 650°C, and MgF_2(s) at ≤ 560°C (fig. 11A). However, only periclase and MgF_2(s) have large enough precipitation rates to extract significant Mg from the gas, specifically by the reactions:

$$MgCl_2 + H_2O \rightarrow \underset{(periclase)}{MgO} + 2HCl, \qquad (26)$$

$$MgCl_2 + 2HF \rightarrow MgF_2(s) + 2HCl. \qquad (27)$$
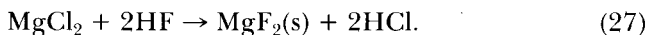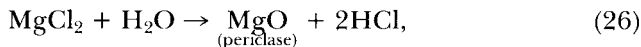
Ca is also removed from the gas mixture during cooling, mostly by the precipitation of fluorite (reaction 17).

Most of the transition metals are transported as simple chlorides. $AgCl$, $CoCl_2$ $CuCl$, $FeCl_2$, $MnCl_2$, and $ZnCl_2$ are the principal gas species of their respective metals, although $Fe(OH)_2$ is more abundant than $FeCl_2$ above 750°C, Zn supersedes $ZnCl_2$ above 780°C, and Ag dominates AgCl above 900°C (figs. 8A-B, 9A-C). Other noteworthy though subordinate species of these six elements include bromides ($AgBr$, $CuBr$, $MnBr_2$, $ZnBr_2$), other chlorides ($FeCl$, $CoCl$, $(CuCl)_3$, $(FeCl_2)_2$, $FeCl_3$), fluorides (CoF_2, CuF, FeF, FeF_2, FeF_3, MnF_2), elemental species (Co, Cu, Fe, Mn), hydrides (CuH), oxides (CuO), and sulfides (AgS, FeS, ZnS).

Transition metals that are not transported as simple chlorides include Au, Cd, Hg, Mo, and W. Of the four species considered for cadmium and gold, Cd prevails over CdS (fig. 9B), and AuS is more abundant than Au (fig. 9C). It is also possible that cadmium and gold are transported as chlorides, and we plan on adding $CdCl_2$ to our data base. Unfortunately, thermochemical data for gold chloride gases are not currently available. Mercury is transported as the elemental gas, which is at least five orders of magnitude more abundant than the main subordinate species, including HgS, $HgCl_2$, HgO, $HgCl$, $HgBr_2$, and HgH (fig. 9B). The group VIB elements, Mo and W, are most stable as oxyacids, H_2MoO_4 and H_2WO_4, at magmatic conditions, but as oxychlorides, MoO_2Cl_2 and WO_2Cl_2, below 320°C (fig. 8C). The only significant secondary species of Mo and W are oxides, MoO_3, MoO_2, and WO_3, and these are only abundant at high temperatures (fig 8C).
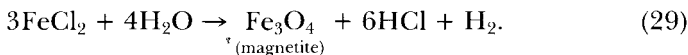
Except for mercury, a highly volatile element, precipitation during cooling removes the transition metals from the gas. Precipitation of
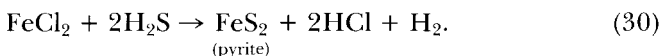
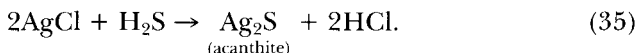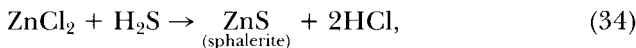magnetite (fig. 11B) removes iron (fig. 8A) from the gas by the following reaction below 910°C:

$$3Fe(OH)_2 \rightarrow \underset{\text{(magnetite)}}{Fe_3O_4} + 2H_2O + H_2, \tag{28}$$

and below 760°C:

$$3FeCl_2 + 4H_2O \rightarrow \underset{\text{(magnetite)}}{Fe_3O_4} + 6HCl + H_2. \tag{29}$$
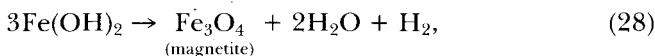
At 300°C, pyrite replaces magnetite and precipitates according to the reaction:

$$FeCl_2 + 2H_2S \rightarrow \underset{\text{(pyrite)}}{FeS_2} + 2HCl + H_2. \tag{30}$$

Similarly, cobalt precipitates as an oxide, $CoFe_2O_4(s)$, between 590° and 510°C, and as a sulfide, $CoS_2(s)$, below 510°C (fig. 11B). Manganese starts precipitating as $MnWO_4(s)$ by reaction (18) but is mostly eliminated from the gas by precipitation of $MnS(s)$ between 400° and 260°C and $MnCl_2(s)$ from 250° to 150°C (fig. 11C). $MnF_2(s)$ forms below 150°C (fig. 11C).

Precipitation of Mn-bearing ferberite (fig. 11C), beginning at 620°C, strips the gas of W (fig. 8C) by reactions such as (18) for $MnWO_4(s)$. In contrast to the unrevised cooling calculations (fig. 5), ferberite (fig. 11C) is richer in Fe, containing 91 mole percent $FeWO_4(s)$ at 620°C, although it contains increasingly more Mn as temperature decreases.

Ag, Cd, Cu, Mo, and Zn all precipitate as sulfides. Bornite (Cu_5FeS_4) starts precipitating at 770°C, molybdenite (MoS_2) begins at 620°C, green-ockite-wurtzite precipitates between 470° and 140°C, sphalerite (ZnS) starts at 460°C, and acanthite (Ag_2S) begins at 440°C (fig. 11C-D). These transition metal sulfides crystallize in the following sequence of reactions:

$$5CuCl + FeCl_2 + 4H_2S \rightarrow \underset{\text{(bornite)}}{Cu_5FeS_4} + 7HCl + 1/2H_2, \tag{31}$$

$$H_2MoO_4 + 2H_2S + H_2 \rightarrow \underset{\text{(molybdenite)}}{MoS_2} + 4H_2O, \tag{32}$$

$$Cd + H_2S \rightarrow \underset{\text{(greenockite)}}{CdS} + H_2, \tag{33}$$

$$ZnCl_2 + H_2S \rightarrow \underset{\text{(sphalerite)}}{ZnS} + 2HCl, \tag{34}$$

$$2AgCl + H_2S \rightarrow \underset{\text{(acanthite)}}{Ag_2S} + 2HCl. \tag{35}$$
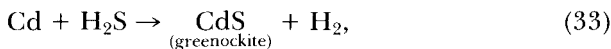
Cd also precipitates as chloride, $CdCl_2(s)$ (not shown in fig. 11C), but only between 130° and 110°C, where little Cd remains in the gas.

Native gold starts precipitating from the gas at 410°C (fig. 11D) by the reaction:

$$AuS + H_2 \rightarrow Au(s) + H_2S. \tag{36}$$

Interestingly, reaction (36) stoichiometrically resembles proposed reactions (Spycher and Reed, 1989) for geothermal-water gold precipitation in that gold deposits by reduction of gold sulfides. However, in geothermal waters, H_2S loss drives the reaction. In volcanic gases, cooling drives the reaction.

In contrast to most trace elements, the refractory elements, Al and Si, have a strong affinity for fluorine (fig. 8D). SiF_4 is the main silicon species from 930° to 110°C. However, it is also possible that Si is transported as H_4SiO_4, a species for which thermochemical data are lacking (Symonds, Reed, and Rose, 1992). Aluminum is dominated by the oxyfluoride, AlF_2O, at high temperatures and the mixed-metal fluoride, $NaAlF_4$, below 560°C. Even the minor species, AlF_3, $AlClF_2$, $AlCl_2F$, $SiOF_2$, AlO_2H, SiO, and SiO_2, are predominantly fluorides. Si is precipitated from the gas between 930° and 730°C, the zone where beta-tridymite, diopside, and forsterite precipitate (fig. 11A). Al is also purged from the gas, but by hercynite between 830° and 290°C and by $AlF_3(s)$ starting at 250°C (fig. 11B).

The group IVA and VA elements, As, Bi, Pb, and Sb, are also unusual in that sulfide and elemental species prevail at magmatic conditions (> 800°C), rather than chlorides (fig. 10A-D). The dominant species of lead are PbS above 560°C, $PbCl_2$ between 560° and 540°, and $PbCl_4$ below 540°C (fig. 10A). Noteworthy secondary Pb species include Pb, PbCl, PbSe, PbO, and PbTe above 540°C and $PbBr_4$ below 150°C. Bismuth is transported as the elemental gas above 740°C, BiS between 740° and 640°C, BiCl between 640° and 230°C, and $BiCl_3$ below 230°C; the most significant secondary species are Bi_2, BiF, $(BiS)_2$, and Bi_2S_3 (fig. 10B). The main species of arsenic are AsS above 640°C, As_4 between 640° and 180°C, and As_4S_4 below 180°C (fig. 10C). Less abundant species of arsenic include As_2, As, As_3, AsH_3, As_4O_6, and $AsCl_3$. Antimony is transported as SbS above 540°C and $SbCl_3$ at ≤ 540°C with the most abundant minor species being Sb, Sb_2, Sb_2S_3, SbF_3, and Sb_4O_6 (fig. 10D). Many of the changes in gas speciation for As, Bi, Pb, and Sb occur because of reactions such as the following:

$$4AsS + 4H_2 \rightarrow As_4 + 4H_2S, \tag{37}$$

$$BiCl + 2HCl \rightarrow BiCl_3 + H_2, \tag{38}$$

$$SbS + 3HCl \rightarrow SbCl_3 + H_2S + 1/2H_2, \tag{39}$$
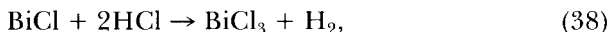
which are apparently driven to the right by entropy effects, as discussed above.

Cooling triggers precipitation of solids containing As and Bi (fig. 11D), but solids of Pb and Sb do not saturate over the entire temperature range. Bismuthinite (Bi_2S_3) starts crystallizing at 400°C according to the reaction:

$$2BiCl + 3H_2S \rightarrow \underset{\text{(bismuthinite)}}{Bi_2S_3} + 2HCl + 2H_2. \tag{40}$$
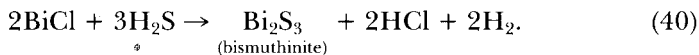
At 270°C, $As_2Te_3(s)$ precipitates by reaction (23). However, most arsenic precipitates as native arsenic, a major phase between 200° and 170°C, as a result of the reaction:

$$1/4As_4 \rightarrow As(s). \qquad (41)$$

The remaining arsenic precipitates as realgar (As_4S_4); it forms from As_4S_4 starting at 110°C.

Overall, the computed mineral assemblage is dominated by magnetite above 620°C, molybdenite and Mn-bearing ferberite between 620° and 590°C, halite and sylvite from 590° to 400°C, bismuthinite between 400° and 340°C, RbCl(s) and CsCl(s) between 340° and 270°C, and various As–S–Te compounds at ≤270°C (fig. 11A-D). The assemblage also includes minor amounts of bornite (≤770°C), Zn-bearing greenockite (≤470°C), sphalerite (≤460°C), pyrite (≤300°C), and $AlF_3(s)$ (≤250°C), and numerous trace solids (fig. 11A-D).

Comparison of predicted solids with observed sublimates, incrustations, and aerosols.—Our model results match both the identity and saturation temperatures of most of Bernard's (Bernard, ms; Bernard and Le Guern, 1986) silica-tube sublimates (fig. 12). Further, it matches the Cd-bearing chloride and FeS_x phases reported by Graeber, Gerlach, and Hlava (1982). The modeling also predicts some unreported minor and trace phases; these may have gone undetected because of the limitations of SEM and XRD, or they may not have formed, perhaps a consequence of
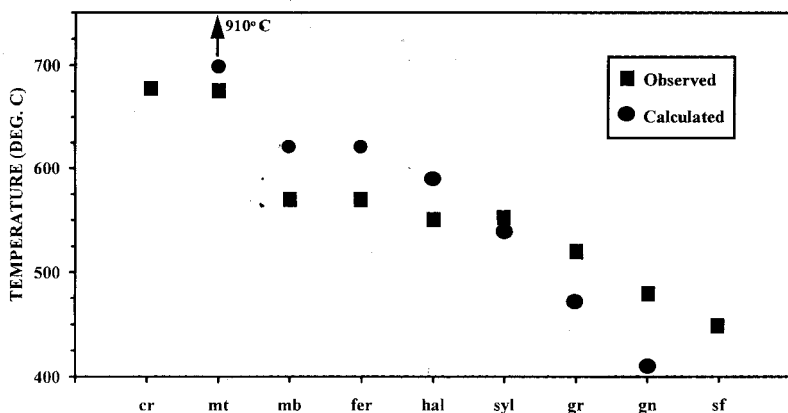
Fig. 12. Comparison of calculated and observed saturation temperatures for sublimates collected (table 3) between 675° and 400°C in silica tubes at Mount St. Helens. The calculated results are the maximum temperatures of precipitation for each phase for the revised cooling case (see text). The plotted deposition temperature for calculated galena is for a calculation with $PbCl_4$ and $PbBr_4$ suppressed; otherwise, galena does not precipitate (see text). Note that calculated magnetite starts precipitating at 910°C. Mineral abbreviations in use here are as follows: cr, cristobalite; mt, magnetite; mb, molybdenite; fer, ferberite; hal, halite; syl, sylvite; gr, greenockite; gn, galena; sf, Pb-Bi sulfosalt ($Pb_3Bi_2S_6$).

kinetically retarded reactions. Our model fails to produce some observed phases, alpha-cristobalite, galena, and Pb-Bi sulfosalt.

In the example chosen, however, it is impossible to test fully the model's predictions below 400°C. Nonetheless, comparison of the model calculations with silica tube studies at other volcanoes suggests that: (1) the precipitation of major amounts of native As between 200° and 170°C is reasonable since native As forms the bulk of the near-200°C sublimates at Momotombo (Quisefit and others, 1989); (2) solids of Rb and Cs may precipitate at lower temperatures than those of Na and K, since that trend is observed at Merapi (Symonds and others, 1987); and (3) we need to incorporate nitrogen-bearing solids (for example, sal ammoniac) in our model since they are often major phases in low-temperature (< 300°C) silica-tube deposits (Bernard, ms). Future studies should do a more complete comparison of the modeling with low-temperature (< 400°C) silica-tube experiments.

The predicted solids also elucidate the origin of many high-temperature chloride and sulfide incrustations (table 4). However, the model does not predict the high-temperature (> 450°C) sulfosalts, galena, Ca-rich powellite, oxides, and sulfates found in the incrustations, nor does it explain the genesis of any observed low-temperature (< 450°C) incrustation phase, except perhaps halite. We discuss these points below.

The volcanic aerosols (table 5) generally differ from the predicted solids. Although the unrevised and revised cooling calculations (figs. 5, 11A-D) support the idea that rock aerosols, halite, and As-S solids exist in the gas stream, they fail to match many of the aerosols, including sulfuric acid, sulfates, and metal oxides.

The overall agreement between the predicted solids and the observed sublimates suggests that the model does a very good job of predicting the identity and saturation temperatures of the sublimates that form in the silica tubes and in the reducing environment of the fumaroles. These results are broadly consistent with the prevalence of equilibrium and lend confidence to the predicted reactions (above), but it is not possible with the data available to check the model's predictions for the amounts of solids formed per unit of gas cooled and the concentrations of trace element gas species. However, recent work by Symonds (1993) uses textural data of silica-tube sublimates from Merapi volcano to evaluate equilibrium conditions in the Merapi tubes. The results show that the sublimates start to form at near-equilibrium conditions, but that the degree of nonequilibrium (supersaturation) increases with decreasing temperature. Thus, silica-tube sublimates may form under quasi-equilibrium conditions where the gas starts precipitating a sublimate phase at its equilibrium saturation temperature but does not maintain equilibrium with the precipitating phase at lower temperatures. This is probably a consequence of the high-velocity carrier gas in the tubes.

The partial match between the predicted solids and the observed incrustations suggests that equilibrium cooling of volcanic gases can also

explain some natural incrustations, especially those crystallizing within hot vents. Like silica-tube precipitates, these natural sublimates may grow under quasi-equilibrium conditions if they form in a roaring vent. However, if they precipitate beneath the surface, especially from a low-velocity carrier gas, they are more likely to form in a state that approaches complete chemical equilibrium. In a silica-tube study at Merapi volcano, Bernard (ms) found that halite and sylvite, which begin precipitating at 630°C, are conspicuously absent or depleted in a silica-tube from a 615°C vent, although these high-temperature phases are prevalent at <400°C in tubes collected from >700°C vents. Bernard's work suggests that subsurface precipitation of sublimates is more efficient than in the silica tubes and is therefore closer to an equilibrium state. Thus, equilibrium thermochemical modeling may be more effective at modeling the natural subsurface precipitation of sublimates than precipitation in the silica tubes.

The model's failure to predict alpha-cristobalite, galena, and sulfosalts in the silica-tube sublimates and galena and sulfosalts in the incrustations can be explained if:

1. The model's predictions are incorrect owing to incorrect or incomplete thermochemical data. As discussed by Symonds and others (1987), the large error (±21 kcal/mole) in $\Delta_f G^0$ values for $PbCl_4$ and $PbBr_4$ is one possible explanation for the lack of galena in the model calculations. Indeed, if one adds 21 kcal/mole to the $\Delta_f G^0$ values of $PbCl_4$ and $PbBr_4$, galena precipitates at 410°C, an excellent agreement with the silica-tube studies. Furthermore, if our model is missing the main gas species of Si, perhaps H_4SiO_4, that might account for the absence of alpha-cristobalite in the computed results (Symonds, Reed, and Rose, 1992). Finally, sulfosalts are not in the computed assemblage because they have not yet been added to our thermochemical data base.

2. There are kinetic effects. Currently our model neglects kinetic effects. Perhaps galena forms instead of gaseous $PbCl_4$ and $PbBr_4$ (fig. 10A) in the fumarole because of kinetic effects. As stated above, if we suppress $PbCl_4$ and $PbBr_4$, galena precipitates.

3. Any of the solids originate from a reaction between the volcanic gas and the silica sampling train. For example, it is possible that cristobalite forms by remobilization of silica from the sampling tube (Symonds, Reed, and Rose, 1992).

However, the absence of several other observed incrustation phases—mostly sulfates and oxides—in the computed assemblage suggests that incrustation formation also includes other chemical processes: (1) mixing of volcanic and atmospheric gases, and (2) reaction between volcanic gases and the wall rock, possibly involving a liquid phase (Stoiber and Rose, 1974; Getahun, Reed, and Symonds, 1992). Mixing of volcanic and atmospheric gases and sulfuric acid-ash reactions are likely origins for the sulfate and oxide aerosols as well (Varekamp and others, 1986). Atmospheric mixing introduces O_2 and N_2, increasing the stability of oxides, sulfates, and nitrogen compounds (for example, sal ammoniac). Reac-

tions with rock or ash might liberate non-volatile cations, such as Al and Ca, that could bond with the sulfate or oxide anions. At high-temperatures, wall rock reactions—for example, as inferred by Bernard and Le Guern (1986) to account for Ca in the natural powellites—may only involve volcanic gas and rock. However, in highly oxidized, <200°C vents, sulfuric acid is stable (Symonds, Reed, and Rose, 1992), consistent with the suggestion of Stoiber and Rose (1974) that incrustations form by acid-rock reactions in low-temperature vents.

ADDITIONAL VOLCANOLOGICAL APPLICATIONS

A complete discussion of the procedures to apply the programs to many other possible geochemical studies of volcanic gases is beyond the scope of this paper. However, it is worthwhile to outline the feasibility of other applications.

Evaluating gas samples.—One of the main uses of SOLVGAS (the homogeneous equilibrium code) is to evaluate equilibrium in samples of the major gases (H_2O, H_2, CO_2, CO, H_2S, SO_2, HCl, HF). Assessing equilibrium among major gas species is important for several reasons: (1) proof of equilibrium is excellent evidence for a good-quality sample, although good samples may also be disequilibrium mixtures, (2) to understand the reasons for disequilibrium if it exists, (3) to return disequilibrium gas mixtures to their initial equilibrium state, if the gases were once in equilibrium, (4) evidence for equilibrium lends credence to further equilibrium calculations, and (5) the evaluation procedure allows determination of a sample's last equilibrium temperature and fO_2; these are intensive quantities that cannot be measured directly.

A simple procedure is used to evaluate equilibrium in a gas sample with SOLVGAS (Symonds and others, 1990; Kodosky, Motyka, and Symonds, 1991). The basic technique is to calculate *correspondence temperatures* (CTs) for all gas species determined in the analysis. CTs are the temperatures at which the calculated equilibrium mole numbers of the various gas species, as determined using the component-species mass balances from the analysis, are equal to their mole numbers in the analysis. If the CTs for all gas species agree at a reasonable temperature, the sample is a quenched equilibrium composition (Gerlach and Casadevall, 1986a). If the CTs do not agree, the specific way in which they disagree may help diagnose the reason(s) for disequilibrium in the sample (Gerlach, 1980a, b, c, d). Once identified, the effects of disequilibrium can often be removed from a sample by using a thermodynamic procedure (Gerlach, 1979, 1980a, b, c, d, 1981; Graeber, Modreski, and Gerlach, 1979; Le Guern, Gerlach, and Nohl, 1982; Gerlach and Casadevall, 1986a; Symonds and others, 1990; Kodosky, Motyka, and Symonds, 1991). Adjusted samples are called restored, apparent, or estimated compositions in decreasing order of quality (see above). This method also allows testing of one's hypothesis for the cause(s) of a sample's disequilibrium and is especially effective on samples that have been degraded by sampling or analytical deficiencies.

Volcanic gas-atmosphere reactions.—Passively degassing and erupting volcanoes release gases and aerosols to the atmosphere. Mixing of high-temperature volcanic gases with the atmosphere triggers a series of cooling and oxidation reactions and the formation of liquid and solid aerosols such as water, sulfuric acid, and metallic solids (Thomas, Varekamp, and Buseck, 1982; Varekamp and others, 1986; Rose, 1987). Little is known about what happens when high-temperature, reduced volcanic gases enter the atmosphere. Thermochemical modeling can help forecast some of the reactions and species that might occur when volcanic gases mix with the atmosphere.

To model this process, air is added in increments to an appropriate initial volcanic gas composition. At each increment, GASWORKS computes the distribution of species in the bulk gas. Such models require a method to compute the temperature of the gas mixture. Currently, GASWORKS calculates temperature as a linear function of mixture composition of 25°C air added to a hot volcanic gas. However, this is unrealistic because volcanic gases and air have markedly different heat capacities. A more realistic heat transfer model (modified from Gerlach and Casadevall, 1986b) is to assume that the heat added to the mixing gas (air) is equal to the heat lost by the volcanic gas, taking into account the different heat capacities of the mixing gases.

Gas-rock alteration and the origin of fumarolic incrustations.—The above cooling calculations cannot explain the low-temperature sulfate incrustations; these may form by complex reactions involving volcanic gases, atmospheric gases, and the wall rock. We model such processes by titrating rock into an appropriate gas mixture. This modeling requires data on the gas composition, the wall rock composition, the temperatures of the vent and each particular incrustation zone, and the appropriate solid solutions for mineral phases.

The reaction progresses using a gas-rock titration procedure as described for the volatility calculations (above). In detail, however, the reaction is fundamentally different from a typical volatility calculation because many incrustations form at low temperatures, high fO_2, and at high G/R ratios. The titrations are done over a range of temperatures and G/R ratios, as constrained by natural samples. Comparison of the predicted alteration assemblages with the natural incrustations helps in identifying possible alteration reactions. A preliminary study of this kind on Augustine's fumaroles shows clearly that observed alteration and incrustations result from a mixture of processes, including gas cooling, gas-rock reaction, and air-gas-rock reaction (Getahun, Reed, and Symonds, 1992).

OTHER SCIENTIFIC APPLICATIONS

SOLVGAS and GASWORKS have potential applications outside the field of volcanic gas studies. Applications include any problems that involve chemical equilibria in gas–solid–liquid systems. The treatment of

gases as ideal limits the suitable problems to those at relatively low pressure and high temperature (app. 1).

Metal volatilities in magmatic vapors.—The contribution of magmas to hydrothermal systems has been disputed for over a century. Most geologists agree that magmas supply heat to overlying hydrothermal systems, but there is considerable debate as to whether they also contribute significant amounts of H_2O, S, halogens, and metals (Muffler and others, 1992). In a recent exploration of this problem, Reed (1992) calculated the consequence of condensing a volcanic gas into hydrothermal water, then reacting the mixture with wall rocks. The conclusion was that a magmatic source of halogens and sulfur is very likely for epithermal systems, but that metals may be leached from wall rocks. The modeling of Reed (1992) applies to magmatic fluids that are diluted significantly (by a factor of ten to one) by meteoric water. Systems that have a greater magmatic component may have a larger percentage of magmatic metals. One unknown is the amount of metal that can be partitioned from a magma to a magmatic vapor phase. Calculating metal volatilities, as was done long ago by Krauskopf (1957, 1964), is one way to investigate the metal contents of magmatic vapors. However, since Krauskropf's initial study, the quality and quantity of thermochemical data have greatly improved, making feasible an improved evaluation of metal transport in magmatic gases at low pressures using Krauskropf's approach. Treatments at high pressures (> 500 atm) await improvements in models of gas non-ideality, including trace gases.

Condensation of the solar nebula.—The primitive solar nebula consisted of a very hot mass of gas. With time, the nebula cooled, and solids and liquids condensed from the gas. The condensation sequence of elements and compounds from the nebula is of fundamental importance to understanding the origin of chondritic meteorites and the planets. Previous workers (for example, Grossman and Larimer, 1974; Saxena and Eriksson, 1983) investigated the condensation of the solar nebula by cooling a solar gas with thermochemical models and comparing the results with appropriate samples. GASWORKS could be used to repeat the modeling, for comparison with previous results, and to model elements and species omitted from earlier studies.

Burning of coal fires.—Fires start occasionally in coal dumps or in underground coal seams by spontaneous combustion, carelessness by people, or lightening. For example, there have been many fires in abandoned coal dumps in Pennsylvania, which have burned for decades before being extinguished (Lapham and others, 1980). The fumes from the fires, often burning at temperatures in excess of 700°C, probably contain CO_2, H_2O, SO_2, soot, and a number of minor gases like CO and NO_x. The smoke also includes volatilized trace elements such as As, Bi, Ge, Pb, Se, and Sn which form colorful incrustations (for example, hematite, various sulfates, native selenium) around the burning vents (Lapham and others, 1980). Such noxious gases may constitute a local

health hazard (Lapham and others, 1980). GASWORKS could model the burning process, the origin of the trace elements, the molecular form of the fumes, and the zoning of incrustations around the vents.

Smoke stack emissions.—With the growing concern over global change and regional air pollution resulting from anthropogenic waste-gas emissions, society needs more information about smoke stack emissions, including better characterization of the molecular form of trace elements. Although much is known about the major gases and aerosols emitted from smoke stacks, little is known about trace species and fly ash. GASWORKS could help characterize the molecular form of stack emissions and model the effects of temperature, fuel mixture, or air/fuel ratio on emission composition. For instance, one could model the transport of toxic metals (for example, Cd, Hg, and Pb) released from the combustion of coal, as investigated previously (Mojtahedi, 1989) using another thermochemical model.

<div align="center">CONCLUSIONS</div>

We have developed a computer model and compiled a large thermochemical data base to study multicomponent chemical equilibria and reaction processes in volcanic gases. Initial applications indicate that the results are favorable. We have used the thermochemical model and its data base to predict the speciation of a number of trace elements in volcanic gases. The numerical simulations have also helped identify which trace elements in gas samples might come from degasing magma. Finally, we have forecasted a number of possible reactions in cooling volcanic gases and tested the predictions by direct comparison with volcanic sublimates.

The degree to which equilibrium modeling reproduces natural systems depends on four factors:

1. *The correctness of the hypothesized geologic process under consideration.* Successful modeling depends critically on having the right geological hypothesis. For example, at the present time, modeling of cooling and precipitation of trace elements in volcanic gases is more effective than modeling of volatilization of trace elements is volcanic gases. In large measure, this reflects the higher level of congruence between the model system and the natural system in the case of the cooling process.

2. *The degree to which equilibrium applies.* The validity of the equilibrium assumption is of fundamental importance to the relevance of natural-system equilibrium calculations. The assumption of chemical equilibrium appears to be adequate for predicting the stable solid phases in a cooling volcanic gas uncontaminated with air. However, whether equilibrium applies to other volcanological processes, such as mixing between volcanic and atmospheric gases, is untested.

3. *The quality of the input gas composition.* Thermochemical modeling, such as presented in this paper, requires excellent gas data. For example, the volatility calculations and unmodified cooling calculations do not

completely reproduce the natural samples becuase the input gas contains rock-aerosol contaminants.

4. *The quality and quantity of thermochemical data.* The quality and quantity of thermochemical data are of fundamental importance to the success of the equilibrium calculations. For example, the absence of galena and sulfosalts in the predicted assemblage illustrates problems with the thermochemical data base.

This work has identified important topics for future research. The numerical simulations of cooling volcanic gases show that the additional modeling of the gas-atmosphere reactions and gas-rock alteration is necessary to explain fumarolic incrustations and plume aerosols. This work and previous studies (Symonds and others, 1987; Le Guern, ms; Quisefit and others, 1989; Bernard, Symonds, and Rose, 1990; Symonds, Reed, and Rose, 1992) have identified a myriad of possible trace gas species in volcanic gases. We need to test whether such species discharge from volcanic fumaroles. Theoretical calculations are not a replacement for direct observations but are a tool to interpret and improve field data so that we can better understand the natural processes.

When new thermochemical data become available, we will incorporate them into the GASTHERM data base, which hopefully will improve the accuracy of the thermochemical calculations. The first such revision (to be started in 1994) is to update our thermochemical data from the JANAF tables with the new edition (Chase and others, 1985). We also plan to add thermochemical data for nitrogen-bearing solids such as sal ammoniac because they are often the dominant sublimates below 350°C (Bernard, ms). In addition, our models need data for sulfosalts since they are important hosts of ore metals (for example, Pb, Cu, Sn, Bi) in volcanic sublimates (Bernard, ms). Finally, this work and previous studies (Symonds and others, 1987; Symonds, Reed and Rose, 1992) suggest that GASTHERM may be missing the main species of Au, Cd, Cr, Ir, and Si, and that the $\Delta_f G^o$ values for $PbCl_4$ and $PbBr_4$ need reevaluation.

The latest versions of programs SOLVGAS and GASWORKS, the GASTHERM data base, and the accompanying manuals are now available for distribution. These are FORTRAN 77 programs and run successfully on 80386- and 80486-level IBM-compatible personal computers, and also on IBM and VAX mainframe computers. They can be obtained for a small distribution cost from either author.

APPENDICES

1: *CALCULATION OF MULTICOMPONENT CHEMICAL EQUILIBRIA IN GAS-SOLID-LIQUID SYSTEMS: CALCULATION METHODS*
MARK H. REED and ROBERT B. SYMONDS

INTRODUCTION

Volcanic gases participate in volatilization, sublimation, and wall rock alteration reactions involving complex multicomponent chemical equilibria among minerals, liquids, and gases. Computation of such equilibria for specified conditions of temperature, pressure, and bulk composition provides a basis for understanding how these natural processes occur. By linking together a series of calculations with incremental changes of temperature, pressure, or composition between calculation segments, one can model processes of magma degassing, ascent of volcanic gases, wall rock reaction, and mixing of volcanic gases with hydrothermal vapor or with 'the atmosphere. Calculated examples of some of these processes in a volcanic gas environment are explored in the main text of this paper and in earlier papers (Naughton and others, 1974; Symonds and others, 1987; Toutain, ms; Le Guern, ms; Quisefit, ms; Quisefit and others, 1989; Symonds, Reed, and Rose, 1992; Getahun, Reed, and Symonds, 1992). Similar processes occur in combustion gases from burning of coal or municipal waste, and the same formulation for heterogeneous equilibrium calculations can be applied to these systems.

In this appendix, we describe the capabilities of computer program GASWORKS and its sister program, SOLVGAS; both descended from the aqueous-solid-gas system programs, CHILLER and SOLVEQ, respectively (Reed, 1982; Reed and Spycher, 1984; Spycher and Reed, 1989). GASWORKS is designed for calculating heterogeneous equilibria among minerals, gases, and liquids during processes of cooling (or heating), pressure change, gas-gas mixing, and gas-rock reaction. Program SOLVGAS calculates homogeneous equilibrium (distribution of species) in a gas phase from a raw gas analysis. It also calculates saturation indices, $\log(Q/K)$, for solid and liquid phases (Reed and Spycher, 1984; Symonds and others, 1987; Spycher and Reed, 1989). One significant use of SOLVGAS and GASWORKS is to restore volcanic gas analyses to their last equilibrium composition (Symonds and others, 1990; Kodosky, Motyka, and Symonds, 1991). Particularly important in this regard is their ability, without recourse to solid phase equilibria, to compute oxygen fugacity, fO_2, and consequent distribution of gas species at any temperature and pressure from knowledge of fO_2 at any other temperature and pressure (see below). The programs can also be used to model the speciation of major and trace elements in volcanic gases, the volatilization of metals from magma, and the precipitation of

sublimates from volcanic gases (Symonds and others, 1987; Symonds, Rose, and Reed, 1988; Bernard, Symonds, and Rose, 1990; Symonds, Reed, and Rose, 1992; this paper). Computational capabilities similar to those of SOLVGAS and GASWORKS based on a Gibbs free energy minimization program by Cheynet (1988a, b) have been applied to volcanic gases by Toutain (ms), Le Guern (ms), Quisefit (ms), and Quisefit and others (1989).

GASWORKS and SOLVGAS are based on an adaptation of a formulation of the basic equilibrium equations and numerical algorithms (Reed, 1982) originally developed for aqueous-solid-gas systems. Interestingly, that early formulation (Reed, 1982) is based, in part, on a formulation primarily for gaseous systems relevant to rocket engine studies by Huff, Gordon, and Morrell (1951) and Zeleznik and Gordon (1960).

In the calculation, a Newton-Raphson method is applied to solving the set of simultaneous non-linear polynomial equations of mass balance and mass action that describe chemical equilibrium in the system. The results of the homogeneous equilibrium calculation (SOLVGAS) include the mole fraction of each of hundreds of gas species in the system and a tabulation of the degree of supersaturation or undersaturation of the gas phase with respect to each of hundreds of solids and liquids. The heterogeneous equilibrium calculation (GASWORKS) produces the gas species mole fractions and the mass and composition of each additional phase in the system, including solid or liquid solutions, at overall equilibrium. The power and speed of the method presented here depend on a judicious choice of a set of thermodynamic component species, reduction of the system of equations to a minimum number, and an algorithm for selecting the stable assemblage of phases at any given temperature, pressure, and bulk composition.

GASWORKS and SOLVGAS use the data base GASTHERM (app. 2) which contains the compositions, equilibrium constants, and stoichiometries of gases, minerals, and a few liquids (for example, hygroscopic sulfuric acid; Symonds, Reed, and Rose, 1992). The stoichiometric data in GASTHERM, applied in the context of the formulation presented below, provides for consideration of all possible reactions among the hundreds of species in all phases of the system. GASTHERM is external to SOLVGAS and GASWORKS, so new gas or mineral species can be added by inserting a few lines in GASTHERM describing the respective stoichiometry and equilibrium constants. This makes it easy to expand or change the data base and to experiment with various, possibly conflicting, equilibrium constants. Most of the constants for equilibrium between the gas phase and minerals in GASTHERM are calculated using free energy program, GASCAL (Reed, Symonds, and Spycher, unpublished), which makes use of fundamental thermochemical data to compute equilibrium constants, as listed in app. 2.

OVERVIEW

For a gas-solid-liquid chemical system at specified temperature, T, pressure, P, and composition, wherein composition is defined by the total number of moles M_i^t, of each thermodynamic component, designated by subscript, i, a set of equations is defined consisting of N_i mass balance equations, one for each thermodynamic component, plus N_k mass action equations, one for each saturated solid, solid solution endmember, and liquid (for simplicity in the following discussion, the terms "mineral" or "solid" may refer to any and all solid and liquid phases). Secondary mass action equations are written for "derived" species in the gas phase, species whose compositions are expressed in terms of the component species. The terms in the mass balance equations for the number of moles (mole number) of each derived species can be replaced by the appropriate secondary mass action expressions, thereby reducing the number of primary equations for simultaneous solution to a minimum number ($N_i + N_k$).

The computer programs apply a Newton-Raphson method to solve the set of equations (Van Zeggren and Storey, 1970), requiring an initial estimate (within several orders of magnitude) of the mole number of each component species in the gas phase and the mass of every saturated phase. These estimates are improved iteratively until each of the $N_i + N_k$ unknowns passes a convergence test.

<div align="center">THERMODYNAMIC RELATIONS</div>

The equations for simultaneous solution of overall heterogeneous equilibrium include the basic equations of mass action and mass balance. The development here is similar to that of Reed (1982), but many details differ. Following a description of the thermodynamic components, formulations of the mass action and mass balance equations for heterogeneous equilibrium (GASWORKS) are given below. The homogeneous equilibrium calculation (SOLVGAS) requires the same equations except that mineral masses are omitted from the mass balance equations, and mass action equations for minerals are excluded from the set for simultaneous solution.

The system of equations is written in terms of the extensive quantities, mole numbers, rather than mole fractions, because this simplifies calculations involving changes in composition owing to mineral fractionation, gas-gas mixing, or rock titrations, and it provides for a direct accounting of the distribution of mass among phases in the total system. The equations are written for a gas–solid–liquid system at overall equilibrium; thus, for purposes of writing the equations, we assume that the phase identities are known. Phase selection is discussed separately, below.

Thermodynamic components.—It is most convenient to describe the composition of the chemical system in terms of a set of thermodynamic components consisting of molecular species actually present in the gas phase in significant concentration, rather than using the chemical elements, themselves. These species are referred to as "component species" (Reed, 1982) and include species such as the following: H_2, H_2O, CO_2, N_2, HCl, HF, NaCl, KCl, $MgCl_2$, SiF_4, H_2S, $FeCl_2$, $CoCl_2$, H_2MoO_4 (a complete list of component species is given in table 1, main text). Most of the component species are the first or second most abundant species containing the various elements at equilibrium in the gas. In volcanic gases, this means most of the trace elements are represented by chlorides, elemental species, hydrides, fluorides, and oxyacids, and the major elements, C, O, H, S, Cl, and F are represented by CO_2, H_2O, H_2, H_2S, HCl, and HF.

The use of component species that are also actual species in the chemical system rather than using the chemical elements, for example, cuts in half the number of descriptive arrays in the program by allowing the same arrays to describe both composition and chemical equilibria. This also cuts the number of program steps needed to set up equations compared to other programs that use one set of species for thermodynamic components and another for writing reactions. The use of molecular components, including relatively abundant species, results in excellent computational speed and numerical stability, a robust treatment of redox reactions, and complete oxygen balance, eliminating in principle any need for recourse to solid phase equilibria to fix oxygen fugacity in homogeneous gas systems.

The selection of both H_2 and H_2O (but not O_2) provides for calculation of oxidation-reduction processes, because all such reactions can be balanced using H_2 and H_2O. These species, in combination with H_2S, also provide for representing SO_2, which is an abundant volcanic gas species. The species, O_2 and SO_2, are two of the large number (N_j) of "derived species" in the chemical system whose compositions are represented by combinations of the component species. Other derived species include the chlorides, fluorides, oxides, and sulfides of metals (app. 2).

The use of thermodynamic components containing multiple chemical elements inevitably requires that negative amounts of some components are necessary to describe the

compositions of most phases and gas species. For example, SO_2 and O_2 compositions are represented as:

$$SO_2 = H_2S + 2H_2O - 3H_2, \tag{A1-1}$$

$$O_2 = 2H_2O - 2H_2. \tag{A1-2}$$

Similarly, hematite is represented as:

$$\underset{\text{(hematite)}}{Fe_2O_3} = 2FeCl_2 + 3H_2O - H_2 - 4HCl. \tag{A1-3}$$
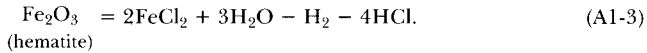
In the same way that description of the composition of individual derived species and minerals requires negative amounts of some components, the description of the bulk composition of a gas phase may require negative amounts of some components. For example, to express the 0.2 mole fraction of oxygen in air in terms of H_2O and H_2, requires $+0.4$ mole H_2O plus -0.4 mole H_2. An example of this compositional transformation applied to a Mount St. Helens gas is shown in table A1-1 where it is apparent that the indicated quantities of H_2, H_2O, SO_2, and H_2S are different where expressed in terms of the thermodynamic components as opposed to the species in the reconstructed gas itself. For example, the quantities of H_2S, H_2O, and H_2 are modified in accordance with eq (A1-1) to express the SO_2 in the gas analysis. A similar modification applies to CO and CO_2.

Mass action equations. Using the component species, i (table 1, main text), we write mass action equations for equilibria involving derived gas species, j:

$$K_j = \frac{\prod_i f_i^{v_{ij}}}{f_j}, \tag{A1-4}$$

in which, K_j is the equilibrium constant for a reaction describing the formation of the derived species (j) in terms of component species, i; f is the fugacity of the subscripted species; v_{ij} is the stoichiometric coefficient referring to the number of moles of component species, i, in one mole of derived species, j; v_{ij} is negative for species appearing on the left hand side of the equilibrium expression. The symbols subscripted with "i", here and below, refer specifically to component species, as distinguished from derived species, which are subscripted with "j."

TABLE A1-1

Mount St. Helens gas composition, major species

	Reconstructed Original Composition* (Moles)	Recomputed to Component Species** (Moles)
H_2O	.986	.987317
CO_2	.00886	.008883
H_2	.0039	.001913
H_2S	.00099	.00166
SO_2	.00067	—
HCl	.00076	.00076
HF	.0003	.0003
CO	.000023	—

* Gerlach and Casadevall (1986a), Bernard (ms), LeGuern (ms)
** SO_2 and CO are not component species, so they are re-expressed in terms of the other species; see text.

To transform eq (A1-4) into a convenient form for numerical solution, we apply a definition of partial pressure (eq A1-5, related to Dalton's Law; for example, Denbigh, 1981, p. 115), and the definitions of fugacity coefficient (eq A1-6) and mole fraction (eq A1-7):

$$P = \sum_g p_g = \sum_g x_g P, \tag{A1-5}$$

$$f_g = \phi_g p_g, \tag{A1-6}$$

$$x_g = \frac{n_g}{\sum_g n_g} = \frac{n_g}{N}. \tag{A1-7}$$

In the preceding equations, P is total fluid pressure; subscript g refers to any gas species in the mixture (encompassing species identified above by i and j); p_g is the partial pressure of species g; x_g is the mole fraction of g; ϕ_g is the fugacity coefficient of g; n_g is number of moles of gas species, g; N is the total number of moles of gas species; the summations in eqs (A1-5) and (A1-7) are over all species in the mixture.

Combining eqs (A1-5), (A1-6), and (A1-7) produces:

$$f_g = \phi_g n_g[P/N], \tag{A1-8}$$

which is substituted into eq (A1-4) to yield:

$$K_j = \frac{\prod_i n_i^{v_{ij}} \phi_i^{v_{ij}}}{n_j \phi_j} [P/N]^{w_j}, \tag{A1-9}$$

in which, w_j is defined as one less than the summation of stoichiometric coefficients of component species, i, contained in derived species, j:

$$w_j = \sum_i v_{ij} - 1. \tag{A1-10}$$

For example, w_j for SO_2 (eq A1-1) is -1. Notice that w_j is equal to the total summation of stoichiometric coefficients in the equilibrium expression, including the coefficient of -1 for the derived species, itself.

For each mineral, or mineral solid solution endmember, indexed as k, below, there is a reaction (app. 2) that relates it to the fugacities of the component species. For that reaction, written with the mineral on the left side, a mass action equation is written:

$$K_k = \frac{\prod_i n_{ik}^{v_{ik}} \phi_{ik}^{v_{ik}}}{a_k} [P/N]^{w_k}, \tag{A1-11}$$

in which, the stoichiometric coefficients, v_{ik}, are negative for component species that appear on the left side of the reaction; w_k is a summation of stoichiometric coefficients of component species, i, contained in mineral k (this excludes the -1 coefficient on the mineral itself); a_k refers to the activity of the solid solution endmember, k. For pure minerals, $a_k = 1$, but for solid solutions, the following equation is substituted for a_k in eq (A1-11):

$$a_k = (\gamma_k n_k / \Sigma \, n_l)^b, \tag{A1-12}$$

in which γ_k is the activity coefficient for endmember, k; n is the number of moles of solid solution endmember, k and l; the summation over n_l in the denominator includes all endmembers in the solid solution. The exponent, b, is unity for solid solutions exhibiting "molecular mixing" or where atoms mix on a single site per formula unit, but b takes a value greater than one in crystals where there are multiple energetically equivalent sites of a given

crystallographic type per formula unit. For example, to model the mixing of forsterite and fayalite endmembers of olivine as ideal, b is set to 2 and γ is set to unity in the mass action equation for each endmember. True multi-site mixing, involving two or more energetically distinct sites, is not currently accommodated in GASWORKS.

Substitution of eq (A1-12) into eq (A1-11) yields:

$$K_k = \frac{\prod_i n_{ik}^{v_{ik}} \phi_{ik}^{v_{ik}}}{\left(\gamma_k n_k / \sum_l n_l \right)^b} [P/N]^{w_k}. \tag{A1-13}$$

There is one mass action equation for each saturated pure mineral or solid solution endmember. The mass action equations for pure liquids or endmembers of ideal liquid mixtures are analogous to eq (A1-13).

Mass balance equations.—For each thermodynamic component in the system as a whole, there is one mass balance equation:

$$M_i^t = n_i + \sum_j v_{ij} n_j + \sum_k v_{ik} n_k. \tag{A1-14}$$

In this equation, M_i^t is the total number of moles of component i in the chemical system; subscript i refers to component species; j refers to derived species; k refers to endmembers of solid and liquid phases. Other symbols are as previously defined.

Eq (A1-9) can be rearranged to express mole number, n_j, of derived species j in terms of the mole numbers and fugacity coefficients of component species, et cetera, and the result substituted into eq (A1-14) to yield a substituted mass balance equation:

$$M_i^t = n_i + \sum_j v_{ij} \frac{\prod_i n_{ij}^{v_{ij}} \phi_{ij}^{v_{ij}}}{\phi_j K_j} [P/N]^{w_j} + \sum_k v_{ik} n_k. \tag{A1-15}$$

Equations such as this one, the number of which is equal to the number of thermodynamic components, N_i, are the master mass balance equations for solving the simultaneous heterogeneous equilibrium system.

Gas non-ideality.—At the current stage of development, the programs treat the gas phase as ideal. This is a reasonable approximation for H_2O, CO_2, CH_4, and H_2 in high temperature ($T > 600°C$) volcanic gases at low to moderate pressures ($P < 500$ atm; Holloway, 1977; Spycher and Reed, 1988). For example, fugacity coefficients for all of the above gases in pure form at 600°C and 500 atm are between 0.77 and 1.20. At 1000°C and 500 atm, they are very nearly 1.0 (except CO_2, which is 1.12). In mixtures, these coefficients are only slightly different. Applications at low temperature ($<500°C$) and moderate pressure (Spycher and Reed, 1988) or at high pressures (Holloway, 1977) will require consideration of non-ideal mixing in the gas phase. For example, in H_2O-CO_2 mixtures at 300°C and 500 atm, fugacity coefficients for H_2O and CO_2 are 0.36 and 2.0, respectively.

For the hundreds of trace-metal gas species, which are fundamentally important to understanding gas phase mass transfer and pneumatolytic wall rock alteration, we have no estimate of the extent of non-ideality, but we can be reasonably confident that ideal treatment is good at high temperature and low pressure, particularly because we are taking into account explicitly the chemical bonding that produces new molecules, including dimers and trimers (Prausnitz and others, 1980). Most of the trace gases are polar molecules, so it is likely that there are significant departures from ideality at lower temperature and high pressure. The equations given above are general, and by applying appropriate methods of calculating ϕ_g, they can be used to describe the thermodynamic behavior of gases under conditions for which gas behavior is non-ideal.

SYSTEM CALCULATIONS

Simultaneous equations.—Among the preceding equations, (A1-13) and (A1-15) constitute the primary set that GASWORKS solves simultaneously by a Newton-Raphson technique to compute overall heterogeneous equilibrium in a model calculation for any given incremental step in P, T, and M_i^t. There are N_i equations such as (A1-15) and N_k such as (A1-13) that are solved for the primary unknowns, n_i and n_k. Computation of n_j's is implicitly included in eq (A1-15), but once new values of n_i and n_k are determined, improved n_j's, are recomputed using eq (A1-9) in a calculational loop that is external to the Newton-Raphson solution to the main system of equations. The value of N, the summation of moles of gas species (eq A1-7), is included within the Newton-Raphson system because that enables faster convergence than when N is computed externally. In the present form of the programs, ϕ_g's are set to unity. They can be computed in an external loop on each Newton-Raphson iteration, as is the treatment of activity coefficients in aqueous systems (Reed, 1982).

For a typical large model calculation, the number of simultaneous equations might be 60, of which 35 are mass balance equations, one for each component, and 25 are mineral mass action equations. In the program, we represent the mineral mass action eq (A1-13) in logarithmic form because this improves convergence rates in most cases.

Program SOLVGAS solves only the substituted mass balance equations (A1-15), truncated after the second term (that is, excluding the mineral mass terms) for homogeneous equilibrium, yielding values for each of the N_i unknown mole numbers (n_i) of component species, which are then substituted into eq (A1-9) to compute n_j.

Calculation of fO_2.—Except in rare cases (for example, at Mount St. Helens in September 1981 by F. Le Guern; Gerlach and Casadevall, 1986a), the oxygen fugacity, fO_2, of a volcanic gas is not measured directly (for example, with an fO_2 probe) but can be computed from analyses of the major gases (H_2O, H_2, CO_2, CO, SO_2, H_2S). Unfortunately, air contamination in fumaroles, sampling difficulties, or changes in gas composition during ascent make it necessary to apply rigorous evaluation and restoration procedures (see main text and Symonds and others, 1990) to obtain the fO_2 from raw gas analyses. However, once restored, a gas analysis can be used directly to compute fO_2 at any temperature; this assumes that fO_2 in the fumarolic gases of interest is controlled by closed-system cooling of the gases. It is also possible to fix fO_2 at any temperature, perhaps with reference to solid buffers, then compute it at other temperatures with a closed system calculation. Finally, it is possible to fix fO_2 at every temperature step of a calculation to model rock-buffered gases.

If oxygen fugacity is set to a specific value, the relationship of fugacities of H_2, O_2, and H_2O are set by the equilibrium condition, and there is only one value of $M_{H_2}^t$ that will satisfy the equilibrium constraint for a given fO_2 and $M_{H_2O}^t$. To determine $M_{H_2}^t$, the following mass action equation for O_2-H_2-H_2O equilibrium (with equilibrium constant, K_{O_2}) is substituted for the H_2 mass balance equation:

$$n_{H_2} = \frac{n_{H_2O}\phi_{H_2O}}{(f_{O_2}K_{O_2})^{1/2}\phi_{H_2}}. \qquad (A1\text{-}16)$$

(Notice that the $[P/N]^{w_j}$ factor (eq A1-9) cancels in this particular case.) Then the system of equations (A1-15 and A1-13) is solved once to yield a distribution of gas species (and mineral masses, if the equilibrium is heterogeneous). The value of $M_{H_2}^t$ is then computed from the distribution of species using eq (A1-15) for H_2. Once the value of $M_{H_2}^t$ is fixed, fO_2 can be determined at any temperature by a closed system calculation using the full set of eqs (A1-15) and (A1-13). The latter is also the approach for computing fO_2 from a reliable complete gas analysis. Figure 2 (main text) illustrates a closed system calculation of fO_2 for a Mount St. Helens gas analysis and shows how H_2O-rich volcanic gases have closed-system fO_2 trends that parallel the Ni-NiO buffer. In contrast, SO_2-rich volcanic gases (for

example, the 1987 Augustine gases; Symonds, Reed, and Rose, 1992) have closed-system fO_2 trends that depart from solid buffers.

Buffering fugacities of major gases.—In order to determine whether the trace metals in volcanic gases could come from direct volatilization of magmatic phases, we carry out a "volatility" calculation wherein we hold the fugacities of the major gases constant, then compute the concentrations of trace gases that would evaporate at equilibrium from magmatic phases. To buffer the major gases, we saturate the gas phase with hypothetical separate gas phases at set fugacities (see also, Delany and Wolery, 1984). To set the fugacity of a gas, g, at a value of f_g, we equilibrate with an arbitrary quantity, n_g, of a hypothetically separate gas phase whose governing equation is a rearrangement of eqs (A1-8) and (A1-9), as follows:

$$K_g f_g = K_g^* = \prod_i n_{ig}^{v_{ig}} \phi_{ig}^{v_{ig}} [P/N]^{w_j+1}. \tag{A1-17}$$

K_g is the ordinary equilibrium constant for the reaction describing the formation of the gas from component species; f_g is set at the desired buffer fugacity; K_g^* is treated as the equilibrium constant for the hypothetical phase.

For the circumstance where the buffered gas species is a component species, i, eq (A1-17) reduces to the simple form:

$$f_i = K_i^* = n_i \phi_i [P/N]. \tag{A1-18}$$

Non-ideal mixing in liquid and solid phases.—For solid solutions, GASWORKS accommodates ideal mixing, as discussed above, and is equipped to handle non-ideal mixing in any minerals for which the necessary mixing properties are programmed into subroutines. For the latter, values of γ_k (eq A1-12) are computed in an external loop using an appropriate mixing law for the solid solution, in which γ is a function of composition and temperature.

Process calculations: cooling, mixing, wall rock reaction, P-change, volatility.—By changing the temperature, pressure, and "total moles" (M_i^t) in a stepwise fashion and computing overall heterogeneous equilibrium at each step, GASWORKS is able to compute a variety of processes, such as gas-rock reactions, gas-gas mixing, and the effects of decrease in temperature or pressure during ascent of a gas. Examples of all these except gas-gas mixing are given in the main text and in Symonds, Reed, and Rose (1992). Temperature change calculations simply require re-calculating for each segment, the equilibrium constants in eqs (A1-13) and (A1-15) using a power function that expresses log K as a function of T (eq 7). For pressure-change calculations, we change P in eqs (A1-13) and (A1-15) from one P-step to the next. In principle, we should also recalculate the gas-solid equilibrium constants at changed pressures, but this effect is small at the low pressures of interest in volcanic gas calculations. Calculation of gas-rock reaction or gas-gas mixing is carried out by incremental changes in the values of M_i^t, computed by adding and subtracting quantities of material appropriate to the addition of rock or gas to an initial quantity of gas.

In any of the above process calculations, depending on the physical model being investigated, it is possible to fractionate solids from the chemical system as they form. This is accomplished after each increment of change by changing the values of M_i^t such that:

$$M_{i,new}^t = M_{i,old}^t - M_{i,old}^s, \tag{A1-19}$$

where $M_{i,old}^s$ is the quantity of material precipitated in solid phases on the previous step. One common process where this capability is used is the ascent of a gas through a fumarole system with consequent decrease of T. At each T-step, we fractionate the solids that formed before taking the next T-step, thereby disallowing back-reaction or buffering by sublimates that are physically distant from the gas (figs. 5-11).

In "volatility" calculations, we determine how much of the various trace elements may evaporate from magmatic phases at equilibrium. We assume that the fugacities of major gas

species are not seriously perturbed by equilibration of trace gas species with magmatic phases. This is equivalent to assuming that the quantities of major species (H_2O, CO_2, HCl, et cetera) are large relative to the trace species and are therefore buffered relative to the perturbations of equilibrium with various minerals. To compute trace element volatilities, we buffer major gas fugacities as described above, then titrate fresh rock into the buffered gas until a large assemblage of phases (including solid solutions and, in principle, magmatic liquid) saturates, thereby buffering the minor species. Examples of such calculatins for Mount St. Helens are given in figure 3 and for Augustine volcano in Symonds, Reed, and Rose (1992). This approach supersedes the one we used for Merapi (Symonds and others, 1987), in which we adjusted the gas composition by trial-and-error until it was saturated with assumed magmatic phases, as computed by SOLVGAS.

NUMERICAL CONSIDERATIONS AND PHASE SELECTION

Trial values.—To begin the Newton-Raphson iterative solution process, trial values of n_i and n_k are supplied. Typically, these need to be within five or ten orders of magnitude of their correct values. Generally, trial values that are smaller rather than larger than the final solution values work better. Because GASWORKS calculations are executed in segments with successive changes in T, P, or composition between segments, we can use the solutions from one segment as trial values·for the next. By cutting the step size between segments to a small amount, the trial values of the unknowns can be made to approach the solutions closely. Thus, a good approach to treating problems with numerical instability is to cut the step size.

Since negative mole numbers of individual component species (n_i, as distinguished from a negative total moles, $M_i^!$, of a component species) cannot prevail at equilibrium, any negative mole numbers that are produced early in the iterative process when the Newton-Raphson correction terms are applied to the current n_i, are arbitrarily reset to small positive values.

Convergence test.—To solve the system of simultaneous equations by the Newton-Raphson method (Van Zeggren and Storey, 1970) the left sides of eqs (A1-13) and (A1-15) are moved to the right, setting the equations to zero, thereby defining functions, F, whose values converge to zero when the system of equations is solved. An additional F function is defined for the total moles of gas where zero is set equal to $\sum_g n_g$ minus N. (Note that N = $\sum_g$ ng in eq A1-7.) The numerical solution is judged to have converged when the value of F for every equation is less than $C \times |X|$, where X is approximately equal to the term in each equation with the largest absolute value, and C is a convergence factor typically set at 10^{-12}. The value of X is ordinarily set equal to $M_i^!$ for mass balance eq (A1-15), to $10 \times K_k$ for mineral mass action eq (A1-13), and to an estimate of N for the total moles of gas equation. If we do not test every function for convergence, it is possible to compute an apparent convergence in which most of the equations are solved, but those with very small terms are not.

Selection of the phase assemblage.—After each increment in a model calculation, it is necessary to scan all possible previously undersaturated phases (pure minerals, solid solutions, liquids) to determine whether any have supersaturated in the gas phase as a consequence of the previous change of T, P, or $M_i^!$. If any are found, a selection of them (see below) is incorporated in the system, and the equilibration step is repeated. The approach to identifying the supersaturated pure phases and choosing among them is the same as that of Reed (1982), except that we compute a scaled (Wolery, 1979) saturation index (eq A1-21) for a mineral in a gas-solid system. We define a gas-system saturation index for pure solid or liquid k as follows:

$$\log (Q/K)_k = \log \left(\prod_i n_{ik}^{v_{ik}} \phi_{ik}^{v_{ik}} [P/N]^{w_k} \right) - \log (K_k), \qquad (A1\text{-}20)$$

where K_k is the equilibrium constant for pure phase, k, and Q_k is the activity quotient for k (for more explanation of this equation, see Reed, 1982). The scaled saturation index is:

$$\log(Q/K)_{k,s} = \frac{\log\ (Q/K)_k}{s_k}\ , \tag{A1-21}$$

where s_k is a scaling factor equal to the sum of the absolute values of the reaction coefficients:

$$s_k = \sum_i |v_{ik}|\ . \tag{A1-22}$$

The mineral with the largest positive scaled saturation index is included in a repeat equilibration calculation. This process is continued in combination with removal of under-saturated minerals (below) until no supersaturated phases remain, at which point the system is at overall equilibrium, and the next increment of change is taken. For ideal and non-ideal solid or liquid solutions, we apply the approach of Reed (1982) as modified by Reed and Spycher (in preparation).

Removal of undersaturated minerals.—When a given pure mineral that is already part of the phase assemblage undersaturates, this is indicated by negative computed mass for the mineral at the end of an equilibration step. Thereupon, the appropriate mass action eq (A1-13) is removed from the system, and the calculation is repeated.

An improved approach eliminates the repeat calculation by testing for negative mineral masses after just five Newton-Raphson iterations and throwing out the undersaturated minerals, if any, at that point, then continuing the iterative process. A variation on this method is used for solid solutions (Reed and Spycher in preparation). If a mineral is incorrectly eliminated because its fifth-iteration computed mass is negative even though it would have become positive again at true equilibrium, that mineral will have a positive scaled saturation index and will be replaced on a repeat equilibration.

<div align="center">CONCLUSIONS</div>

The chemical equilibrium condition provides strict limits on the compositions of phases in volcanic gas-mineral systems. By establishing the equilibrium constraints for a given system, we can deduce what departures from equilibrium result from reaction kinetics effects, and we can identify the effects of cooling, mixing with hydrothermal steam or air, and reaction with wall rock, for example. The formulation of equations presented above provides a straightforward and numerically well-behaved approach to solving for the equilibrium conditions and to exploring various reaction processes.

Although developed for volcanic gas systems, the same method can be used to model other natural and industrial processes that involve reactions with gases, solids, and liquids. Other applications include modeling of the condensation of the solar nebular, incineration and combustion processes such as underground coal fires, and the speciation of metals in smoke stack emissions.

2: COEFFICIENTS FOR CALCULATING LOG K^T VALUES[a] WITH EQ (7)[b]

ROBERT B. SYMONDS and MARK H. REED

Gas Species						
Reaction[c]	l_0	$l_1 \times 10^{-2}$	$l_2 \times 10^3$	$l_3 \times 10^{-3}$	$l_4 \times 10^1$	Ref.[d]
$O_2 + 2H_2 = 2H_2O$	4.414	248.415	0.326	6.036	-31.546	e
$Ag + HCl = 0.5H_2 + AgCl$	-3.063	45.590	-0.079	-5.089	3.951	e
$AgBr + HCl = HBr + AgCl$	0.005	-11.689	0.010	-3.464	-0.383	f,g
$AgS + 0.5H_2 + HCl = H_2S + AgCl$	0.381	111.397	0.188	-6.476	-10.871	h
$Al + 3HF = 1.5H_2 + AlF_3$	-17.022	381.694	-0.020	-43.146	18.688	e
$AlBr + 3HF = H_2 + HBr + AlF_3$	-12.826	235.829	0.049	-34.963	14.874	i
$AlBr_3 + 3HF = 3HBr + AlF_3$	1.768	47.535	0.223	-20.857	-6.967	i
$(AlBr_3)_2 + 6HF = 6HBr + 2AlF_3$	17.353	31.740	0.452	-42.758	-34.256	i
$AlC + 2H_2O + 3HF = 3.5H_2 + CO_2 + AlF_3$	-24.360	527.563	-0.280	-59.241	50.736	j,k
$AlCl + 3HF = H_2 + HCl + AlF_3$	-12.699	229.627	0.047	-32.168	14.522	i
$AlClF + 2HF = 0.5H_2 + HCl + AlF_3$	-7.647	141.705	0.083	-18.199	7.228	j,l
$AlClF_2 + HF = HCl + AlF_3$	0.939	15.444	0.106	1.209	-4.818	j,l
$AlCl_2 + 3HF = 0.5H_2 + 2HCl + AlF_3$	-6.890	156.528	0.138	-21.737	5.543	i
$AlCl_2F + 2HF = 2HCl + AlF_3$	0.907	30.338	0.132	-8.326	-5.192	j,l
$AlCl_3 + 3HF = 3HCl + AlF_3$	1.565	43.874	0.168	-14.796	-5.987	i
$(AlCl_3)_2 + 6HF = 6HCl + 2AlF_3$	17.662	18.344	0.381	-22.775	-34.125	i
$AlF + 2HF = H_2 + AlF_3$	-3.006	207.712	-0.010	-29.184	-18.609	i
$AlFO + 2HF = H_2O + AlF_3$	-3.865	169.072	0.192	-8.358	-8.805	j,l
$AlF_2 + HF = 0.5H_2 + AlF_3$	-8.037	129.187	0.013	-14.454	9.853	i
$AlF_2O + 0.5H_2 + HF = H_2O + AlF_3$	1.437	34.709	0.237	2.040	-17.193	j,l
$(AlF_3)_2 = 2AlF_3$	14.641	-111.270	-0.001	17.820	-19.727	i

Reaction						Ref
$AlH + 3HF = 2H_2 + AlF_3$	-16.497	345.094	-0.130	-35.282	24.931	j,k
$HAlO + 3HF = H_2 + H_2O + AlF_3$	-9.258	348.855	-0.029	-0.057	6.662	j,m
$AlH_2 + 3HF = 2.5H_2 + AlF_3$	-16.806	339.345	-0.300	-29.690	33.706	j,k
$AlH_3 + 3HF = 3H_2 + AlF_3$	-13.683	317.540	-0.483	-2.840	37.291	j,k
$AlO + 3HF = 0.5H_2 + H_2O + AlF_3$	-13.845	369.859	0.021	-35.225	8.752	e
$(AlO)_2 + 6HF = H_2 + 2H_2O + 2AlF_3$	-13.299	436.603	0.333	-43.641	-2.763	e
$AlOCl + 3HF = H_2O + HCl + AlF_3$	-3.742	197.010	0.221	-17.023	-9.343	j,m
$AlOH + 3HF = H_2 + H_2O + AlF_3$	-12.595	239.701	-0.102	-14.486	17.565	j,m
$AlO_2 + 0.5H_2 + 3HF = 2H_2O + AlF_3$	-3.172	357.169	0.362	-15.621	-22.274	e
$2H^{\cdot} + 3HF = 2H_2O + AlF_3$	-3.618	215.355	0.173	-0.210	-9.693	j,m
$AlS + 3HF = 0.5H_2 + H_2S + AlF_3$	-14.290	341.701	0.025	-43.515	10.789	h
$(AlS)_2 + 6HF = H_2 + 2H_2S + 2AlF_3$	-14.254	487.809	0.434	-62.765	0.896	h
$Al_2O + 6HF = 2H_2 + H_2O + 2AlF_3$	-21.697	473.381	0.123	-64.390	18.777	e
$Al_2S + 6HF = 2H_2 + H_2S + 2AlF_3$	-22.106	546.992	0.173	-75.036	20.147	h
$As + 3HCl = 1.5H_2 + AsCl_3$	-19.100	154.440	-0.231	-23.730	27.224	f,e
$AsBr_3 + 3HCl = 3HBr + AsCl_3$	-0.463	-17.898	0.023	-11.542	0.905	f,i
$AsF_3 + 3HCl = 3HF + AsCl_3$	-1.839	9.336	-0.238	17.429	7.283	f,i
$AsF_5 + H_2 + 3HCl = 5HF + AsCl_3$	18.879	51.232	0.064	71.710	-28.671	n
$AsH_3 + 3HCl = 3H_2 + AsCl_3$	-17.037	31.917	-0.651	7.221	48.629	g
$AsS + 3HCl = 0.5H_2 + H_2S + AsCl_3$	-12.509	102.928	0.090	-9.044	5.750	h
$As_2 + 6HCl = 3H_2 + 2AsCl_3$	-33.186	108.602	-0.409	-34.122	56.856	f,e
$As_3 + 9HCl = 4.5H_2 + 3AsCl_3$	-45.524	125.964	-0.650	-58.040	79.671	f,e
$As_4 + 12HCl = 6H_2 + 4AsCl_3$	-55.705	65.249	-0.843	-68.583	104.784	f,e
$As_4O_6 + 12HCl = 4AsCl_3 + 6H_2O$	0.340	94.132	0.018	25.482	-38.062	f,e
$As_4S_4 + 12HCl = 2H_2 + 4H_2S + 4AsCl_3$	-18.266	14.858	0.199	-60.166	6.895	h
$AuS + H_2 = H_2S + Au$	3.488	-61.921	0.265	0.220	-14.713	h
$Bi + 3HCl = 1.5H_2 + BiCl_3$	-18.048	106.200	-0.233	-11.806	27.204	f,e

Gas Species (continued)

Reaction[c]	l_0	$l_1 \times 10^{-2}$	$l_2 \times 10^3$	$l_3 \times 10^{-3}$	$l_4 \times 10^1$	Ref.[d]
$BiBr_3 + 3HCl = 3HBr + BiCl_3$	-0.117	-30.323	0.006	-7.534	1.609	f,i
$BiCl + 2HCl = H_2 + BiCl_3$	-14.113	58.625	-0.181	-7.910	23.322	f,n
$BiF + 3HCl = H_2 + HF + BiCl_3$	-14.365	124.529	-0.217	-4.663	24.010	n
$BiF_3 + 3HCl = 3HF + BiCl_3$	-0.017	51.361	-0.106	15.395	0.951	f,i
$BiS + 3HCl = 0.5H_2 + H_2S + BiCl_3$	-14.189	96.650	-0.016	-14.859	14.157	h
$(BiS)_2 + 6HCl = H_2 + 2H_2S + 2BiCl_3$	-16.658	104.313	0.028	-17.250	17.081	h
$Bi_2 + 6HCl = 3H_2 + 2BiCl_3$	-32.095	111.435	-0.449	-21.885	58.685	f,e
$Bi_2S_3 + 6HCl = 3H_2S + 2BiCl_3$	-9.147	115.146	0.325	-23.187	-9.679	h
$Br + 0.5H_2 = HBr$	0.015	76.536	0.044	-0.921	-7.642	e
$BrCl + H_2 = HCl + HBr$	4.150	73.119	0.129	5.102	-11.645	i
$BrF + H_2 = HF + HBr$	4.364	128.752	0.118	13.529	-12.427	i
$BrF_3 + 2H_2 = 3HF + HBr$	18.759	306.815	0.200	40.934	-33.480	i
$BrF_5 + 3H_2 = 5HF + HBr$	36.462	495.990	0.271	78.695	-59.734	i
$BrSF_5 + 4H_2 = H_2S + 5HF + HBr$	44.689	218.693	0.382	109.105	-75.398	j,o
$Br_2 + H_2 = 2HBr$	4.536	52.519	0.148	3.062	-11.953	e
$C + 2H_2O = 2H_2 + CO_2$	-10.839	332.287	-0.233	-28.272	25.767	e
$CBr + 2H_2O = 1.5H_2 + CO_2 + HBr$	-6.385	242.650	-0.142	-22.863	20.890	i
$CBrF_3 + 2H_2O = CO_2 + 3HF + HBr$	12.752	58.760	-0.301	42.009	4.741	j,m
$CBr_4 + 2H_2O = CO_2 + 4HBr$	17.335	68.589	0.052	8.632	-10.402	f,i
$CCl + 2H_2O = 1.5H_2 + CO_2 + HCl$	-7.321	267.451	-0.195	-16.744	23.912	i
$CClF_3 + 2H_2O = CO_2 + HCl + 3HF$	12.640	56.888	-0.325	47.221	5.492	j,m
$CCl_2 + 2H_2O = H_2 + CO_2 + 2HCl$	-2.279	177.044	-0.314	-8.984	21.635	i

Reaction						
$CCl_2F_2 + 2H_2O = CO_2 + 2HCl + 2HF$	14.011	75.075	-0.211	41.907	-0.119	j,m
$CCl_3 + 2H_2O = 0.5H_2 + CO_2 + 3HCl$	7.763	138.545	-0.057	14.630	3.642	i
$CCl_3F + 2H_2O = CO_2 + 3HCl + HF$	15.700	86.287	-0.098	36.529	-5.582	j,m
$CCl_4 + 2H_2O = CO_2 + 4HCl$	17.257	89.153	-0.006	25.113	-9.201	i
$CF + 2H_2O = 1.5H_2 + CO_2 + HF$	-8.347	233.451	-0.254	-17.394	27.263	i
$CF_2 + 2H_2O = H_2 + CO_2 + 2HF$	-3.098	146.181	-0.287	1.215	24.487	i
$CF_3 + 2H_2O = 0.5H_2 + CO_2 + 3HF$	3.899	135.513	-0.311	28.582	16.613	i
$CF_3OF + H_2 + H_2O = CO_2 + 4HF$	17.629	245.362	-0.234	57.971	-10.021	j,m
$CF_4 + 2H_2O = CO_2 + 4HF$	11.955	34.169	-0.360	49.233	9.951	i
$CH + 2H_2O = 2.5H_2 + CO_2$	-11.729	269.669	-0.367	-30.557	36.256	j,k
$CHCl + 2H_2O = 2H_2 + CO_2 + HCl$	-8.872	181.225	-0.635	-8.359	40.293	j,m
$CHClF_2 + 2H_2O = H_2 + CO_2 + HCl + 2HF$	5.574	34.819	-0.503	42.378	22.987	j,m
$CHCl_2F + 2H_2O = H_2 + CO_2 + 2HCl + HF$	6.535	43.760	-0.421	38.568	19.500	j,m
$CHCl_3 + 2H_2O = H_2 + CO_2 + 3HCl$	8.218	43.199	-0.332	32.610	15.254	j,m
$CHF + 2H_2O = 2H_2 + CO_2 + HF$	-8.539	166.367	-0.433	-7.472	38.503	j,m
$CHFO + H_2O = H_2 + CO_2 + HF$	-2.748	27.185	-0.419	16.312	25.716	j,m
$CHF_3 + 2H_2O = H_2 + CO_2 + 3HF$	3.811	17.470	-0.641	46.110	30.939	j,m
$CH_2 + 2H_2O = 3H_2 + CO_2$	-10.877	161.201	-0.476	-17.626	43.789	j,k
$CH_2ClF + 2H_2O = 2H_2 + CO_2 + HCl + HF$	-2.043	10.120	-0.743	31.262	44.461	j,m
$CH_2Cl_2 + 2H_2O = 2H_2 + CO_2 + 2HCl$	-0.031	1.931	-0.627	29.738	38.558	j,m
$CH_2F_2 + 2H_2O = 2H_2 + CO_2 + 2HF$	-3.358	6.506	-0.845	34.530	50.135	j,m
$CH_2O + H_2O = 2H_2 + CO_2$	-8.278	23.431	-0.595	2.979	41.845	j,m
$CH_3 + 2H_2O = 3.5H_2 + CO_2$	-11.034	36.631	-0.712	-13.294	56.674	j,k
$CH_3Cl + 2H_2O = 3H_2 + CO_2 + HCl$	-7.463	-36.705	-0.909	18.027	60.580	j,p
$CH_3F + 2H_2O = 3H_2 + CO_2 + HF$	-9.161	-20.279	-1.014	19.600	66.380	j,m
$CH_4 + 2H_2O = 4H_2 + CO_2$	-12.869	-77.318	-1.101	4.447	77.549	j,k
$CO + H_2O = H_2 + CO_2$	-7.768	25.445	-0.115	-24.619	18.435	e

Gas Species (continued)

Reaction[c]	l_0	$l_1 \times 10^{-2}$	$l_2 \times 10^3$	$l_3 \times 10^{-3}$	$l_4 \times 10^1$	Ref.[d]
$COCl + H_2O = 0.5H_2 + CO_2 + HCl$	-1.482	96.004	0.001	-6.792	6.832	j,m
$COClF + H_2O = CO_2 + HCl + HF$	4.838	46.189	-0.149	22.527	3.988	j,m
$COCl_2 + H_2O = CO_2 + 2HCl$	6.589	59.394	-0.033	16.859	-1.347	j,m
$COF + H_2O = 0.5H_2 + CO_2 + HF$	-3.519	134.405	-0.185	-3.447	15.128	j,m
$COF_2 + H_2O = CO_2 + 2HF$	3.594	30.290	-0.256	26.093	9.544	j,m
$COS + H_2O = CO_2 + H_2S$	0.482	16.166	0.081	-5.715	-2.224	h
$CS + 2H_2O = H_2 + CO_2 + H_2S$	-6.977	117.091	-0.032	-24.047	16.303	h
$CSF_8 + 3H_2 + 2H_2O = CO_2 + H_2S + 8HF$	52.300	191.865	-0.129	145.240	-55.394	j,o
$CS_2 + 2H_2O = CO_2 + 2H_2S$	1.979	35.719	0.201	-11.191	-5.909	h
$C_2 + 4H_2O = 4H_2 + 2CO_2$	-18.953	356.240	-0.535	-78.480	62.409	e
$C_2Cl_2 + 4H_2O = 3H_2 + 2CO_2 + 2HCl$	-3.999	118.764	-0.477	-26.437	43.473	i
$C_2Cl_4 + 4H_2O = 2H_2 + 2CO_2 + 4HCl$	11.288	94.256	-0.371	9.029	22.899	i
$C_2Cl_6 + 4H_2O = H_2 + 2CO_2 + 6HCl$	31.389	120.811	-0.164	38.612	-11.644	i
$C_2F_2 + 4H_2O = 3H_2 + 2CO_2 + 2HF$	-5.092	208.874	-0.602	-13.022	48.329	i
$C_2F_4 + 4H_2O = 2H_2 + 2CO_2 + 4HF$	6.450	135.897	-0.690	21.199	39.022	i
$C_2F_6 + 4H_2O = H_2 + 2CO_2 + 6HF$	23.578	56.937	-0.609	72.892	15.122	i
$C_2HCl + 4H_2O = 4H_2 + 2CO_2 + HCl$	-9.233	73.995	-0.651	-20.960	57.323	j,m
$C_2HF + 4H_2O = 4H_2 + 2CO_2 + HF$	-10.233	122.724	-0.720	-20.402	60.430	j,m
$C_2H_2 + 4H_2O = 5H_2 + 2CO_2$	-14.064	34.133	-0.830	-19.174	71.628	j,k
$C_2H_4 + 4H_2O = 6H_2 + 2CO_2$	-16.747	-55.324	-1.393	11.777	103.302	j,k
$C_2H_4O + 3H_2O = 5H_2 + 2CO_2$	-10.568	12.413	-1.389	39.481	89.306	j,m
$C_2H_6 + 4H_2O = 7H_2 + 2CO_2$	-22.586	-120.710	-2.322	-12.262	146.035	f,j,k

Reaction						
$C_3 + 6H_2O = 6H_2 + 3CO_2$	-29.481	306.089	-0.916	-82.779	109.904	e
$C_3O_2 + 4H_2O = 4H_2 + 3CO_2$	-10.215	71.510	-0.715	-29.447	59.172	j,m
$C_4 + 8H_2O = 8H_2 + 4CO_2$	-27.681	338.276	-1.210	-68.553	123.980	e
$C_5 + 10H_2O = 10H_2 + 5CO_2$	-31.620	299.535	-1.531	-75.628	152.908	e
$C_6H_6 + 12H_2O = 15H_2 + 6CO_2$	-42.996	-204.032	-4.202	-34.372	282.012	f,j,k
$Ca + 2HCl = H_2 + CaCl_2$	-10.737	245.423	-0.146	-7.751	17.564	e
$CaBr + 2HCl = 0.5H_2 + HBr + CaCl_2$	-7.843	145.160	-0.075	-5.073	13.924	i
$CaBr_2 + 2HCl = 2HBr + CaCl_2$	-0.503	-12.638	0.000	-5.610	1.353	i
$CaCl + HCl = 0.5H_2 + CaCl_2$	-8.105	149.174	-0.101	-6.336	14.767	i
$CaF° + 2HCl = 0.5H_2 + HF + CaCl_2$	-8.274	152.547	-0.139	-2.016	15.383	i
$CaF_2 + 2HCl = 2HF + CaCl_2$	-1.870	22.027	-0.057	10.404	5.194	i
$CaH + 2HCl = 1.5H_2 + CaCl_2$	-10.848	272.354	-0.241	-0.913	21.705	j,k
$CaO + 2HCl = H_2O + CaCl_2$	-7.323	299.835	-0.045	-2.275	4.648	e
$CaOH + 2HCl = 0.5H_2 + H_2O + CaCl_2$	-3.692	174.605	-0.008	6.604	1.350	j,l
$Ca(OH)_2 + 2HCl = 2H_2O + CaCl_2$	6.745	79.286	0.145	23.099	-21.040	j,l
$CaS + 2HCl = H_2S + CaCl_2$	-10.895	228.907	-0.245	-25.429	17.172	h
$Ca_2 + 4HCl = 2H_2 + 2CaCl_2$	-21.524	487.836	-0.204	-28.557	44.178	e
$CdS + H_2 = H_2S + Cd$	4.347	48.687	0.277	2.898	-16.110	h
$Cl + 0.5H_2 = HCl$	1.565	109.561	0.122	6.195	-13.220	e
$ClF + H_2 = HCl + HF$	4.016	162.431	0.089	13.111	-11.315	i
$ClF_3 + 2H_2 = HCl + 3HF$	18.318	386.480	0.161	44.889	-31.901	i
$ClF_5 + 3H_2 = HCl + 5HF$	36.037	624.472	0.231	84.176	-57.748	i
$ClF_5S + 4H_2 = H_2S + HCl + 5HF$	44.436	213.318	0.344	112.280	-73.965	j,o
$ClO + 1.5H_2 = H_2O + HCl$	4.714	223.837	0.261	13.948	-24.639	e
$ClO_2 + 2.5H_2 = 2H_2O + HCl$	11.067	348.407	0.379	31.213	-41.115	j,m
$ClO_3F + 4H_2 = 3H_2O + HCl + HF$	27.091	545.159	0.459	75.700	-68.643	j,m
$Cl_2O + 2H_2 = H_2O + 2HCl$	11.380	259.176	0.332	23.199	-32.929	e

APPENDIX 2

(continued)

Gas Species (continued)

Reaction[c]	l_0	$l_1 \times 10^{-2}$	$l_2 \times 10^3$	$l_3 \times 10^{-3}$	$l_4 \times 10^1$	Ref.[d]
$Cl_2 + H_2 = 2HCl$	4.835	94.135	0.139	11.284	-12.877	e
$Co + 2HCl = H_2 + CoCl_2$	-9.148	175.415	-0.089	0.906	9.394	e
$CoCl + HCl = 0.5H_2 + CoCl_2$	-7.387	103.301	-0.027	-2.392	13.030	i
$(CoCl_2)_2 = 2CoCl_2$	10.949	-86.706	0.061	0.631	-11.428	i
$CoCl_3 + 0.5H_2 = HCl + CoCl_2$	9.169	8.524	0.190	19.515	-15.730	i
$CoF_2 + 2HCl = 2HF + CoCl_2$	-1.709	51.779	-0.032	10.540	5.314	i
$Cr + 4HCl = 2H_2 + CrCl_4$	-27.945	245.148	-0.344	-34.619	42.303	e
$CrBr_4 + 4HCl = 4HBr + CrCl_4$	-0.495	-28.067	0.050	-13.201	0.042	f,i
$CrO + 4HCl = H_2 + H_2O + CrCl_4$	-23.258	259.280	-0.109	-21.713	24.996	e
$CrO_2 + 4HCl = 2H_2O + CrCl_4$	-15.548	244.008	0.128	-0.818	3.830	e
$CrO_2Cl_2 + H_2 + 2HCl = 2H_2O + CrCl_4$	3.083	93.218	0.309	24.299	-26.828	f,n
$CrO_3 + H_2 + 4HCl = 3H_2O + CrCl_4$	-5.558	252.549	0.274	17.892	-19.056	e
$Cs + HCl = 0.5H_2 + CsCl$	-3.359	117.976	-0.058	-3.387	4.168	e
$(CsCl)_2 = 2CsCl$	9.357	-94.792	0.025	-2.138	-9.194	i
$CsF + HCl = HF + CsCl$	0.373	31.924	-0.002	6.220	-1.100	i
$(CsF)_2 + 2HCl = 2HF + 2CsCl$	10.150	-26.880	-0.012	8.068	-10.608	i
$CsO + 0.5H_2 + HCl = H_2O + CsCl$	0.935	234.362	0.169	2.949	-14.735	e
$CsOH + HCl = H_2O + CsCl$	4.411	65.862	0.121	5.567	-14.613	j,p
$(CsOH)_2 + 2HCl = 2H_2O + 2CsCl$	12.617	43.478	-0.124	35.933	-13.916	j,p
$(Cs)_2 + 2HCl = H_2 + 2CsCl$	-4.884	212.132	-0.198	-7.913	14.056	e
$Cs_2O + 2HCl = H_2O + 2CsCl$	3.200	231.456	0.109	1.216	-9.548	e
$Cs_2SO_4 + 4H_2 + 2HCl = H_2S + 2CsCl + 4H_2O$	36.927	67.447	0.704	74.779	-94.968	j,k

Reaction						
$Cu + HCl = 0.5H_2 + CuCl$	-3.989	81.323	-0.075	-7.953	4.462	e
$CuBr + HCl = HBr + CuCl$	-0.170	-12.478	0.003	-4.216	0.551	i
$(CuBr)_3 + 3HCl = 3HBr + 3CuCl$	22.255	-312.237	0.051	-7.394	-23.968	f,i
$(CuCl)_3 = 3CuCl$	22.105	-275.129	0.046	3.845	-25.345	i
$CuF + HCl = HF + CuCl$	-0.209	77.222	-0.040	4.321	0.544	i
$CuF_2 + 0.5H_2 + HCl = 2HF + CuCl$	8.043	39.574	0.016	23.238	-12.920	i
$CuH + HCl = H_2 + CuCl$	-4.137	49.304	-0.180	-3.258	11.668	j,k
$CuO + 0.5H_2 + HCl = H_2O + CuCl$	-0.596	156.685	0.042	-9.922	-9.341	e
$F + 0.5H_2 = HF$	0.395	182.666	0.063	-0.007	-10.517	e
$FO_. + 1.5H_2 = H_2O + HF$	3.908	322.386	0.196	11.285	-22.376	e
$FO_2 + 2.5H_2 = 2H_2O + HF$	9.797	395.734	0.369	20.217	-39.816	e
$FS_2F + 3H_2 = 2H_2S + 2HF$	19.218	123.188	0.561	26.350	-53.085	i
$F_2 + H_2 = 2HF$	3.990	283.169	0.048	14.702	-10.718	e
$F_2O + 2H_2 = H_2O + 2HF$	10.143	419.132	0.226	27.966	-29.288	e
$Fe + 2HCl = H_2 + FeCl_2$	-9.904	196.652	-0.049	-15.174	11.263	e
$FeBr_2 + 2HCl = 2HBr + FeCl_2$	-1.008	-5.776	0.012	-8.264	0.515	i
$(FeBr_2)_2 + 4HCl = 4HBr + 2FeCl_2$	10.322	-102.498	0.124	-12.293	-12.965	i
$Fe(CO)_5 + 5H_2O + 2HCl = 6H_2 + 5CO_2 + FeCl_2$	3.055	2.854	-0.959	-38.360	60.786	j,o
$FeCl + HCl = 0.5H_2 + FeCl_2$	-6.303	157.693	0.012	-2.860	7.199	i
$(FeCl_2)_2 = 2FeCl_2$	10.904	-79.719	0.086	0.499	-13.613	i
$FeCl_3 + 0.5H_2 = HCl + FeCl_2$	7.319	-12.503	0.147	5.143	-11.504	i
$(FeCl_3)_2 + H_2 = 2HCl + 2FeCl_2$	28.426	-104.181	0.297	8.021	-43.372	i
$FeF + 2HCl = 0.5H_2 + HF + FeCl_2$	-7.381	146.322	-0.048	0.855	11.915	i
$FeF_2 + 2HCl = 2HF + FeCl_2$	4.528	55.824	0.118	26.895	-13.362	i
$FeF_3 + 0.5H_2 + 2HCl = 3HF + FeCl_2$	6.196	-25.968	-0.012	26.959	-6.358	i
$Fe(OH)_2 + 2HCl = 2H_2O + FeCl_2$	10.883	50.085	0.237	46.457	-32.466	j,m
$FeS + 2HCl = H_2S + FeCl_2$	-5.250	181.774	0.237	-7.917	-4.862	h

(continued)

Gas Species (continued)

Reaction[c]	l_0	$l_1 \times 10^{-2}$	$l_2 \times 10^3$	$l_3 \times 10^{-3}$	$l_4 \times 10^1$	Ref.[d]
$Ga + 3HCl = 1.5H_2 + GaCl_3$	-15.080	228.010	-0.060	-11.545	14.079	e
$GaCl + 2HCl = H_2 + GaCl_3$	-14.817	95.949	-0.155	-15.819	22.253	i
$GaCl_2 + HCl = 0.5H_2 + GaCl_3$	-9.142	53.454	-0.074	-8.070	13.786	i
$(GaCl_3)_2 = 2GaCl_3$	13.766	-52.215	0.005	4.236	-20.319	i
$GaF + 3HCl = H_2 + HF + GaCl_3$	-15.171	105.708	-0.205	-12.206	23.593	i
$GaF_2 + 3HCl = 0.5H_2 + 2HF + GaCl_3$	-9.803	87.551	-0.153	3.881	15.821	i
$GaF_3 + 3HCl = 3HF + GaCl_3$	-0.965	26.716	-0.120	18.936	2.998	i
$GaH + 3HCl = 2H_2 + GaCl_3$	-18.838	197.949	-0.359	-18.061	33.583	j,k
$Ga_2S + 6HCl = 2H_2 + H_2S + 2GaCl_3$	-27.395	190.019	-0.210	-24.865	40.896	n
$H = 0.5H_2$	0.025	112.616	0.048	2.042	-8.973	e
$HCO + H_2O = 1.5H_2 + CO_2$	-7.927	105.949	-0.295	-11.694	26.719	j,p
$HClO + H_2 = HCl + H_2O$	4.950	123.264	0.138	20.540	-15.035	j,m
$(HF)_2 = 2HF$	5.240	-15.391	-0.168	30.037	2.991	i
$(HF)_3 = 3HF$	16.867	-36.758	-0.197	58.233	-13.554	i
$(HF)_4 = 4HF$	26.246	-55.957	-0.262	77.585	-24.644	i
$(HF)_5 = 5HF$	35.691	-75.759	-0.331	96.690	-35.679	i
$(HF)_6 = 6HF$	44.866	-101.669	-0.418	115.190	-45.557	i
$(HF)_7 = 7HF$	53.974	-115.348	-0.517	131.154	-55.090	i
$OH + 0.5H_2 = H_2O$	0.348	145.545	0.142	-5.589	-12.501	e
$HO_2 + 1.5H_2 = 2H_2O$	4.478	249.864	0.224	14.215	-23.815	e
$HS + 0.5H_2 = H_2S$	0.262	83.093	0.185	-13.656	-11.687	h
$HSO_3F + 4H_2 = 3H_2O + H_2S + HF$	28.786	124.905	0.510	74.266	-74.537	j,p

Reaction						
$H_2O_2 + H_2 = 2H_2O$	4.822	178.603	0.026	15.396	-13.765	f,e
$H_2SO_4 + 4H_2 = H_2S + 4H_2O$	32.042	116.817	0.597	73.366	-83.473	h
$H_2S_2 + H_2 = 2H_2S$	6.222	27.164	0.200	4.928	-19.045	f,h
$HgBr + 0.5H_2 = HBr + Hg$	2.856	40.944	0.047	0.284	-3.299	i
$HgBr_2 + H_2 = 2HBr + Hg$	11.243	-44.135	0.159	4.722	-16.996	i
$HgCl + 0.5H_2 = HCl + Hg$	2.952	56.501	0.045	3.142	-3.562	i
$HgCl_2 + H_2 = 2HCl + Hg$	11.632	-12.335	0.147	11.934	-17.714	i
$HgF + 0.5H_2 = HF + Hg$	3.093	111.112	0.031	9.015	-4.066	i
$HgF_2 + H_2 = 2HF + Hg$	11.984	96.178	0.100	24.731	-17.882	i
$HgH = 0.5H_2 + Hg$	0.381	92.084	-0.101	10.979	2.993	g
$HgO + H_2 = H_2O + Hg$	3.998	113.920	0.163	5.623	-14.930	e
$HgS + H_2 = H_2S + Hg$	3.702	47.255	0.236	-3.489	-14.089	h
$IrF_6 + 3H_2 = 6HF + Ir$	45.782	210.766	0.326	89.770	-65.078	i
$K + HCl = 0.5H_2 + KCl$	-3.672	111.169	-0.075	-6.212	4.874	e
$KBr + HCl = HBr + KCl$	-0.055	-11.296	0.010	-1.529	0.178	i
$(KBr)_2 + 2HCl = 2HBr + 2KCl$	9.133	-117.927	0.051	-4.522	-9.154	i
$KCN + 2H_2O + HCl = 2.5H_2 + CO_2 + KCl + 0.5N_2$	-6.238	63.326	-0.329	-21.791	31.624	j,m
$(KCl)_2 = 2KCl$	9.694	-100.419	0.056	2.367	-10.881	i
$KF + HCl = HF + KCl$	-0.371	36.482	-0.054	0.478	1.299	i
$(KF)_2 + 2HCl = 2HF + 2KCl$	10.106	-39.821	-0.006	8.403	-10.730	i
$KH + HCl = H_2 + KCl$	-1.536	131.998	-0.070	8.806	3.036	j,k
$KO + 0.5H_2 + HCl = H_2O + KCl$	0.596	225.455	0.139	0.015	-13.511	e
$KOH + HCl = H_2O + KCl$	4.145	66.422	0.093	5.288	-13.400	j,p
$(KOH)_2 + 2HCl = 2H_2O + 2KCl$	12.249	33.771	-0.149	34.538	-12.860	j,p
$KS + 0.5H_2 + HCl = H_2S + KCl$	-0.015	131.675	0.203	-5.112	-10.732	h
$K_2 + 2HCl = H_2 + 2KCl$	-4.389	195.545	-0.156	-6.187	12.522	e
$K_2S + 2HCl = H_2S + 2KCl$	1.858	129.920	0.125	-8.556	-5.468	h

APPENDIX 2

(continued)

Gas Species (continued)

Reaction[c]	l_0	$l_1 \times 10^{-2}$	$l_2 \times 10^3$	$l_3 \times 10^{-3}$	$l_4 \times 10^1$	Ref.[d]
$K_2SO_4 + 4H_2 + 2HCl = H_2S + 2KCl + 4H_2O$	37.341	55.003	0.708	76.181	-95.207	j,k
$Li + HCl = 0.5H_2 + LiCl$	-3.513	138.872	-0.052	-10.731	3.272	e
$LiAlF_4 + HCl = HF + AlF_3 + LiCl$	13.846	-143.428	0.075	27.008	-20.106	j,m
$LiBr + HCl = HBr + LiCl$	0.094	-7.539	0.017	-0.857	-0.330	i
$(LiBr)_2 + 2HCl = 2HBr + 2LiCl$	9.904	-117.006	0.046	-2.341	-10.021	i
$LiClO + H_2 = LiCl + H_2O$	6.050	217.391	0.169	21.149	-17.719	j,m
$(LiCl)_2 = 2LiCl$	10.028	-107.512	0.015	3.956	-9.746	i
$(LiCl)_3 = 3LiCl$	22.248	-201.518	-0.014	35.146	-20.726	i
$LiF + HCl = HF + LiCl$	-0.548	19.177	-0.054	1.846	1.987	i
$LiFO + H_2 + HCl = HF + LiCl + H_2O$	6.136	271.078	0.143	22.454	-18.399	j,m
$(LiF)_2 + 2HCl = 2HF + 2LiCl$	10.291	-101.083	-0.038	26.818	-8.969	i
$(LiF)_3 + 3HCl = 3HF + 3LiCl$	21.710	-206.765	-0.072	40.041	-22.473	i
$LiH + HCl = H_2 + LiCl$	-2.678	127.392	-0.134	-0.493	6.900	j,k
$LiNaO + 2HCl = H_2O + NaCl + LiCl$	1.300	168.327	0.017	11.284	-3.835	j,m
$LiO + 0.5H_2 + HCl = H_2O + LiCl$	0.165	222.773	0.113	-2.254	-11.895	e
$LiOH + HCl = H_2O + LiCl$	4.563	55.512	0.122	6.440	-14.937	j,p
$(LiOH)_2 + 2HCl = 2H_2O + 2LiCl$	12.779	-16.035	-0.157	44.624	-13.218	j,p
$Li_2 + 2HCl = H_2 + 2LiCl$	-4.199	220.322	-0.140	-16.840	11.520	e
$Li_2ClF + HCl = HF + 2LiCl$	10.292	-97.998	-0.014	25.969	-8.385	j,m
$Li_2O + 2HCl = H_2O + 2LiCl$	4.557	144.746	0.094	5.498	-13.520	g
$Li_2O_2 + H_2 + 2HCl = 2H_2O + 2LiCl$	12.219	228.714	0.327	2.774	-37.980	g
$Li_2SO_4 + 4H_2 + 2HCl = H_2S + 2LiCl + 4H_2O$	36.390	63.038	0.659	74.264	-93.511	j,k

Reaction						
$Mg + 2HCl = H_2 + MgCl_2$	-11.020	187.975	-0.142	-12.305	17.103	e
$MgBr + 2HCl = 0.5H_2 + HBr + MgCl_2$	-8.304	111.711	-0.086	-11.042	14.376	i
$MgBr_2 + 2HCl = 2HBr + MgCl_2$	-0.285	-11.215	0.009	-5.105	0.683	i
$(MgBr_2)_2 + 4HCl = 4HBr + 2MgCl_2$	10.130	-108.195	0.050	-14.779	-10.412	i
$MgCl + HCl = 0.5H_2 + MgCl_2$	-7.729	135.886	-0.061	-3.847	12.549	i
$MgClF + HCl = HF + MgCl_2$	-1.298	2.385	-0.027	8.412	5.056	j,m
$(MgCl_2)_2 = 2MgCl_2$	10.453	-90.050	0.029	0.865	-11.726	i
$MgF + 2HCl = 0.5H_2 + HF + MgCl_2$	-8.456	129.682	-0.134	-3.547	15.089	i
$MgF_2 + 2HCl = 2HF + MgCl_2$	-2.129	14.585	-0.083	10.404	6.847	i
$(MgF_2)_2 + 4HCl = 4HF + 2MgCl_2$	11.224	-112.774	-0.155	33.494	-7.438	i
$MgH + 2HCl = 1.5H_2 + MgCl_2$	-11.332	199.960	-0.244	-6.484	22.345	j,k
$MgO + 2HCl = H_2O + MgCl_2$	-3.764	262.952	-0.086	17.539	-7.942	e
$MgOH + 2HCl = 0.5H_2 + H_2O + MgCl_2$	-3.326	148.045	0.032	10.903	-0.615	j,l
$Mg(OH)_2 + 2HCl = 2H_2O + MgCl_2$	6.788	57.929	0.137	26.699	-20.132	j,p
$MgS + 2HCl = H_2S + MgCl_2$	0.286	190.617	0.259	30.575	-21.230	h
$Mg_2 + 4HCl = 2H_2 + 2MgCl_2$	-23.855	375.523	-0.287	-35.072	49.649	e
$Mn + 2HCl = H_2 + MnCl_2$	-14.202	194.335	-0.211	-16.097	25.853	e
$MnBr_2 + 2HCl = 2HBr + MnCl_2$	-2.268	-26.814	-0.111	-14.670	10.886	g
$MnF_2 + 2HCl = 2HF + MnCl_2$	-3.061	51.944	-0.143	8.724	9.556	f,i
$Mo + 4H_2O = 3H_2 + H_2MoO_4$	-35.073	298.815	-0.531	-71.965	84.885	e
$MoBr + 4H_2O = 2.5H_2 + HBr + H_2MoO_4$	-31.699	211.974	-0.460	-70.316	81.439	i
$MoBr_2 + 4H_2O = 2H_2 + 2HBr + H_2MoO_4$	-19.027	75.487	-0.189	-62.502	52.293	i
$MoBr_3 + 4H_2O = 1.5H_2 + 3HBr + H_2MoO_4$	-17.106	3.678	-0.346	-63.622	60.184	i
$MoBr_4 + 4H_2O = H_2 + 4HBr + H_2MoO_4$	-7.659	-64.911	-0.170	-54.543	43.748	i
$MoCl_4 + 4H_2O = H_2 + 4HCl + H_2MoO_4$	-7.346	-60.660	-0.207	-42.470	43.190	i
$MoCl_5 + 4H_2O = 0.5H_2 + 5HCl + H_2MoO_4$	1.525	-47.402	-0.150	-34.668	30.059	i
$MoCl_6 + 4H_2O = 6HCl + H_2MoO_4$	10.961	3.200	-0.061	-32.271	15.429	i

Gas Species (continued)

Reaction[c]	l_0	$l_1 \times 10^{-2}$	$l_2 \times 10^3$	$l_3 \times 10^{-3}$	$l_4 \times 10^1$	Ref.[d]
$MoF + 4H_2O = 2.5H_2 + HF + H_2MoO_4$	-31.973	244.155	-0.514	-62.574	82.459	i
$MoF_2 + 4H_2O = 2H_2 + 2HF + H_2MoO_4$	-22.705	151.547	-0.408	-54.721	65.554	i
$MoF_3 + 4H_2O = 1.5H_2 + 3HF + H_2MoO_4$	-17.074	60.360	-0.495	-34.511	62.294	i
$MoF_4 + 4H_2O = H_2 + 4HF + H_2MoO_4$	-9.000	22.436	-0.391	-18.315	48.493	i
$MoF_5 + 4H_2O = 0.5H_2 + 5HF + H_2MoO_4$	1.513	7.511	-0.307	9.380	29.352	i
$MoF_6 + 4H_2O = 6HF + H_2MoO_4$	8.689	-16.026	-0.352	14.545	23.887	i
$MoO + 3H_2O = 2H_2 + H_2MoO_4$	-30.360	241.220	-0.322	-70.280	68.032	e
$MoOF_4 + 3H_2O = H_2MoO_4 + 4HF$	1.813	-17.152	-0.182	12.184	22.215	j,m
$MoO_2 + 2H_2O = H_2 + H_2MoO_4$	-23.572	196.848	-0.140	-45.162	49.386	e
$MoO_2Cl_2 + 2H_2O = 2HCl + H_2MoO_4$	-5.804	-38.003	0.013	-23.025	21.583	j,m
$MoO_3 + H_2O = H_2MoO_4$	-14.302	142.907	0.008	-32.756	26.930	e
$N = 0.5N_2$	-0.269	245.553	0.081	2.785	-9.456	e
$NBr + 0.5H_2 = HBr + 0.5N_2$	2.736	174.330	0.116	8.054	-10.455	i
$CN + 2H_2O = 2H_2 + CO_2 + 0.5N_2$	-10.265	196.927	-0.294	-26.070	33.187	j,k
$ClCN + 2H_2O = 1.5H_2 + CO_2 + HCl + 0.5N_2$	-1.541	75.769	-0.234	-3.617	19.724	j,m
$HCN + 2H_2O = 2.5H_2 + CO_2 + 0.5N_2$	-6.594	27.882	-0.354	-5.679	33.367	j,m
$CNC + 4H_2O = 4H_2 + 2CO_2 + 0.5N_2$	-10.609	203.593	-0.430	-21.313	47.248	j,m
$CF_3CN + 4H_2O = 2.5H_2 + 2CO_2 + 3HF + 0.5N_2$	8.631	75.761	-0.496	45.187	30.055	j,m
$NCO + H_2O = H_2 + CO_2 + 0.5N_2$	-1.353	163.168	-0.093	4.905	8.477	j,m
$NF + 0.5H_2 = HF + 0.5N_2$	1.935	270.921	0.046	12.430	-8.246	i
$NF_2 + H_2 = 2HF + 0.5N_2$	7.543	303.710	0.052	32.222	-13.545	i
$NF_3 + 1.5H_2 = 3HF + 0.5N_2$	15.969	352.341	0.055	57.497	-24.019	i

Reaction						Ref
$NH = 0.5H_2 + 0.5N_2$	-1.246	196.860	-0.008	-1.569	0.632	j,o
$HNCO + H_2O = 1.5H_2 + CO_2 + 0.5N_2$	-0.485	123.695	-0.185	14.048	16.668	j,p
$NH_2 = H_2 + 0.5N_2$	-1.432	100.332	-0.132	6.328	11.138	j,o
$NH_3 = 1.5H_2 + 0.5N2$	-0.260	-23.186	-0.295	23.204	20.171	j,o
$NO + H_2 = H_2O + 0.5N_2$	1.228	171.695	0.140	-0.549	-14.711	e
$NOBr + 1.5H_2 = H_2O + HBr + 0.5N_2$	8.473	183.786	0.284	18.455	-26.517	j,m
$ONCl + 1.5H_2 = H_2O + HCl + 0.5N_2$	8.585	196.799	0.253	22.486	-26.687	j,q
$ONF + 1.5H_2 = H_2O + HF + 0.5N_2$	8.348	229.748	0.231	28.350	-25.514	j,m
$HNO + 0.5H_2 = H_2O + 0.5N_2$	3.844	175.243	0.118	22.584	-12.840	j,m
$NO_2 + 2H_2 = 2H_2O + 0.5N_2$	7.322	264.892	0.271	21.091	-29.916	e
$NO_2Cl + 2.5H_2 = 2H_2O + HCl + 0.5N_2$	17.476	297.901	0.414	50.888	-47.908	j,m
$cis\text{-}HNO_2 + 1.5H_2 = 2H_2O + 0.5N_2$	11.690	205.350	0.273	44.832	-33.962	j,m
$trans\text{-}HNO2 + 1.5H_2 = 2H_2O + 0.5N_2$	12.208	203.933	0.309	47.054	-35.720	j,m
$NO_3 + 3H_2 = 3H_2O + 0.5N_2$	20.078	403.506	0.596	70.944	-64.323	j,m
$HNO_3 + 2.5H_2 = 3H_2O + 0.5N_2$	20.488	296.590	0.446	79.740	-55.865	j,m
$NS + H_2 = H_2S + 0.5N_2$	3.097	146.412	0.304	5.458	-20.272	h
$CNN + 2H_2O = 2H_2 + CO_2 + N_2$	-3.919	261.396	-0.235	-3.801	24.078	j,m
$NCN + 2H_2O = 2H_2 + CO_2 + N_2$	-2.082	201.795	-0.221	5.126	19.090	j,p
$C_2N_2 + 4H_2O = 4H_2 + 2CO_2 + N_2$	-9.143	75.959	-0.684	-26.456	57.789	g
$C_4N_2 + 8H_2O = 8H_2 + 4CO_2 + N_2$	-14.952	105.569	-1.102	-40.493	104.330	j,m
$cis\text{-}N_2F_2 + H_2 = 2HF + N_2$	13.534	315.406	0.005	54.235	-17.763	i
$trans\text{-}N_2F_2 + H_2 = 2HF + N_2$	12.935	322.788	-0.018	43.915	-16.565	i
$N_2F_4 + 2H_2 = 4HF + N_2$	29.995	554.679	0.024	98.946	-41.168	i
$cis\text{-}N_2H_2 = H_2 + N_2$	3.404	109.346	-0.179	43.065	8.928	j,m
$N_2H_4 = 2H_2 + N_2$	9.660	45.201	-0.313	82.003	9.031	j,m
$N_2O + H_2 = H_2O + N_2$	6.901	165.554	0.078	20.564	-17.734	e
$N_2O_3 + 3H_2 = 3H_2O + N_2$	18.628	413.430	0.386	39.889	-53.098	e

Gas Species (continued)

Reaction[c]	l_0	$l_1 \times 10^{-2}$	$l_2 \times 10^3$	$l_3 \times 10^{-3}$	$l_4 \times 10^1$	Ref.[d]
$N_2O_4 + 4H_2 = 4H_2O + N_2$	28.714	496.230	0.481	65.724	-75.639	e
$N_2O_5 + 5H_2 = 5H_2O + N_2$	39.135	618.368	0.841	85.648	-108.557	e
$N_3 = 1.5N_2$	7.447	212.334	0.065	34.994	-13.459	j,p
$Na + HCl = 0.5H_2 + NaCl$	-3.526	101.147	-0.055	-5.374	3.873	e
$NaAlF_4 + HCl = HF + NaCl + AlF_3$	13.771	-160.692	0.077	21.218	-20.141	j,m
$NaBr + HCl = HBr + NaCl$	-0.157	-11.485	-0.002	-1.909	0.531	i
$(NaBr)_2 + 2HCl = 2HBr + 2NaCl$	9.505	-128.892	0.037	-4.036	-8.831	i
$(NaCl)_2 = 2NaCl$	10.048	-115.245	0.045	2.284	-10.474	i
$NaF + HCl = HF + NaCl$	-0.025	34.403	-0.030	4.331	0.147	i
$(NaF)_2 + 2HCl = 2HF + 2NaCl$	10.586	-62.169	-0.031	20.773	-9.331	i
$NaH + HCl = H_2 + NaCl$	-2.561	112.612	-0.133	2.777	6.538	j,k
$NaO + 0.5H_2 + HCl = H_2O + NaCl$	0.407	212.552	0.129	-0.805	-12.944	e
$NaOH + HCl = H_2O + NaCl$	4.430	64.850	0.120	6.389	-14.639	j,p
$(NaOH)_2 + 2HCl = 2H_2O + 2NaCl$	12.826	18.786	-0.121	40.099	-14.338	j,p
$Na_2 + 2HCl = H_2 + 2NaCl$	-4.621	162.245	-0.167	-10.797	13.344	e
$Na_2SO_4 + 4H_2 + 2HCl = H_2S + 2NaCl + 4H_2O$	36.923	47.606	0.672	76.196	-93.537	j,k
$Ni + 2HCl = H_2 + NiCl_2$	-12.174	168.169	-0.145	-13.565	18.816	e
$NiBr + 2HCl = 0.5H_2 + HBr + NiCl_2$	-9.360	58.444	-0.111	-10.005	18.733	i
$NiBr_2 + 2HCl = 2HBr + NiCl_2$	-0.589	-14.789	-0.021	-8.491	1.864	i
$Ni(CO)_4 + 4H_2O + 2HCl = 5H_2 + 4CO_2 + NiCl_2$	-1.531	-47.279	-0.597	-53.489	51.428	j,o
$NiCl + HCl = 0.5H_2 + NiCl_2$	-9.571	85.543	-0.131	-10.296	19.376	i
$NiF + 2HCl = 0.5H_2 + HF + NiCl_2$	-10.145	140.698	-0.197	-6.712	21.385	i

Reaction						
$NiF_2 + 2HCl = 2HF + NiCl_2$	-1.037	50.044	-0.099	13.539	4.101	i
$NiH + 2HCl = 1.5H_2 + NiCl_2$	-14.493	150.974	-0.306	-17.676	33.578	j,k
$NiO + 2HCl = H_2O + NiCl_2$	-8.167	229.275	-0.002	-5.028	4.910	e
$NiS + 2HCl = H_2S + NiCl_2$	-8.204	139.192	0.083	-9.540	5.775	h
$O + H_2 = H_2O$	1.000	253.915	0.214	-2.688	-22.436	e
$O_3 + 3H_2 = 3H_2O$	11.767	445.443	0.502	28.944	-51.928	e
$Pb + 2HCl = H_2 + PbCl_2$	-9.330	98.948	-0.178	-9.738	13.889	e
$PbBr + 2HCl = 0.5H_2 + HBr + PbCl_2$	-6.231	52.210	-0.093	-7.772	9.647	i
$PbBr_2 + 2HCl = 2HBr + PbCl_2$	-0.297	-21.494	0.004	-6.076	1.025	i
$PbBr_4 + H_2 + 2HCl = 4HBr + PbCl_2$	17.084	-171.175	0.176	0.252	-26.547	i
$PbCl + HCl = 0.5H_2 + PbCl_2$	-5.804	51.847	-0.080	-3.733	8.491	i
$PbCl_4 + H_2 = 2HCl + PbCl_2$	17.210	-105.266	0.133	10.333	-26.962	i
$PbF + 2HCl = 0.5H_2 + HF + PbCl_2$	-6.017	96.315	-0.112	0.513	8.835	i
$PbF_2 + 2HCl = 2HF + PbCl_2$	0.192	51.708	-0.048	13.812	-0.365	i
$PbF_4 + H_2 + 2HCl = 4HF + PbCl_2$	17.023	-32.270	0.006	35.675	-25.901	i
$PbH + 2HCl = 1.5H_2 + PbCl_2$	-9.336	120.141	-0.244	-0.848	17.945	j,k
$PbO + 2HCl = H_2O + PbCl_2$	-4.987	157.356	0.024	-2.253	-2.309	e
$PbS + 2HCl = H_2S + PbCl_2$	-5.316	74.830	0.084	-11.409	-0.659	j,k
$PbSe + 2HCl = H_2Se + PbCl_2$	-5.473	46.261	0.117	-15.141	-0.170	n
$PbTe + 2HCl = H_2Te + PbCl_2$	-6.322	25.201	0.074	-17.739	3.091	n
$Pb_2 + 4HCl = 2H_2 + 2PbCl_2$	-15.860	167.476	-0.337	-16.538	30.689	e
$Rb + HCl = 0.5H_2 + RbCl$	-3.524	114.407	-0.065	-4.719	4.561	e
$Rb_2 + 2HCl = H_2 + 2RbCl$	2.573	174.678	-0.154	-5.913	12.957	n
$S + H_2 = H2S$	1.094	153.537	0.276	-8.943	-21.310	e
$SBr_2 + 2H_2 = H_2S + 2HBr$	11.145	37.945	0.423	8.130	-31.660	n
$SCl + 1.5H_2 = H_2S + HCl$	4.893	137.931	0.343	-1.935	-24.889	i
$SClF_5 + 4H_2 = H2S + HCl + 5HF$	45.009	213.163	0.418	111.252	-76.110	h

Gas Species (continued)

Reaction[c]	l_0	$l_1 \times 10^{-2}$	$l_2 \times 10^3$	$l_3 \times 10^{-3}$	$l_4 \times 10^1$	Ref.[d]
$SCl_2 + 2H_2 = H_2S + 2HCl$	10.831	93.570	0.387	11.729	-31.010	i
$SF + 1.5H_2 = H_2S + HF$	4.872	157.012	0.323	5.932	-24.691	i
$SF_2 + 2H_2 = H2S + 2HF$	9.918	136.556	0.288	21.377	-27.700	i
$SF_3 + 2.5H_2 = H_2S + 3HF$	17.665	168.220	0.282	45.823	-37.510	i
$SF_4 + 3H_2 = H_2S + 4HF$	26.906	172.354	0.361	63.244	-53.262	i
$SF_5 + 3.5H_2 = H_2S + 5HF$	36.073	235.878	0.373	90.830	-65.179	i
$SF_6 + 4H_2 = H_2S + 6HF$	44.622	212.631	0.326	122.552	-71.422	i
$SO + 2H_2 = H_2O + H_2S$	4.323	135.752	0.391	3.409	-31.442	e
$SOCl_2 + 3H_2 = H_2O + H_2S + 2HCl$	18.328	114.828	0.468	24.406	-50.784	f,n
$SOF_2 + 3H_2 = H2O + H2S + 2HF$	18.233	129.594	0.434	43.468	-49.158	h
$SO_2 + 3H_2 = 2H_2O + H_2S$	10.275	101.810	0.509	15.317	-45.939	e
$SO_2ClF + 4H_2 = 2H_2O + H_2S + HCl + HF$	26.386	151.474	0.536	57.250	-68.324	j,p
$SO_2Cl_2 + 4H_2 = 2H_2O + H_2S + 2HCl$	26.787	163.269	0.600	40.816	-69.566	h
$SO_2F_2 + 4H_2 = 2H_2O + H_2S + 2HF$	26.538	139.962	0.544	66.780	-67.398	h
$SO_3 + 4H_2 = 3H_2O + H_2S$	19.691	171.979	0.706	42.441	-68.791	e
$SSF_2 + 3H_2 = 2H_2S + 2HF$	19.237	88.877	0.558	34.062	-52.648	i
$S_2 + 2H_2 = 2H_2S$	4.741	85.123	0.451	-1.518	-31.279	e
$S_2Br_2 + 3H_2 = 2H_2S + 2HBr$	18.479	69.215	0.580	2.780	-52.674	f,h
$S_2Cl + 2.5H_2 = 2H_2S + HCl$	10.835	105.511	0.574	6.546	-41.838	i
$S_2Cl_2 + 3H_2 = 2H2S + 2HCl$	19.299	101.611	0.599	15.369	-55.128	f,i
$S_2F_{10} + 7H_2 = 2H_2S + 10HF$	87.148	338.585	0.641	213.601	-142.348	i
$S_2O + 3H_2 = H_2O + 2H_2S$	11.492	119.664	0.671	15.234	-50.836	h

Reaction						
$S_3 + 3H_2 = 3H_2S$	12.464	100.580	0.779	7.535	-52.755	e
$S_4 + 4H_2 = 4H_2S$	22.049	103.853	1.022	17.455	-75.998	e
$S_5 + 5H_2 = 5H_2S$	30.582	105.916	1.271	15.075	-100.330	e
$S_6 + 6H_2 = 6H_2S$	40.531	101.475	1.521	12.513	-124.600	e
$S_7 + 7H_2 = 7H_2S$	48.900	112.817	1.768	15.521	-148.519	e
$S_8 + 8H_2 = 8H_2S$	58.691	116.391	2.047	19.602	-173.799	e
$Sb + 3HCl = 1.5H_2 + SbCl_3$	-18.570	160.752	-0.222	-18.108	26.659	e
$SbBr_3 + 3HCl = 3HBr + SbCl3$	-0.348	-24.621	0.021	-9.062	0.786	f,i
$SbCl_5 + H_2 = 2HCl + SbCl_3$	17.616	49.926	0.170	14.299	-28.000	f,n
$SbF_3 + 3HCl = 3HF + SbCl_3$	-0.338	21.831	-0.118	20.679	1.601	f,i
$SbH_3 + 3HCl = 3H_2 + SbCl_3$	-14.072	98.280	-0.556	19.742	39.038	f,n
$SbS + 3HCl = 0.5H_2 + H_2S + SbCl_3$	-13.905	129.546	-0.007	-15.584	11.315	h
$(SbS)_2 + 6HCl = H_2 + 2H_2S + 2SbCl_3$	-17.484	152.659	0.061	-23.203	15.823	h
$(SbS)_3 + 9HCl = 1.5H_2 + 3H_2S + 3SbCl_3$	-16.513	165.719	0.101	-29.423	12.984	h
$(SbS)_4 + 12HCl = 2H_2 + 4H_2S + 4SbCl_3$	-19.604	189.785	0.179	-63.477	7.621	h
$Sb_2 + 6HCl = 3H_2 + 2SbCl_3$	-32.896	170.890	-0.427	-33.432	57.755	e
$Sb_2S_3 + 6HCl = 3H_2S + 2SbCl_3$	-10.111	134.667	0.328	-34.003	-9.500	h
$Sb_2S_4 + H_2 + 6HCl = 4H_2S + 2SbCl_3$	0.060	128.589	0.618	-30.776	-35.507	h
$Sb_3S_2 + 9HCl = 2.5H_2 + 2H_2S + 3SbCl_3$	-28.157	168.809	-0.128	-41.931	35.710	h
$Sb_4 + 12HCl = 6H_2 + 4SbCl_3$	-54.727	201.628	-0.865	-67.885	106.126	e
$Sb_4O_6 + 12HCl = 4SbCl_3 + 6H_2O$	2.364	192.908	0.114	23.876	-42.854	f,e
$Sb_4S_3 + 12HCl = 3H_2 + 3H_2S + 4SbCl_3$	-28.669	199.706	-0.067	-61.729	31.675	h
$Se + H2 = H_2Se$	1.117	105.367	0.255	-1.926	-20.317	e
$SeBr_2 + 2H_2 = H_2Se + 2HBr$	9.790	8.435	0.460	2.543	-27.701	i
$CSe + 2H_2O = H_2 + CO_2 + H_2Se$	-8.358	134.032	-0.057	-31.165	21.034	j,k
$CSe_2 + 2H_2O = CO_2 + 2H_2Se$	2.138	57.836	0.279	-19.164	-6.743	j,k
$SeCl_2 + 2H_2 = H_2Se + 2HCl$	11.146	59.273	0.449	8.389	-32.505	i

Gas Species (continued)

Reaction[c]	l_0	$l_1 \times 10^{-2}$	$l_2 \times 10^3$	$l_3 \times 10^{-3}$	$l_4 \times 10^1$	Ref.[d]
$SeF + 1.5H_2 = H_2Se + HF$	4.320	102.643	0.317	6.026	-21.862	i
$SeF_2 + 2H_2 = H_2Se + 2HF$	11.149	101.636	0.389	22.900	-31.882	i
$SeF_4 + 3H_2 = H_2Se + 4HF$	27.863	120.045	0.403	77.038	-53.172	i
$SeF_5 + 3.5H_2 = H_2Se + 5HF$	36.563	193.315	0.450	80.837	-68.165	i
$SeF_6 + 4H_2 = H_2Se + 6HF$	46.883	240.473	0.499	107.403	-81.718	i
$SeO + 2H_2 = H_2O + H_2Se$	5.087	134.518	0.465	5.590	-33.954	e
$SeO_2 + 3H_2 = 2H_2O + H_2Se$	11.406	172.990	0.580	16.156	-50.176	e
$Se_2 + 2H_2 = 2H_2Se$	8.508	37.400	0.660	-2.422	-42.735	e
$Se_2Br_2 + 3H_2 = 2H_2Se + 2HBr$	19.033	16.271	0.703	-1.275	-55.245	f,i
$Se_2Cl_2 + 3H_2 = 2H_2Se + 2HCl$	19.726	47.217	0.725	7.519	-57.227	f,i
$Se_3 + 3H_2 = 3H_2Se$	12.127	40.665	0.791	-10.071	-52.712	e
$Se_4 + 4H_2 = 4H_2Se$	20.527	26.234	1.183	-11.112	-78.137	e
$Se_5 + 5H_2 = 5H_2Se$	31.070	-15.200	1.428	-13.112	-100.186	e
$Se_6 + 6H_2 = 6H_2Se$	40.359	-34.868	1.746	-15.617	-125.693	e
$Se_7 + 7H_2 = 7H_2Se$	48.988	-48.432	2.027	-15.535	-149.568	e
$Se_8 + 8H_2 = 8H_2Se$	57.917	-60.339	2.309	-23.760	-173.340	e
$Si + 4HF = 2H_2 + SiF_4$	-25.800	516.392	-0.049	-71.937	28.779	e
$SiBr + 4HF = 1.5H_2 + HBr + SiF_4$	-20.950	421.565	0.075	-64.493	21.795	i
$SiBr_2 + 4HF = H_2 + 2HBr + SiF_4$	-15.125	289.040	0.140	-55.038	15.565	i
$SiBr_3 + 4HF = 0.5H_2 + 3HBr + SiF_4$	-6.852	227.905	0.208	-47.315	2.866	i
$SiBr_4 + 4HF = 4HBr + SiF_4$	2.318	133.432	0.270	-43.733	-9.656	i
$SiC + 2H_2O + 4HF = 4H_2 + CO_2 + SiF_4$	-26.746	611.760	0.003	-76.484	41.183	j,k

Reaction						
$SiCH_3Cl_3 + 2H_2O + 4HF = 4H_2 + CO_2 + 3HCl + SiF_4$	-7.684	101.217	-0.725	-11.932	55.318	f,j,m
$SiCH_3F_3 + 2H_2O + HF = 4H_2 + CO_2 + SiF_4$	-9.848	16.786	-0.939	7.111	63.488	f,j,m
$SiC_2 + 4H_2O + 4HF = 6H_2 + 2CO_2 + SiF_4$	-37.332	517.537	-0.644	-99.156	91.187	j,k
$Si(CH_3)_4 + 8H_2O + 4HF = 16H_2 + 4CO_2 + SiF_4$	-37.519	-36.371	-3.647	13.773	255.381	f,j,m
$SiCl + 4HF = 1.5H_2 + HCl + SiF_4$	-21.632	431.566	0.038	-61.133	23.949	i
$ClSiF_3 + HF = HCl + SiF_4$	1.014	60.100	0.104	-4.073	-6.143	j,m
$SiCl_2 + 4HF = H_2 + 2HCl + SiF_4$	-14.833	286.106	0.129	-47.178	14.928	i
$SiCl_3 + 4HF = 0.5H_2 + 3HCl + SiF_4$	-6.467	216.045	0.200	-35.519	1.692	i
$SiCl_4 + 4HF = 4HCl + SiF_4$	3.038	119.545	0.258	-22.765	-11.095	i
$SiF + 3HF = 1.5H_2 + SiF_4$	-22.333	412.085	-0.022	-58.353	26.417	i
$FSiCl_3 + 3HF = 3HCl + SiF_4$	2.345	120.601	0.244	-19.231	-11.834	j,m
$SiF_2 + 2HF = H_2 + SiF_4$	-15.794	255.803	0.027	-35.368	18.624	i
$SiF_3 + HF = 0.5H_2 + SiF_4$	-8.500	136.320	0.015	-18.570	9.064	i
$SiH + 4HF = 2.5H_2 + SiF_4$	-26.020	478.243	-0.151	-66.570	36.259	j,k
$SiHBr_3 + 4HF = H_2 + 3HBr + SiF_4$	-2.770	173.272	0.120	-23.376	2.346	j,o
$SiHCl_3 + 4HF = H_2 + 3HCl + SiF_4$	-2.522	158.921	0.100	-9.033	1.877	j,o
$SiHF_3 + HF = H_2 + SiF_4$	-6.115	74.953	-0.216	5.735	14.890	j,l
$SiH_2 + 4HF = 3H_2 + SiF_4$	-20.958	406.383	-0.228	-29.263	30.479	j,k
$SiH_2Br_2 + 4HF = 2H_2 + 2HBr + SiF_4$	-9.906	214.908	-0.214	-16.196	22.413	j,o
$SiH_2Cl_2 + 4HF = 2H_2 + 2HCl + SiF_4$	-10.091	204.921	-0.256	-8.099	23.387	j,o
$SiH_2F_2 + 2HF = 2H_2 + SiF_4$	-11.559	148.087	-0.387	5.035	28.900	j,l
$SiH_3 + 4HF = 3.5H_2 + SiF_4$	-22.763	389.427	-0.495	-27.140	47.394	j,k
$SiH_3Br + 4HF = 3H_2 + HBr + SiF_4$	-15.306	255.764	-0.448	-7.813	38.079	j,o
$SiH_3Cl + 4HF = 3H_2 + HCl + SiF_4$	-15.322	251.501	-0.460	-3.841	38.303	j,o
$SiH_3F + 3HF = 3H_2 + SiF_4$	-16.128	223.318	-0.534	2.969	41.339	j,l
$SiH_4 + 4HF = 4H_2 + SiF_4$	-20.649	297.627	-0.710	-9.448	55.086	j,k
$SiO + 4HF = H_2 + H_2O + SiF_4$	-21.066	352.713	0.131	-56.649	15.334	e

Gas Species (continued)

Reaction[c]	l_0	$l_1 \times 10^{-2}$	$l_2 \times 10^3$	$l_3 \times 10^{-3}$	$l_4 \times 10^1$	Ref.[d]
$SiOF_2 + 2HF = H_2O + SiF_4$	-8.276	180.552	0.083	-11.450	1.382	j,m
$SiO_2 + 4HF = 2H_2O + SiF_4$	-12.561	358.967	0.275	-39.623	-6.243	e
$SiS + 4HF = H_2 + H_2S + SiF_4$	-20.868	344.960	0.201	-62.484	15.124	h
$SiS_2 + 4HF = 2H_2S + SiF_4$	-11.869	300.920	0.449	-56.945	-8.082	h
$SiSe + 4HF = H_2 + H_2Se + SiF_4$	-20.448	369.498	0.267	-63.425	13.823	n
$SiTe + 4HF = H2 + H2Te + SiF4$	-21.733	342.546	0.194	-70.817	18.407	j,k
$Si_2 + 8HF = 4H_2 + 2SiF_4$	-45.569	868.367	-0.111	-118.198	56.885	e
$Si_2C + 2H_2O + 8HF = 6H_2 + CO_2 + 2SiF_4$	-51.070	798.428	-0.404	-138.861	90.816	j,k
$Si_3 + 12HF = 6H_2 + 3SiF_4$	-64.459	1173.233	-0.101	-187.398	85.203	e
$Sn + 2HCl = H_2 + SnCl_2$	-6.422	164.113	-0.223	6.852	3.843	e
$SnBr_2 + 2HCl = 2HBr + SnCl_2$	-1.211	-13.896	0.000	-8.855	-0.288	f,n
$SnBr_4 + H_2 + 2HCl = 4HBr + SnCl_2$	17.306	-84.910	0.177	3.453	-26.819	f,i
$SnCl + HCl = 0.5H_2 + SnCl_2$	-5.955	74.375	-0.137	-2.051	8.263	i
$SnCl_4 + H_2 = 2HCl + SnCl_2$	17.408	-50.780	0.116	14.750	-26.499	f,i
$SnF + 2HCl = 0.5H_2 + HF + SnCl_2$	-6.161	100.954	-0.173	1.928	8.973	i
$SnF_2 + 2HCl = 2HF + SnCl_2$	-0.198	38.920	-0.067	12.187	0.827	i
$SnH_4 + 2HCl = 3H_2 + SnCl_2$	-5.810	94.655	-0.941	24.782	39.944	f,n
$SnO + 2HCl = H_2O + SnCl_2$	-4.759	143.565	0.066	3.009	-3.632	n
$SnS + 2HCl = H_2S + SnCl_2$	-5.502	76.834	0.086	-10.900	-0.432	h
$SnSe + 2HCl = H_2Se + SnCl_2$	-5.378	58.820	0.133	-14.180	-0.882	j,k
$SnTe + 2HCl = H_2Te + SnCl_2$	-6.390	40.265	0.074	-17.342	2.945	j,k
$Sr + 2HCl = H_2 + SrCl_2$	-8.898	238.802	-0.175	-10.914	14.142	e

Reaction						
$SrBr + 2HCl = 0.5H_2 + HBr + SrCl_2$	-5.618	124.627	-0.077	-5.005	9.015	i
$SrBr_2 + 2HCl = 2HBr + SrCl_2$	1.919	-24.062	0.003	-4.912	-3.822	i
$SrCl + HCl = 0.5H2 + SrCl2$	-5.307	135.355	-0.067	-1.676	8.000	i
$SrF + 2HCl = 0.5H_2 + HF + SrCl_2$	-5.458	140.500	-0.106	2.523	8.611	i
$SrF_2 + 2HCl = 2HF + SrCl_2$	-0.030	35.552	-0.062	7.718	0.238	i
$SrH + 2HCl = 1.5H_2 + SrCl_2$	-8.313	267.049	-0.224	0.529	15.753	j,k
$SrO + 2HCl = H_2O + SrCl_2$	-5.447	270.423	-0.069	-4.565	0.986	e
$SrOH + 2HCl = 0.5H_2 + H_2O + SrCl_2$	-1.300	168.694	-0.001	6.787	-4.195	j,l
$Sr(OH)_2 + 2HCl = 2H_2O + SrCl_2$	8.928	87.307	0.172	21.276	-27.490	j,l
$SrS + 2HCl = H_2S + SrCl_2$	-6.246	219.479	-0.055	-14.680	4.013	h
$Te + H_2 = H_2Te$	-0.905	57.905	0.169	-12.778	-12.858	e
$TeCl_2 + 2H_2 = H_2Te + 2HCl$	9.811	-18.030	0.377	2.395	-28.000	i
$TeF + 1.5H_2 = H_2Te + HF$	3.330	43.087	0.259	1.214	-18.146	i
$TeF_2 + 2H_2 = H2Te + 2HF$	9.319	28.345	0.273	16.502	-24.766	i
$TeF_4 + 3H_2 = H_2Te + 4HF$	26.473	13.738	0.374	53.549	-52.412	i
$TeF_5 + 3.5H_2 = H_2Te + 5HF$	35.288	43.170	0.414	69.149	-65.728	i
$TeF_6 + 4H_2 = H_2Te + 6HF$	45.249	73.611	0.455	89.751	-78.933	i
$TeO + 2H_2 = H_2O + H_2Te$	3.903	109.831	0.396	-1.341	-29.392	n
$TeO_2 + 3H_2 = 2H_2O + H_2Te$	10.784	161.016	0.554	12.053	-48.442	f,e
$Te_2 + 2H_2 = 2H_2Te$	3.011	-21.768	0.317	-17.495	-22.854	e
$Te_2F10 + 7H_2 = 2H_2Te + 10HF$	88.918	7.419	0.813	183.920	-150.003	i
$Te_2O_2 + 4H_2 = 2H_2O + 2H_2Te$	20.581	81.894	0.755	13.844	-74.345	n
$Ti + 4HF = 2H_2 + TiF_4$	-26.650	494.867	-0.151	-59.677	35.934	e
$TiBr + 4HF = 1.5H_2 + HBr + TiF_4$	-20.104	374.924	-0.038	-36.892	23.658	i
$TiBr_2 + 4HF = H_2 + 2HBr + TiF_4$	-13.817	188.915	0.064	-41.519	16.877	i
$TiBr_3 + 4HF = 0.5H_2 + 3HBr + TiF_4$	-4.940	102.853	0.199	-28.255	1.528	i
$TiBr_4 + 4HF = 4HBr + TiF_4$	1.666	30.264	0.226	-32.882	-4.593	i

APPENDIX 2

(continued)

Gas Species (continued)

Reaction[c]	l_0	$l_1 \times 10^{-2}$	$l_2 \times 10^3$	$l_3 \times 10^{-3}$	$l_4 \times 10^1$	Ref.[d]
$TiCl + 4HF = 1.5H_2 + HCl + TiF_4$	-19.993	373.557	-0.038	-34.850	23.231	i
$TiCl_2 + 4HF = H_2 + 2HCl + TiF_4$	-13.912	217.014	0.001	-40.130	18.627	i
$TiCl_3 + 4HF = 0.5H_2 + 3HCl + TiF_4$	-5.091	102.775	0.121	-17.358	3.869	i
$(TiCl_3)_2 + 8HF = H_2 + 6HCl + 2TiF_4$	-16.184	130.240	0.144	-108.933	53.005	n
$TiCl_4 + 4HF = 4HCl + TiF_4$	1.513	34.722	0.169	-22.234	-4.137	i
$TiF + 3HF = 1.5H_2 + TiF_4$	-20.198	352.265	-0.077	-30.684	23.955	i
$TiF_2 + 2HF = H_2 + TiF_4$	-14.344	169.986	-0.076	-31.027	19.993	i
$TiF_3 + HF = 0.5H_2 + TiF_4$	-6.146	47.554	0.018	-0.130	5.845	i
$TiO + 4HF = H_2 + H_2O + TiF_4$	-21.102	399.205	0.088	-39.963	18.030	e
$TiOCl + 4HF = 0.5H_2 + H_2O + HCl + TiF_4$	-12.602	289.095	0.165	-28.430	5.506	j,m
$TiOCl_2 + 4HF = H_2O + 2HCl + TiF_4$	-6.227	178.323	0.268	-22.836	-4.896	j,m
$TiOF + 3HF = 0.5H_2 + H_2O + TiF_4$	-12.701	284.512	0.129	-21.340	6.178	j,m
$TiOF_2 + 2HF = H_2O + TiF_4$	-5.968	168.098	0.184	-3.152	-3.029	j,m
$TiO_2 + 4HF = 2H_2O + TiF_4$	-14.043	334.346	0.290	-24.767	-0.422	e
$TiS + 4HF = H_2 + H_2S + TiF_4$	-21.820	430.624	0.149	-48.292	20.752	h
$V + 4HCl = 2H_2 + VCl_4$	-28.171	359.308	-0.392	-51.187	41.498	e
$VBr_4 + 4HCl = 4HBr + VCl_4$	2.278	-45.535	-0.066	-24.158	5.538	f,n
$VF_5 + 0.5H_2 + 4HCl = 5HF + VCl_4$	5.674	43.000	-0.277	28.531	-0.479	i
$VO + 4HCl = H_2 + H_2O + VCl_4$	-24.737	280.945	-0.219	-37.027	31.607	e
$VOCl_3 + 0.5H_2 + HCl = H_2O + VCl_4$	2.759	-3.290	0.086	-17.223	-10.380	f,g
$VO_2 + 4HCl = 2H_2O + VCl_4$	-17.505	215.450	-0.034	-19.086	11.294	j,q
$W + 4H_2O = 3H_2 + H_2WO_4$	-29.885	423.930	-0.533	-46.239	68.836	e

Reaction						
$WBr + 4H_2O = 2.5H_2 + HBr + H_2WO_4$	-32.206	308.238	-0.439	-74.347	81.759	i
$WBr_5 + 4H_2O = 0.5H_2 + 5HBr + H_2WO_4$	0.397	-33.069	-0.080	-60.816	31.300	i
$WBr_6 + 4H_2O = 6HBr + H_2WO_4$	10.285	-38.913	0.011	-58.211	17.332	i
$WCl + 4H_2O = 2.5H_2 + HCl + H_2WO_4$	-31.879	319.913	-0.425	-68.899	80.614	i
$WCl_2 + 4H_2O = 2H_2 + 2HCl + H_2WO_4$	-24.466	70.704	-0.396	-66.021	68.467	i
$WCl_4 + 4H_2O = H_2 + 4HCl + H_2WO_4$	-8.058	-5.909	-0.173	-50.487	43.303	i
$WCl_5 + 4H_2O = 0.5H_2 + 5HCl + H_2WO_4$	0.752	0.117	-0.123	-42.114	30.312	i
$(WCl_5)_2 + 8H_2O = H_2 + 10HCl + 2H_2WO_4$	12.618	-24.325	-0.213	-97.267	39.369	i
$WCl_6 + 4H_2O = 6HCl + H_2WO_4$	10.666	3.801	-0.029	-37.320	15.619	i
$WF + 4H_2O = 2.5H_2 + HF + H_2WO_4$	-32.174	326.777	-0.464	-63.804	81.548	i
$WF_6 + 4H_2O = 6HF + H_2WO_4$	8.873	-72.797	-0.320	10.593	24.127	i
$WO + 3H_2O = 2H_2 + H_2WO_4$	-31.596	343.590	-0.322	-66.610	71.035	e
$WOCl_4 + 3H_2O = 4HCl + H_2WO_4$	2.013	-8.877	-0.004	-14.023	20.556	j,m
$WOF_4 + 3H_2O = 4HF + H_2WO_4$	1.656	-31.095	-0.120	11.916	21.215	j,p
$WO_2 + 2H_2O = H_2 + H_2WO_4$	-24.649	254.504	-0.121	-52.641	50.601	e
$WO_2Cl_2 + 2H_2O = 2HCl + H_2WO_4$	-6.956	-28.780	0.048	-33.181	21.538	j,m
$WO_3 + H_2O = H_2WO_4$	-13.696	199.274	0.118	-34.374	23.421	e
$(WO_3)_2 + 2H_2O = 2H_2WO_4$	-10.234	93.710	0.345	-86.900	15.192	e
$(WO_3)_3 + 3H_2O = 3H_2WO_4$	-8.330	-6.229	0.419	-106.454	21.067	e
$(WO_3)_4 + 4H_2O = 4H_2WO_4$	-5.537	-63.882	0.566	-155.407	20.548	e
$W_3O_8 + 4H_2O = H_2 + 3H_2WO_4$	-18.891	35.854	0.196	-126.564	48.543	e
$Zn + 2HCl = H_2 + ZnCl_2$	-11.875	113.848	-0.166	-7.288	17.290	e
$ZnBr_2 + 2HCl = 2HBr + ZnCl_2$	0.407	-21.209	0.036	-0.209	-0.836	g
$ZnS + 2HCl = H_2S + ZnCl_2$	-7.562	160.728	0.105	-3.920	1.681	h

Liquid Species

Reaction[c]	l_0	$l_1 \times 10^{-2}$	$l_2 \times 10^3$	$l_3 \times 10^{-3}$	$l_4 \times 10^1$	Ref.[d]
$Bi_2S_3(liq) + 6HCl = 3H_2S + 2BiCl_3$	38.907	-74.466	3.189	-39.706	-131.007	f,h
$Br_2(liq) + H_2 = 2HBr$	22.779	30.625	1.821	0.144	-58.133	f,e
$CCl_4(liq) + 2H_2O = CO_2 + 4HCl$	30.318	70.907	-4.685	-17.753	-38.068	f,i
$CuFeS_2(liq) + 0.5H_2 + 3HCl = 2H_2S + FeCl_2 + CuCl$	32.740	-167.062	3.983	-24.722	-85.947	f,h
$Cu_2S(liq) + 2HCl = H_2S + 2CuCl$	21.317	-217.696	1.052	-22.071	-43.124	f,h
$FeS(liq) + 2HCl = H_2S + FeCl_2$	10.587	-48.076	1.874	-14.579	-29.988	f,h
$H_2O(liq) = H_2O$	22.489	-30.265	3.240	3.741	-56.512	f,e
$H_2SO_4(liq) + 4H_2 = 4H_2O + H_2S$	31.470	80.992	-38.362	-0.233	-49.814	f,h
$H_2SO_4.H_2O(liq) + 4H_2 = 5H_2O + H_2S$	57.685	35.979	-24.184	-3.010	-118.864	f,h
$H_2SO_4.2H_2O(liq) + 4H_2 = 6H_2O + H_2S$	56.106	6.202	-66.150	7.367	-82.210	f,h
$H_2SO_4.3H_2O(liq) + 4H_2 = 7H_2O + H_2S$	73.680	-24.573	-54.693	0.037	-123.748	f,h
$H_2SO_4.4H_2O(liq) + 4H_2 = 8H_2O + H_2S$	97.971	-57.559	-38.838	5.860	-188.822	f,h
$H_2SO_4.6.5H_2O(liq) + 4H_2 = 10.5H_2O + H_2S$	164.368	-140.143	0.518	22.818	-370.919	f,h
$Hg(liq) = Hg$	6.872	-32.529	-0.336	-5.101	-5.975	f,e
$MnS(liq) + 2HCl = H_2S + MnCl_2$	9.540	-54.895	0.584	-19.717	-24.729	f,h
$NiS(liq) + 2HCl = H_2S + NiCl_2$	11.734	-85.734	0.882	-23.499	-30.234	f,h
$PbS(liq) + 2HCl = H2S + PbCl2$	14.362	-47.498	1.332	-11.013	-38.352	f,h
$S(liq) + H_2 = H_2S$	12.376	8.065	3.464	-16.688	-36.633	f,e
$SiBr_4(liq) + 4HF = 4HBr + SiF_4$	21.349	106.790	2.984	-64.741	-57.833	f,i
$SnCl_4(liq) + H_2 = 2HCl + SnCl_2$	21.136	-73.421	-63.172	-6.888	-7.885	f,i
$SnS(liq) + 2HCl = H_2S + SnCl_2$	16.703	-35.922	1.126	-15.111	-47.377	f,h
$TiCl_4(liq) + 4HF = 4HCl + TiF_4$	19.581	8.878	-0.469	-43.954	-48.298	f,i

Solid Species

Reaction[c]	l_0	$l_1 \times 10^{-2}$	$l_2 \times 10^3$	$l_3 \times 10^{-3}$	$l_4 \times 10^1$	Ref.[d]
$Ag(c) + HCl = 0.5H_2 + AgCl$	3.967	-103.128	-2.998	-10.514	3.449	f,e
$AgBr(c) + HCl = HBr + AgCl$	-15.429	-124.223	-46.786	-89.653	88.367	f,i
$AgCl(c) = AgCl$	6.253	-120.642	-14.019	-22.947	9.550	f,i
$Ag_2O(c) + 2HCl = H_2O + 2AgCl$	13.973	-99.908	-11.219	-0.711	-8.099	f,e
$Ag_2O_2(c) + H_2 + 2HCl = 2H_2O + 2AgCl$	22.887	27.911	-10.016	-7.332	-28.060	f,e
$Ag_2S(acanthite) + 2HCl = H_2S + 2AgCl$	20.099	-212.087	1.667	-98.425	-35.621	f,h
$Al(c) + 3HF = 1.5H_2 + AlF_3$	-10.082	209.265	-3.877	-41.929	20.057	f,e
$AlBr_3(c) + 3HF = 3HBr + AlF3$	28.748	-16.221	4.391	31.003	-67.782	f,i
$AlCl_3(c) + 3HF = 3HCl + AlF_3$	7.450	-17.107	-21.082	-39.362	14.341	f,i
$AlF_3(c) = AlF_3$	25.953	-167.501	3.995	75.908	-49.481	f,i
$AlO(OH)(diaspore) + 3HF = 2H_2O + AlF_3$	13.260	-71.322	-0.959	40.516	-26.329	f,r
$Al_2O_3(corundum) + 6HF = 3H_2O + 2AlF_3$	14.188	-94.785	2.419	21.659	-43.657	r
$Al_2O_3(glass) + 6HF = 3H_2O + 2AlF_3$	13.463	-83.871	0.444	6.663	-41.576	f,e
$Al_2O_4O_{10}(OH)_2(pyrophyllite) + 22HF = 12H_2O + 2AlF_3 + 4SiF_4$	31.075	50.428	4.078	24.003	-127.064	f,r
$Al_2S_3(c) + 6HF = 3H_2S + 2AlF_3$	10.787	99.744	2.552	-55.330	-37.660	f,h
$Al_2(SO_4)_3(c) + 12H_2 + 6HF = 12H_2O + 3H_2S + 2AlF_3$	151.085	82.667	40.081	417.126	-406.768	f,J,s
$Al_2SiO_5(andalusite) + 10HF = 5H_2O + 2AlF_3 + SiF_4$	16.320	-49.550	4.941	19.394	-65.161	f,r
$Al_2SiO_5(kyanite) + 10HF = 5H_2O + 2AlF_3 + SiF_4$	15.479	-50.901	3.427	13.018	-60.567	f,r
$Al_2SiO_5(sillimanite) + 10HF = 5H_2O + 2AlF_3 + SiF_4$	13.558	-45.632	3.448	5.547	-56.703	f,r
$Al_2Si_2O_5(OH)_4(kaolinite) + 14HF = 9H_2O + 2AlF_3 + 2SiF_4$	44.401	-81.107	5.009	66.272	-118.607	f,r
$As(c) + 3HCl = 1.5H_2 + AsCl_3$	-10.664	-3.914	-3.542	-21.520	23.403	f,e
$As_2O_3(arsenolite) + 6HCl = 3H_2O + 2AsCl_3$	-0.397	19.189	-16.431	-9.532	2.906	f,e

Solid Species (continued)

Reaction[c]	l_0	$l_1 \times 10^{-2}$	$l_2 \times 10^3$	$l_3 \times 10^{-3}$	$l_4 \times 10^1$	Ref.[d]
$As_2O_3(claudetite) + 6HCl = 3H_2O + 2AsCl_3$	1.517	19.138	-12.452	-1.943	-5.292	f,e
$As_2O_5(c) + 2H_2 + 6HCl = 5H_2O + 2AsCl_3$	9.512	128.862	-23.059	5.460	-7.981	f,e
$As_2S_3(orpiment) + 6HCl = 3H_2S + 2AsCl_3$	6.700	-32.648	0.193	-36.689	-26.847	f,h
$As_2S_3(glass) + 6HCl = 3H_2S + 2AsCl_3$	-119.909	46.892	-189.920	-417.501	431.928	f,h
$As_2Te_3(c) + 6HCl = 3H_2Te + 2AsCl_3$	-29.013	-173.178	-53.556	-143.469	103.532	f,j,k
$As_4S_4(orthorhombic) + 12HCl = 2H_2 + 4H_2S + 4AsCl_3$	-10.658	-52.572	-15.448	-90.013	17.615	f,h
$As_4S_4(realgar) + 12HCl = 2H_2 + 4H_2S + 4AsCl_3$	-10.693	-54.240	-15.434	-91.325	17.706	f,h
$Au(c) = Au$	7.889	-191.681	-1.466	-0.830	-2.972	f,e
$Bi(c) + 3HCl = 1.5H_2 + BiCl_3$	-13.596	-0.683	-9.481	-23.385	36.321	f,e
$BiBr_3(c) + 3HCl = 3HBr + BiCl_3$	-1.876	-74.926	-6.019	-225.930	35.289	f,i
$BiCl_3(c) = BiCl_3$	10.576	-60.555	-15.015	-5.319	-1.118	f,i
$BiF_3(c) + 3HCl = 3HF + BiCl_3$	-3.500	-46.899	-33.034	-28.906	52.771	f,i
$Bi_2O_3(c) + 6HCl = 3H_2O + 2BiCl_3$	-31.436	89.274	-47.833	-176.849	112.455	f,e
$Bi_2S_3(bismuthinite) + 6HCl = 3H_2S + 2BiCl_3$	8.882	-76.559	-2.582	-18.537	-28.853	f,h
$C(diamond) + 2H_2O = 2H_2 + CO_2$	-6.599	-40.581	-6.191	-11.900	40.554	f,e
$C(graphite) + 2H_2O = 2H_2 + CO_2$	-4.599	-42.590	-3.923	-8.945	32.730	e
$CBr_4(c) + 2H_2O = CO_2 + 4HBr$	57.306	35.534	38.653	-147.263	-137.068	f,i
$Ca(c) + 2HCl = H_2 + CaCl_2$	-7.030	153.475	-8.797	-14.281	26.396	f,e
$CaAl_2SiO_6(Ca\text{-}Al\ pyroxene) + 2HCl + 10HF = 6H_2O + 2AlF_3 + SiF_4 + CaCl_2$	23.460	-146.477	3.515	34.228	-78.804	f,r
$CaAl_2Si_2O_7(OH)_2 \cdot H_2O(lawsonite) + 2HCl + 14HF = 10H_2O + 2AlF_3 + 2SiF_4 + CaCl_2$	48.103	-198.042	-9.149	119.490	-112.286	f,r

Reaction						
$CaAl_2Si_2O_8$(anorthite) + $2HCl$ + $14HF$ = $8H_2O$ + $2AlF_3$ + $2SiF_4$ + $CaCl_2$	19.113	-104.995	2.451	-4.214	-82.045	f,r
$CaAl_4Si_2O_{10}(OH)_2$(margarite) + $2HCl$ + $20HF$ = $12H_2O$ + $4AlF_3$ + $2SiF_4$ + $CaCl_2$	52.633	-256.032	3.441	89.919	-157.808	f,r
$CaBr_2$(c) + $2HCl$ = $2HBr$ + $CaCl_2$	15.172	-171.922	-2.158	8.546	-18.350	f,i
$CaCO_3$(calcite) + $2HCl$ = H_2O + CO_2 + $CaCl_2$	20.096	-155.270	-3.189	45.645	-25.951	f,r
$CaCl_2$(hydrophilite) = $CaCl_2$	12.679	-170.830	-3.921	-1.770	-9.538	f,i
CaF_2(fluorite) + $2HCl$ = $2HF$ + $CaCl_2$	3.556	-203.072	-14.970	-25.905	24.855	f,i
$CaFeSi_2O_6$(hedenbergite) + $4HCl$ + $8HF$ = $6H_2O$ + $2SiF_4$ + $FeCl_2$ + $CaCl_2$	20.413	-63.176	1.656	14.277	-73.519	f,t
$CaMgSiO_4$(monticellite) + $4HCl$ + $4HF$ = $4H_2O$ + SiF_4 + $MgCl_2$ + $CaCl_2$	15.864	-146.125	0.127	21.052	-44.035	f,r
$CaMgSi_2O_6$(diopside) + $4HCl$ + $8HF$ = $6H_2O$ + $2SiF_4$ + $MgCl_2$ + $CaCl_2$	20.075	-121.547	3.077	34.693	-71.048	f,r
CaO(lime) + $2HCl$ = H_2O + $CaCl_2$	8.824	-59.064	0.086	18.909	-17.514	f,r
CaS(c) + $2HCl$ = H_2S + $CaCl_2$	6.636	-87.546	-0.107	-6.860	-11.267	h
$CaSO4$(anhydrite) + $4H_2$ + $2HCl$ = $4H_2O$ + H_2S + $CaCl_2$	22.403	-87.905	-15.407	-7.416	-29.593	f,s
$CaSO_4.2H_2O$(gypsum) + $4H_2$ + $2HCl$ = $6H_2O$ + H_2S + $CaCl_2$	27.303	-141.481	-66.622	-4.897	16.235	f,t
$CaSiO3$(pseudowollastonite) + $2HCl$ + $4HF$ = $3H_2O$ + SiF_4 + $CaCl_2$	9.896	-54.240	2.135	15.368	-36.575	f,r
$CaSiO_3$(wollastonite) + $2HCl$ + $4HF$ = $3H_2O$ + SiF_4 + $CaCl_2$	9.752	-56.017	1.651	11.350	-35.495	f,r
$CaTiSiO_5$(sphene) + $2HCl$ + $8HF$ = $5H_2O$ + SiF_4 + $CaCl_2$ + TiF_4	13.029	-70.557	3.981	10.876	-56.252	f,r
$Ca_2Al_2Si_3O_{10}(OH)_2$(prehnite) + $4HCl$ + $18HF$ = $12H_2O$ + $2AlF_3$ + $3SiF_4$ + $2CaCl_2$	43.422	-217.230	0.161	61.358	-132.084	f,r
$Ca_2Al_3Si_3O_{12}(OH)$(zoisite, orthorhombic) + $4HCl$ + $21HF$ = $13H_2O$ + $3AlF_3$ + $3SiF_4$ + $2CaCl_2$	41.402	-246.929	1.455	42.293	-137.705	f,r
$Ca_2Al_3Si_3O_{12}(OH)$(clinozoisite) + $4HCl$ + $21HF$ = $13H_2O$ + $3AlF_3$ + $3SiF_4$ + $2CaCl_2$	42.164	-249.984	1.588	44.036	-138.401	f,r
$Ca_2MgSi_2O_7$(akermanite) + $6HCl$ + $8HF$ = $7H_2O$ + $2SiF_4$ + $MgCl_2$ + $2CaCl_2$	16.990	-183.733	-0.982	-36.326	-55.851	f,r

Solid Species (continued)

Reaction[c]	l_0	$l_1 \times 10^{-2}$	$l_2 \times 10^3$	$l_3 \times 10^{-3}$	$l_4 \times 10^1$	Ref.[d]
$Ca_2Mg_5O_{22}(OH)_2$(tremolite) + 14HCl + 32HF = 24H_2O + 8SiF_4 + 5$MgCl_2$ + 2$CaCl_2$	87.913	-421.017	12.712	167.401	-293.278	f,r
$Ca_3Al_2Si_3O_{12}$(grossular) + 6HCl + 18HF = 12H_2O + 2AlF_3 + 3SiF_4 + 3$CaCl_2$	47.572	-297.678	9.926	77.944	-156.598	f,r
$Ca_3MgSi_2O_8$(merwinite) + 8HCl + 8HF = 8H_2O + 2SiF_4 + $MgCl_2$ + 3$CaCl_2$	28.914	-268.449	0.054	20.667	-83.112	f,r
$Ca_4Al_6Si_6O_{25}(CO_2)$(meionite) + 8HCl + 42HF = 25H_2O + CO_2 + 6AlF_3 + 6SiF_4 + 4$CaCl_2$	75.150	-447.864	2.941	37.815	-270.587	f,r
Cd(c) = Cd	6.697	-58.863	-3.195	-0.667	-1.591	f,e
$CdBr_2$(c) + H_2 = 2HBr + Cd	22.557	-189.176	-6.738	1.091	-22.802	f,i
$CdCl_2$(c) + H_2 = 2HCl + Cd	23.918	-171.068	-4.096	9.122	-28.002	f,i
CdO(c) + H_2 = H_2O + Cd	18.085	-71.850	0.626	13.905	-31.060	f,e
CdS(greenockite) + H_2 = H_2S + Cd	17.205	-129.513	1.023	3.620	-28.600	f,h
Co(c) + 2HCl = H_2 + CoCl	-4.687	-44.348	-6.444	-14.034	21.460	f,e
$CoCl_2$(c) = CoCl	17.280	-118.094	-1.210	6.711	-24.923	f,i
CoF_2(c) + 2HCl = 2HF + CoCl	17.180	-118.195	-1.637	27.166	-23.513	f,i
CoF_3(c) + 0.5H_2 + 2HCl = 3HF + CoCl	24.800	-37.999	-0.426	24.806	-32.869	f,i
$CoFe_2O_4$(c) + H_2 + 6HCl = 4H_2O + 2$FeCl_2$ + CoCl	69.204	-198.490	20.156	269.820	-185.978	f,n
CoO(c) + 2HCl = H_2O + CoCl	6.289	-45.600	-1.310	-21.396	-11.308	f,e
$CoS_{.89}$(c) + 2HCl = 0.11H_2 + 0.89H_2S + CoCl	4.651	-149.035	-5.655	-2.271	-1.175	f,h
$CoSO_4$(c) + 4H_2 + 2HCl = 4H_2O + H_2S + CoCl	38.604	-10.546	-0.550	58.634	-86.278	f,j,u
$CoSO_4 \cdot H_2O$(c) + 4H_2 + 2HCl = 5H_2O + H_2S + CoCl	8.889	-32.057	-84.457	-5.807	54.050	f,u

Reaction						
$CoSO_4 \cdot 6H_2O(C) + 4H_2 + 2HCl = 10H_2O + H_2S + CoCl$	56.260	-190.412	-157.613	105.599	45.498	f,j,u
$CoSO_4 \cdot 7H_2O(C) + 4H_2 + 2HCl = 11H_2O + H_2S + CoCl$	36.227	-205.283	-211.241	34.299	149.614	f,j,u
$CoS_2(c) + H_2 + 2HCl = 2H_2S + CoCl$	15.123	-109.821	-3.373	0.212	-27.826	f,h
$Co_3O_4(c) + H_2 + 6HCl = 4H_2O + 3CoCl$	24.153	-124.851	-10.490	49.307	-27.022	f,e
$Cr(c) + 4HCl = 2H_2 + CrCl_4$	-19.790	37.005	-6.572	-31.143	42.069	e
$CrBr_3(c) + 4HCl = 0.5H_2 + 3HBr + CrCl_4$	7.786	-138.678	-2.616	-18.100	-5.634	f,i
$CrCl_2(c) + 2HCl = H_2 + CrCl_4$	-1.598	-78.746	-4.356	-11.492	7.012	f,i
$CrCl_3(c) + HCl = 0.5H_2 + CrCl_4$	8.505	-117.240	-4.076	0.532	-6.868	f,i
$CrF_2(c) + 4HCl = H_2 + 2HF + CrCl_4$	-3.995	-88.735	-6.357	-10.197	16.118	f,i
$CrF_3(c) + 4HCl = 0.5H_2 + 3HF + CrCl_4$	6.769	-156.454	-3.758	20.430	-2.039	f,i
$CrS(c) + 4HCl = H_2 + H_2S + CrCl_4$	-5.260	-29.086	0.942	-16.122	-2.410	f,h
$Cr_2O_3(c) + 8HCl = H_2 + 3H_2O + 2CrCl_4$	-9.411	-152.545	-2.862	-58.548	3.671	e
$Cr_2S_3(c) + 8HCl = H_2 + 3H_2S + 2CrCl_4$	-19.073	-76.150	-10.133	-89.871	34.164	f,h
$Cr_2(SO_4)_3(c) + 11H_2 + 8HCl = 12H_2O + 3H_2S + 2CrCl_4$	84.847	30.707	-11.574	128.474	-208.791	f,j,u
$Cs(c) + HCl = 0.5H_2 + CsCl$	-0.259	77.560	-17.270	-2.340	13.172	f,e
$CsBr(c) + HCl = HBr + CsCl$	8.174	-115.485	-8.419	-12.876	0.887	f,i
$CsCl(c) = CsCl$	32.355	-126.942	6.498	178.863	-78.561	f,i
$CsF(c) + HCl = HF + CsCl$	-0.570	-65.135	-25.265	-29.978	32.892	f,i
$Cs_2O(c) + 2HCl = H_2O + 2CsCl$	15.213	97.409	-7.687	-7.036	-18.620	f,e
$Cs_2SO_4(c) + 4H_2 + 2HCl = H_2S + 2CsCl + 4H_2O$	63.041	-116.235	-3.634	225.004	-142.612	f,j,k
$Cu(c) + HCl = 0.5H_2 + CuCl$	3.875	-95.419	-2.308	-6.134	1.703	e
$CuBr(c) + HCl = HBr + CuCl$	73.074	-184.574	35.209	426.461	-215.447	f,i
$CuBr_2(c) + 0.5H_2 + HCl = 2HBr + CuCl$	22.430	-134.419	-0.052	2.326	-31.541	f,i
$CuCl(c) = CuCl$	53.084	-168.373	16.241	339.327	-146.931	f,i
$CuCl2(c) + 0.5H_2 = HCl + CuCl$	29.534	-124.227	3.662	63.884	-54.984	f,i
$CuF(c) + HCl = HF + CuCl$	16.587	-67.463	-1.243	21.294	-27.368	f,i
$CuF_2(c) + 0.5H_2 + HCl = 2HF + CuCl$	21.396	-97.905	-5.312	26.555	-25.780	f,i

Solid Species (continued)

Reaction[c]	l_0	$l_1 \times 10^{-2}$	$l_2 \times 10^3$	$l_3 \times 10^{-3}$	$l_4 \times 10^1$	Ref.[d]
$CuFeS_2$(chalopyrite) $+ 0.5H_2 + 3HCl = 2H_2S + FeCl_2 + CuCl$	24.247	-203.490	-19.968	150.260	-39.241	f,h
CuO(tenorite) $+ 0.5H_2 + HCl = H_2O + CuCl$	14.852	-55.278	-0.447	13.533	-26.906	f,e
CuS(covellite) $+ 0.5H_2 + HCl = H_2S + CuCl$	11.483	-116.003	-3.388	-9.748	-16.970	f,h
$CuSO_4$(chalcocyanite) $+ 4.5H_2 + HCl = 4H_2O + H_2S + CuCl$	44.766	0.925	-0.938	60.421	-95.022	f,j,u
$CuSO_4 \cdot H_2O$(c) $+ 4.5H_2 + HCl = 5H_2O + H_2S + CuCl$	14.043	-20.943	-84.391	-7.143	52.423	f,u
$CuSO_4 \cdot 3H_2O$(c) $+ 4.5H_2 + HCl = 7H_2O + H_2S + CuCl$	18.975	-79.059	-123.747	1.091	98.099	f,u
$CuSO_4 \cdot 5H_2O$(chalcanthite) $+ 4.5H_2 + HCl = 9H_2O + H_2S + CuCl$	22.349	-135.102	-170.048	4.172	149.698	f,u
Cu_2O(cuprite) $+ 2HCl = H_2O + 2CuCl$	13.625	-156.094	-5.456	-4.939	-10.554	f,e
Cu_2OSO_4(c) $+ 5H_2 + 2HCl = 5H_2O + H_2S + 2CuCl$	58.010	-48.391	0.014	69.276	-119.881	f,j,u
Cu_2S(chalcocite) $+ 2HCl = H_2S + 2CuCl$	12.772	-209.609	-1.120	-210.515	-16.532	f,h
Cu_2SO_4(c) $+ 4H_2 + 2HCl = 4H_2O + H_2S + 2CuCl$	34.606	-76.579	-20.053	-0.326	-50.848	f,j,u
Cu_5FeS_4(bornite) $+ 0.5H_2 + 7HCl = 4H_2S + FeCl_2 + 5CuCl$	133.790	-725.415	37.528	373.812	-349.599	f,h
Fe(c) $+ 2HCl = H_2 + FeCl_2$	0.555	-25.031	-5.591	40.475	5.734	f,e
$FeAl_2O_4$(hercynite) $+ 2HCl + 6HF = 4H_2O + FeCl_2 + 2AlF_3$	18.775	-146.806	0.726	-9.509	-49.651	n
$FeBr_2$(c) $+ 2HCl = 2HBr + FeCl_2$	16.700	-118.757	-3.422	9.176	-23.705	f,i
$FeCl_2$(lawrencite) $= FeCl_2$	15.720	-107.749	-2.032	0.560	-21.045	f,i
$FeCl_3$(molysite) $+ 0.5H_2 = HCl + FeCl_2$	15.865	-88.298	-18.848	-4.410	-1.838	f,i
$FeCr_2O_4$(chromite) $+ 10HCl = H_2 + 4H_2O + FeCl_2 + 2CrCl_4$	0.832	-200.367	-2.872	18.733	-19.640	n
FeF_2(c) $+ 2HCl = 2HF + FeCl_2$	14.665	-109.097	-2.304	12.708	-16.064	f,i
FeF_3(c) $+ 0.5H_2 + 2HCl = 3HF + FeCl_2$	26.321	-144.096	1.597	26.852	-38.955	f,i
$Fe_{.947}O$(wustite) $+ 0.053H_2 + 1.894HCl = H_2O + 0.947FeCl_2$	8.772	-37.194	-0.273	3.021	-20.330	f,e
FeO(c) $+ 2HCl = H_2O + FeCl_2$	7.863	-40.706	-1.099	-2.213	-17.286	f,e

Reaction						Notes
$Fe_{.877}S$(pyrrhotite) + $0.113H_2$ + $1.774HCl$ = H_2S + $0.887FeCl_2$	12.235	-67.255	3.197	-20.909	-31.689	f,h
FeS(troilite) + 2HCl = H_2S + $FeCl_2$	5.993	-56.261	0.303	-155.726	-12.764	f,h
$FeSO_4$(c) + $4H_2$ + 2HCl = $4H_2O$ + H_2S + $FeCl_2$	47.126	-14.791	6.431	99.405	-115.872	j,u
$FeSO_4 \cdot H_2O$(szomolnokite) + $4H_2$ + 2HCl = $5H_2O$ + H_2S + $FeCl_2$	9.073	-29.960	-84.495	-9.248	56.662	f,u
$FeSO_4 \cdot 4H_2O$(c) + $4H_2$ + 2HCl = $8H_2O$ + H_2S + $FeCl_2$	29.241	-116.924	-133.879	-0.175	77.085	f,u
$FeSO_4 \cdot 7H_2O$(melanterite) + $4H_2$ + 2HCl = $11H_2O$ + H_2S + $FeCl_2$	60.702	-212.771	-181.166	113.192	61.908	f,j,u
FeS_2(marcasite) + H_2 + 2HCl = $2H_2S$ + $FeCl_2$	16.801	-92.779	0.191	3.402	-30.298	f,h
FeS_2(pyrite) + H_2 + 2HCl = $2H_2S$ + $FeCl_2$	17.070	-95.053	0.657	3.528	-31.127	f,h
$FeSiO_3$(ferrosilite) + 2HCl + 4HF = $3H_2O$ + $FeCl_2$ + SiF_4	10.051	-0.622	0.765	10.979	-37.265	f,r
$FeTiO_3$(ilmenite) + 2HCl + 4HF = $3H_2O$ + $FeCl_2$ + TiF_4	13.680	-54.772	2.647	16.066	-46.404	f,r
$FeWO_4$(ferberite) + 2HCl = $FeCl_2$ + H_2WO_4	3.671	-165.091	-6.262	-77.311	11.877	g
Fe_2O_3(hematite) + H_2 + 4HCl = $3H_2O$ + $2FeCl_2$	49.200	-127.293	9.177	211.777	-127.629	f,r
$Fe_2(SO_4)_3$(c) + $13H_2$ + 4HCl = $12H_2O$ + $3H_2S$ + $2FeCl_2$	162.322	68.817	29.934	532.400	-409.679	f,j,u
Fe_2SiO_4(fayalite) + 4HCl + 4HF = $4H_2O$ + $2FeCl_2$ + SiF_4	19.319	-49.554	0.491	24.415	-57.912	f,r
Fe_2TiO_4(ulvospinel) + 4HCl + 4HF = $4H_2O$ + $2FeCl_2$ + TiF_4	19.826	-100.846	-0.163	25.373	-55.896	f,v,w
$Fe_3Al_2Si_3O_{12}$(almandine) + 6HCl + 18HF = $12H_2O$ + $3FeCl_2$ + $2AlF_3$ + $3SiF_4$	47.623	-102.394	10.133	74.043	-167.515	f,r
Fe_3O_4(magnetite) + H_2 + 6HCl = $4H_2O$ + $3FeCl_2$	97.737	-213.572	32.295	520.898	-278.177	f,r
Ga(c) + 3HCl = $1.5H_2$ + $GaCl_3$	-9.636	84.378	-2.325	-21.339	18.360	f,e
GaF_3(c) + 3HCl = 3HF + $GaCl_3$	8.744	-103.771	-10.569	-16.318	5.546	f,i
GaS(c) + 3HCl = $0.5H_2$ + H_2S + $GaCl_3$	-1.708	-16.895	-4.829	-14.162	2.320	f,h
Ga_2O_3(c) + 6HCl = $3H_2O$ + $2GaCl_3$	8.577	-33.025	-1.187	15.654	-26.727	e
$HgBr_2$(c) + H_2 = 2HBr + Hg	21.091	-89.183	-6.037	1.619	-22.523	f,i
$HgCl_2$(calomel) + H_2 = 2HCl + Hg	-14.831	-36.921	-57.372	-103.786	107.453	f,i
HgF_2(c) + H_2 = 2HF + Hg	22.101	28.795	-4.563	3.043	-25.478	f,i
HgO(montroydite) + H_2 = H_2O + Hg	16.027	42.463	-3.014	13.429	-24.755	f,e
HgS(cinnabar) + H_2 = H_2S + Hg	16.755	-53.511	-0.770	3.238	-27.252	f,h

Solid Species (continued)

Reaction[c]	l_0	$l_1 \times 10^{-2}$	$l_2 \times 10^3$	$l_3 \times 10^{-3}$	$l_4 \times 10^1$	Ref.[d]
$HgS(metacinnabar) + H_2 = H_2S + Hg$	16.871	-51.758	-0.468	7.412	-28.788	f,h
$Hg_2Br_2(c) + H_2 = 2HBr + 2Hg$	33.531	-140.988	-4.011	14.013	-42.515	f,i
$Hg_2Cl_2(c) + H_2 = 2HCl + 2Hg$	31.785	-111.972	-5.131	12.190	-35.906	f,i
$Hg_2F_2(c) + H_2 = 2HF + 2Hg$	32.222	-38.334	-5.372	15.520	-36.198	f,i
$Ir(c) = Ir$	10.009	-348.356	-0.169	1.255	-5.948	e
$IrBr_3(c) + 1.5H_2 = 3HBr + Ir$	38.733	-390.069	-1.369	3.445	-49.098	f,i
$IrS_2(c) + 2H_2 = 2H_2S + Ir$	24.760	-398.895	-1.298	-6.843	-36.185	f,h
$Ir_2S_3(c) + 3H_2 = 3H_2S + 2Ir$	44.067	-778.167	-0.658	-7.595	-63.751	f,h
$K(c) + HCl = 0.5H_2 + KCl$	-2.865	64.980	-22.581	-4.097	23.803	f,e
$KAl(SO_4)_2(c) + 8H_2 + HCl + 3HF = 8H_2O + 2H_2S + KCl + AlF_3$	79.669	12.253	1.854	108.351	-183.912	f,s
$KAlSi_3O_8(microcline) + HCl + 15HF = 8H_2O + KCl + AlF_3 + 3SiF_4$	18.251	11.150	6.321	-0.209	-88.047	f,r
$KAlSi_3O_8(sanidine) + HCl + 15HF = 8H_2O + KCl + AlF_3 + 3SiF_4$	18.101	16.313	6.699	6.379	-90.101	f,r
$KAl_3(OH)_6(SO_4)_2(alunite) + 8H_2 + HCl + 9HF = 14H_2O + 2H_2S + KCl + 3AlF_3$	193.086	-290.895	38.061	482.190	-473.356	f,t
$KAl_3Si_3O_{10}(OH)_2(muscovite) + HCl + 21HF = 12H_2O + KCl + 3AlF_3 + 3SiF_4$	54.108	-141.057	7.404	107.486	-173.911	f,r
$KBr(c) + HCl = HBr + KCl$	11.382	-124.456	-4.045	-5.231	-10.686	f,i
$KCl(sylvite) = KCl$	9.866	-116.853	-6.106	-8.963	-4.924	f,i
$KF(c) + HCl = HF + KCl$	12.976	-92.707	-3.042	8.681	-15.059	f,i
$KMg_3(AlSi_3O_{10})(OH)_2(phlogopite) + 7HCl + 15HF = 12H_2O + KCl + AlF_3 + 3SiF_4 + 3MgCl_2$	63.757	-346.159	9.995	129.849	-178.382	f,r
$KO_2(c) + 1.5H_2 + HCl = 2H_2O + KCl$	25.110	157.857	0.148	19.418	-65.634	f,e

Reaction						
$K_2O(c) + 2HCl = H_2O + 2KCl$	19.175	71.252	-3.445	6.709	-30.634	f,e
$K_2O_2(c) + H_2 + 2HCl = 2H_2O + 2KCl$	26.324	113.523	-9.758	14.426	-44.652	f,e
$K_2S(c) + 2HCl = H_2S + 2KCl$	-3.045	-66.633	-28.412	-51.200	49.066	f,h
$K_2SO_4(arcanite, orthorhombic) + 4H_2 + 2HCl = H_2S + 2KCl + 4H_2O$	33.021	-115.154	-23.717	-2.874	-42.850	f,j,o
$K_2SO_4(hexagonal) + 4H_2 + 2HCl = H_2S + 2KCl + 4H_2O$	37.873	-109.475	-10.775	-9.009	-65.433	f,j,o
$K_2S_5(c) + 4H_2 + 2HCl = 5H_2S + 2KCl$	40.841	-76.925	-48.290	0.981	-67.471	f,h
$Li(c) + HCl = 0.5H_2 + LiCl$	-1.655	56.303	-12.264	-16.565	18.718	f,e
$LiBr(c) + HCl = HBr + LiCl$	10.112	-111.319	-5.600	-10.195	-6.965	f,i
$LiCl(c) = LiCl$	10.134	-112.225	-5.739	-7.024	-6.371	f,i
$LiF(c) + HCl = HF + LiCl$	11.083	-126.864	-4.483	4.959	-7.513	f,i
$Li_2O(c) + 2HCl = H_2O + 2LiCl$	17.368	-83.051	-4.008	24.003	-21.531	f,e
$Li_2O_2(c) + H_2 + 2HCl = 2H_2O + 2LiCl$	16.419	28.241	-10.007	-28.115	-11.974	f,e
$Li_2SO_4(c) + 4H_2 + 2HCl = H_2S + 2LiCl + 4H_2O$	105.074	-205.354	9.118	705.345	-271.503	f,j,k
$Mg(c) + 2HCl = H_2 + MgCl_2$	-4.629	111.207	-4.491	-13.456	16.530	f,e
$MgBr_2(c) + 2HCl = 2HBr + MgCl_2$	12.593	-128.282	-4.507	-9.758	-9.825	f,i
$MgCO_3(magnesite) + 2HCl = H_2O + CO_2 + MgCl_2$	21.859	-149.952	-2.238	65.115	-29.084	f,r
$MgCl_2(chloromagnesite) = MgCl_2$	15.543	-134.875	-2.064	10.596	-18.969	f,i
$MgCr_2O_4(picrochromite) + 10HCl = H_2 + 4H_2O + MgCl_2 + 2CrCl_4$	3.109	-263.378	-1.401	35.876	-23.872	f,j,s
$MgF_2(sellaite) + 2HCl = 2HF + MgCl2$	14.705	-196.922	-2.732	25.052	-14.300	f,i
$MgFe_2O_4(magnesioferrite) + H_2 + 6HCl = 4H_2O + 2FeCl_2 + MgCl_2$	55.374	-206.588	12.899	175.588	-140.587	f,j,s
$MgO(periclase) + 2HCl = H_2O + MgCl_2$	7.496	-82.233	-0.280	17.564	-13.357	f,r
$Mg(OH)_2(brucite) + 2HCl = 2H_2O + MgCl_2$	27.023	-134.184	1.087	78.229	-51.058	f,r
$MgS(c) + 2HCl = H_2S + MgCl_2$	5.978	-61.962	0.120	-9.244	-10.403	h
$MgSiO_3(clinoenstatite) + 2HCl + 4HF = 3H_2O + SiF_4 + MgCl_2$	9.557	-52.428	2.327	10.758	-34.555	f,r
$MgSiO_3(orthoenstatite) + 2HCl + 4HF = 3H_2O + SiF_4 + MgCl_2$	9.121	-52.370	0.231	14.393	-32.482	f,r
$MgSiO_3(protoenstatite) + 2HCl + 4HF = 3H_2O + SiF_4 + MgCl_2$	9.070	-51.530	0.261	14.106	-32.547	f,r
$MgTiO_3(geikelite) + 2HCl + 4HF = 3H_2O + MgCl_2 + TiF_4$	12.963	-101.481	2.169	25.829	-41.349	f,s,w

APPENDIX 2

(continued)

Solid Species (continued)

Reaction[c]	l_0	$l_1 \times 10^{-2}$	$l_2 \times 10^3$	$l_3 \times 10^{-3}$	$l_4 \times 10^1$	Ref.[d]
$Mg_2Al_4Si_5O_{18}$(cordierite) + 4HCl + 32HF = 18H_2O + 4AlF_3 + 5SiF_4 + 2MgCl_2	35.798	-133.526	7.236	-21.515	-170.878	f,r
Mg_2SiO_4(forsterite) + 4HCl + 4HF = 4H_2O + SiF_4 + 2MgCl_2	14.082	-147.136	-1.058	20.467	-37.527	f,r
$Mg_3Al_2Si_3O_{12}$(pyrope) + 6HCl + 18HF = 12H_2O + 2AlF_3 + 3SiF_4 + 3MgCl_2	37.706	-235.058	4.881	33.138	-132.481	f,r
$Mg_3Si_2O_5(OH)_4$(chrysotile) + 6HCl + 8HF = 9H_2O + 2SiF_4 + 3MgCl_2	55.862	-296.832	-3.336	142.092	-120.727	f,r
$Mg_3Si_4O_{10}(OH)_2$(talc) + 6HCl + 16HF = 12H_2O + 4SiF_4 + 3MgCl_2	42.085	-168.483	4.257	44.540	-132.314	f,r
$Mg_5Al(AlSi_3O_{10})(OH)_8$(clinochlore) + 10HCl + 18HF = 18H_2O + 2AlF_3 + 3SiF_4 + 5MgCl_2	118.374	-667.734	-2.680	343.281	-258.187	f,r
$Mg_7Si_8O_{22}(OH)_2$(anthophyllite) + 14HCl + 32HF = 24H_2O + 8SiF_4 + 7MgCl_2	93.726	-383.701	15.122	182.545	-315.050	f,r
$Mg_{48}Si_{34}O_{85}(OH)_{62}/16$(antigorite/16) + 6HCl + 8.5HF = 9.188H_2O + 2.125SiF_4 + 3MgCl_2	71.345	-301.195	9.009	222.847	-177.265	f,r
Mn(c) + 2HCl = H_2 + MnCl_2	-8.242	48.328	-8.969	-22.717	31.925	f,e
$MnCl_2$(scacchite) = MnCl_2	11.137	-112.729	-4.418	-0.301	-6.590	f,i
MnF_2(c) + 2HCl = 2HF + MnCl_2	6.355	-113.342	-9.145	-12.888	10.162	f,i
$MnFe_2O_4$(jacobsite) + H_2 + 6HCl = 4H_2O + 2FeCl_2 + MnCl_2	24.111	-144.571	-16.996	16.956	-34.719	f,g
MnO(manganosite) + 2HCl = H_2O + MnCl_2	3.683	-32.084	-1.745	-0.833	-4.234	f,e
MnO_2(pyrolusite) + H_2 + 2HCl = 2H_2O + MnCl_2	15.064	18.367	0.575	31.844	-30.940	f,e
MnS(alabandite) + 2HCl = H_2S + MnCl_2	2.358	-56.613	-1.481	-19.631	-1.123	f,h
$MnSO_4$(c) + 4H_2 + 2HCl = 4H_2O + H_2S + MnCl_2	37.439	-12.035	-0.237	61.641	-82.767	f,j,u
$MnSO_4 \cdot H_2O$(c) + 4H_2 + 2HCl = 5H_2O + H_2S + MnCl_2	5.686	-31.161	-85.731	-15.323	68.681	f,u

Reaction						
$MnSO_4 \cdot 4H_2O(c) + 4H_2 + 2HCl = 8H_2O + H_2S + MnCl_2$	19.417	-112.391	-134.929	-3.035	111.146	f,u
$MnSO_4 \cdot 5H_2O(c) + 4H_2 + 2HCl = 9H_2O + H_2S + MnCl_2$	27.810	-142.653	-171.501	-4.977	116.114	f,u
$MnSO_4 \cdot 7H_2O(c) + 4H_2 + 2HCl = 11H_2O + H_2S + MnCl_2$	19.892	-189.901	-230.563	2.601	209.218	f,u
$MnS_2(hauerite) + H_2 + 2HCl = 2H_2S + MnCl_2$	11.754	-54.252	-1.331	-11.411	-23.181	f,h
$MnSiO_3(rhodonite) + 2HCl + 4HF = 3H_2O + SiF_4 + MnCl_2$	5.177	3.454	0.476	-11.528	-24.120	f,j,s
$MnWO_4(huebnerite) + 2HCl = MnCl_2 + H_2WO_4$	-0.820	-157.390	-7.578	-81.263	24.169	f,g
$Mn_2O_3(bixbyite) + H_2 + 4HCl = 3H_2O + 2MnCl_2$	12.741	-33.709	-6.558	-60.866	-16.529	f,e
$Mn_2SiO_4(tephroite) + 4HCl + 4HF = 4H_2O + SiF_4 + 2MnCl_2$	9.781	-41.672	-0.021	-6.079	-31.686	j,s
$Mn_3O_4(hausmannite) + H_2 + 6HCl = 4H_2O + 3MnCl_2$	13.746	-90.167	-12.064	-16.622	-6.336	f,e
$Mo(c) + 4H_2O = 3H_2 + H_2MoO_4$	-27.487	-45.036	-7.596	-76.942	86.592	e
$MoBr_2(c) + 4H_2O = 2H_2 + 2HBr + H_2MoO_4$	-7.835	-118.148	-6.220	-69.988	49.642	f,i
$MoBr_3(c) + 4H_2O = 1.5H_2 + 3HBr + H_2MoO_4$	0.230	-142.962	-6.567	-70.544	36.967	f,i
$MoBr_4(c) + 4H_2O = H_2 + 4HBr + H_2MoO_4$	10.076	-136.914	-6.854	-68.272	20.959	f,i
$MoCl_3(c) + 4H_2O = 1.5H_2 + 3HCl + H_2MoO_4$	2.953	-115.359	-6.672	-37.638	32.662	f,i
$MoCl_4(c) + 4H_2O = H_2 + 4HCl + H_2MoO_4$	11.168	-112.506	-4.399	-36.613	18.789	f,i
$MoCl_5(c) + 4H_2O = 0.5H_2 + 5HCl + H_2MoO_4$	7.621	-87.901	-31.104	-65.143	42.589	f,i
$MoO_2(c) + 2H_2O = H_2 + H_2MoO_4$	-8.048	-108.575	-5.984	-40.108	38.567	e
$MoO_3(molybdite) + H_2O = H_2MoO_4$	-2.311	-65.676	-6.552	-41.949	23.668	f,e
$MoS_2(molybdenite) + 4H_2O = H_2 + 2H_2S + H_2MoO_4$	-6.380	-175.208	-2.042	-58.707	34.473	h
$Mo_2S_3(c) + 8H_2O = 3H_2 + 3H_2S + 2H_2MoO_4$	-25.479	-280.715	-11.086	-132.039	101.871	h
$Na(c) + HCl = 0.5H_2 + NaCl$	0.978	44.597	-10.679	-5.365	8.814	f,e
$NaAlSi_2O_6(jadeite) + HCl + 11HF = 6H_2O + NaCl + AlF_3 + 2SiF_4$	18.765	-37.681	3.733	1.231	-70.146	f,r
$NaAlSi_3O_8(high\ albite) + HCl + 15HF = 8H_2O + NaCl + AlF_3 + 3SiF_4$	17.086	17.940	6.203	-10.218	-87.922	f,r
$NaAlSi_3O_8(low\ albite) + HCl + 15HF = 8H_2O + NaCl + AlF_3 + 3SiF_4$	17.841	11.018	6.107	-11.431	-87.488	f,r
$NaAl_3Si_3O_{10}(OH)_2(paragonite) + HCl + 21HF = 12H_2O + NaCl + 3AlF_3 + 3SiF_4$	58.632	-146.850	12.706	134.931	-188.432	f,r
$NaBr(c) + HCl = HBr + NaCl$	9.699	-125.970	-5.986	-10.673	-4.757	f,i

Solid Species *(continued)*

Reaction[c]	l_0	$l_1 \times 10^{-2}$	$l_2 \times 10^3$	$l_3 \times 10^{-3}$	$l_4 \times 10^1$	Ref.[d]
NaCl(halite) = NaCl	10.018	-123.076	-5.709	-9.013	-5.330	f,i
NaF(villiaumite) + HCl = HF + NaCl	11.706	-114.735	-4.274	4.625	-9.526	f,i
NaO_2(c) + $1.5H_2$ + HCl = $2H_2O$ + NaCl	15.745	156.604	-5.992	-15.285	-33.989	f,e
Na_2O(c) + 2HCl = H_2O + 2NaCl	12.832	-4.377	-9.761	-12.651	-6.826	f,e
Na_2O_2(c) + H_2 + 2HCl = $2H_2O$ + 2NaCl	56.890	38.846	13.848	263.472	-146.432	f,e
Na_2S(c) + 2HCl = H_2S + 2NaCl	-10.321	-71.675	-26.327	-220.422	68.084	f,h
Na_2SO_4(c, I) + $4H_2$ + 2HCl = H_2S + 2NaCl + $4H_2O$	45.540	-127.837	-6.402	-24.768	-90.871	f,j,o
Na_2SO_4(c, IV) + $4H_2$ + 2HCl = H_2S + 2NaCl + $4H_2O$	39.252	-132.063	-16.871	25.729	-63.368	f,j,o
Na_2SO_4(thenardite) + $4H_2$ + 2HCl = H_2S + 2NaCl + $4H_2O$	39.177	-132.094	-16.929	24.669	-63.035	f,j,o
Ni(c) + 2HCl = H_2 + $NiCl_2$	-1.007	-58.771	-1.352	-0.418	8.294	f,e
$NiBr_2$(c) + 2HCl = 2HBr + $NiCl_2$	12.167	-132.662	-3.594	-11.306	-5.772	f,i
$NiCl_2$(c) = $NiCl_2$	12.564	-123.784	-3.543	-2.283	-6.637	f,i
NiF_2(c) + 2HCl = 2HF + NiCl2	9.966	-117.809	-4.535	-1.048	2.240	f,i
$NiFe_2O_4$(trevorite) + H_2 + 6HCl = $4H_2O$ + $2FeCl_2$ + $NiCl_2$	54.237	-195.793	4.584	198.525	-131.212	f,g
NiO(bunsenite) + 2HCl = H_2O + $NiCl_2$	7.933	-59.354	0.754	-19.682	-14.395	e
NiS(millerite) + 2HCl = H_2S + $NiCl_2$	32.262	-120.604	12.268	190.835	-92.568	f,h
$NiSO_4$(c) + $4H_2$ + 2HCl = $4H_2O$ + H_2S + $NiCl_2$	38.817	-14.738	1.687	61.442	-84.461	f,j,u
$NiSO_4 \cdot H_2O$(c) + $4H_2$ + 2HCl = $5H_2O$ + H_2S + $NiCl_2$	5.989	-36.500	-85.540	-19.944	70.652	f,u
$NiSO_4 \cdot 4H_2O$(c) + $4H_2$ + 2HCl = $8H_2O$ + H_2S + $NiCl_2$	19.787	-126.460	-134.825	-9.371	114.126	f,u
$NiSO_4 \cdot 6H_2O$(c) + $4H_2$ + 2HCl = $10H_2O$ + H_2S + $NiCl_2$	89.527	-216.451	-74.975	184.517	-76.864	f,j,u
$NiSO_4 \cdot 7H_2O$(c) + $4H_2$ + 2HCl = $11H_2O$ + H_2S + $NiCl_2$	138.724	-263.821	-4.791	287.334	-230.497	f,j,u
NiS_2(c) + H_2 + 2HCl = $2H_2S$ + $NiCl_2$	11.033	-106.665	-2.330	-33.710	-14.800	f,h

Reaction						
$Ni_2SiO_4 + 4HCl + 4HF = 4H_2O + SiF_4 + 2NiCl_2$	15.225	-81.513	-4.304	7.450	-35.952	f,j,k
Ni_3S_2(heazlewoodite) $+ 6HCl = H_2 + 2H_2S + 3NiCl_2$	112.324	-383.300	18.975	1156.819	-318.776	f,h
$Ni_3S_4(c) + H_2 + 6HCl = 4H_2S + 3NiCl_2$	7.958	-287.411	-32.577	-80.587	26.336	f,h
$Pb(c) + 2HCl = H_2 + PbCl_2$	-3.112	-3.471	-5.242	-12.406	12.953	f,e
$PbBr_2(c) + 2HCl = 2HBr + PbCl_2$	9.568	-112.341	-12.402	-25.588	0.837	f,i
$PbCl_2$(cotunnite) $= PbCl_2$	12.265	-97.955	-8.794	-10.407	-8.253	f,i
$PbF_2(c) + 2HCl = 2HF + PbCl_2$	66.203	-115.400	24.895	414.915	-185.503	f,i
PbO(litharge) $+ 2HCl = H_2O + PbCl_2$	7.282	4.641	-3.148	-2.428	-12.681	f,e
PbO(massicot) $+ 2HCl = H_2O + PbCl_2$	7.460	5.453	-2.636	-3.158	-13.803	f,e
PbO_2(plattnerite) $+ H_2 + 2HCl = 2H_2O + PbCl_2$	14.494	97.862	-4.373	6.125	-27.411	f,e
PbS(galena) $+ 2HCl = H_2S + PbCl_2$	7.065	-47.155	-0.986	-13.060	-14.181	f,h
$PbSO_4$(anglesite) $+ 4H_2 + 2HCl = 4H_2O + H_2S + PbCl_2$	13.624	31.589	-23.687	-60.415	-2.421	f,s
Pb_3O_4(minium) $+ H_2 + 6HCl = 4H_2O + 3PbCl_2$	40.169	97.606	-4.145	51.190	-91.645	f,e
$Rb(c) + HCl = 0.5H_2 + RbCl$	-3.533	72.676	-25.859	-3.077	26.544	f,e
$RbCl(c) = RbCl$	12.065	-107.060	-2.564	-2.040	-12.662	f,n
$RbF(c) + HCl = HF + RbCl$	12.834	-80.204	-4.489	9.819	-14.785	f,i
$RbO_2(c) + 1.5H_2 + HCl = 2H_2O + RbCl$	23.970	169.365	-1.596	14.610	-60.973	f,e
S(monoclinic sulfur) $+ H_2 = H_2S$	9.285	8.138	2.674	-2.831	-25.014	f,e
S(orthorhombic sulfur) $+ H_2 = H_2S$	8.900	8.256	2.551	-4.806	-23.560	f,e
$Sb(c) + 3HCl = 1.5H_2 + SbCl_3$	-11.135	23.538	-4.665	-20.486	25.696	f,e
$SbF_3(c) + 3HCl = 3HF + SbCl_3$	3.879	-29.074	-23.506	-12.546	21.972	f,i
Sb_2O_3(valentinite) $+ 6HCl = 3H_2O + 2SbCl_3$	8.282	43.386	0.391	2.913	-28.362	f,e
$Sb_2O_4(c) + H_2 + 6HCl = 4H_2O + 2SbCl_3$	16.430	63.126	3.028	11.932	-46.839	f,e
$Sb_2O_5(c) + 2H_2 + 6HCl = 5H_2O + 2SbCl_3$	22.032	154.459	7.830	20.449	-55.948	f,e
Sb_2S_3(stibnite) $+ 6HCl = 3H_2S + 2SbCl_3$	2.808	-1.975	-6.482	-49.689	-11.683	f,h
$Se(c) + H_2 = H_2Se$	8.576	-17.788	0.247	-3.948	-21.464	f,e
$SeO_2(c) + 3H_2 = 2H_2O + H_2Se$	21.128	112.468	-7.121	7.954	-46.106	f,e

Solid Species (continued)

Reaction[c]	l_0	$l_1 \times 10^{-2}$	$l_2 \times 10^3$	$l_3 \times 10^{-3}$	$l_4 \times 10^1$	Ref.[d]
$Si(c) + 4HF = 2H_2 + SiF_4$	-16.339	279.192	-0.919	-54.690	23.756	f,e
$SiO_2(coesite) + 4HF = 2H_2O + SiF_4$	0.886	49.937	1.598	-13.719	-17.240	f,r
$SiO_2(alpha-cristobalite) + 4HF = 2H_2O + SiF_4$	1.555	49.561	2.465	-15.275	-20.409	f,r
$SiO_2(beta-cristobalite) + 4HF = 2H_2O + SiF_4$	1.355	50.029	2.317	-10.268	-20.030	f,r
$SiO_2(glass) + 4HF = 2H_2O + SiF_4$	-1.270	53.524	0.415	-25.967	-11.348	e
$SiO_2(alpha-quartz) + 4HF = 2H_2O + SiF_4$	7.819	42.044	5.697	43.210	-40.260	f,r
$SiO_2(beta-quartz) + 4HF = 2H_2O + SiF_4$	1.800	48.484	2.549	-6.393	-21.149	f,r
$SiO_2(alpha-tridymite) + 4HF = 2H_2O + SiF_4$	1.176	49.780	1.990	-16.115	-19.158	f,r
$SiO_2(beta-tridymite) + 4HF = 2H_2O + SiF_4$	2.287	48.616	2.546	1.220	-22.794	f,r
$SiS(c) + 4HF = H_2 + H_2S + SiF_4$	-10.690	200.877	-1.545	-71.535	9.373	f,h
$SiS_2(c) + 4HF = 2H_2S + SiF_4$	-4.825	149.211	-2.396	-78.544	0.118	f,h
$Sn(c) + 2HCl = H_2 + SnCl_2$	-3.011	8.935	-6.695	-12.753	13.312	f,e
$SnBr_2(c) + 2HCl = 2HBr + SnCl_2$	8.841	-81.768	-16.160	-21.009	3.774	f,i
$SnCl_2(c) = SnCl_2$	11.884	-69.451	-11.636	-8.374	-7.970	f,i
$SnF_2(c) + 2HCl = 2HF + SnCl_2$	9.391	-46.795	-15.999	-6.579	3.668	f,i
$SnO(c) + 2HCl = H_2O + SnCl_2$	9.496	-19.169	-1.649	3.568	-20.737	f,e
$SnO_2(cassiterite) + H_2 + 2HCl = 2H_2O + SnCl_2$	17.650	-50.778	-1.639	31.282	-36.359	f,e
$SnS(herzenbergite) + 2HCl = H_2S + SnCl_2$	13.070	-45.741	1.278	39.715	-32.914	f,h
$SnS_2(c) + H_2 + 2HCl = 2H_2S + SnCl_2$	17.433	-54.075	1.354	-6.733	-37.965	f,h
$Sn_2S_3(c) + H_2 + 4HCl = 3H_2S + 2SnCl_2$	24.841	-92.074	0.089	-20.372	-52.594	f,h
$Sr(c) + 2HCl = H_2 + SrCl_2$	2.822	147.865	-2.878	32.923	-4.242	f,e
$SrBr_2(c) + 2HCl = 2HBr + SrCl_2$	1.563	-181.783	-23.908	-29.977	33.306	f,i

Reaction						
$SrCl_2(c) = SrCl_2$	5.218	-183.443	-20.070	-17.166	21.485	f,i
$SrF_2(c) + 2HCl = 2HF + SrCl_2$	3.423	-194.163	-16.410	-42.066	27.295	f,i
$SrO(c) + 2HCl = H_2O + SrCl_2$	9.938	-34.606	-0.915	8.080	-19.835	f,e
$SrS(c) + 2HCl = H_2S + SrCl_2$	9.097	-85.151	-0.475	-5.166	-17.033	h
$SrSiO_3(c) + 2HCl + 4HF = 3H_2O + SiF_4 + SrCl_2$	9.791	-54.698	0.474	-10.187	-34.132	j,k
$Sr_2SiO_4(c) + 4HCl + 4HF = 4H_2O + SiF_4 + 2SrCl_2$	22.628	-133.662	-0.586	12.612	-63.699	j,k
$Te(c) + H_2 = H_2Te$	6.246	-53.257	-3.678	-10.177	-12.391	f,e
$TeCl_4(c) + 3H_2 = H_2Te + 4HCl$	46.719	-39.618	5.341	-3.540	-92.996	f,i
$TeO_2(tellurite) + 3H_2 = 2H_2O + H_2Te$	28.490	21.551	5.095	21.702	-73.913	f,e
$Ti(c) + 4HF = 2H_2 + TiF_4$	-24.989	252.492	-9.776	-99.417	57.397	f,e
$TiBr_2(c) + 4HF = H_2 + 2HBr + TiF_4$	1.081	69.041	-2.391	-50.289	1.922	f,i
$TiBr_3(c) + 4HF = 0.5H_2 + 3HBr + TiF_4$	-12.106	22.038	-34.281	-104.208	63.408	f,i
$TiBr_4(c) + 4HF = 4HBr + TiF_4$	3.912	-3.949	-39.086	-47.902	23.400	f,i
$TiCl_2(c) + 4HF = H_2 + 2HCl + TiF_4$	-0.712	69.833	-4.013	-37.432	8.451	f,i
$TiCl_3(c) + 4HF = 0.5H_2 + 3HCl + TiF_4$	7.433	9.187	-1.610	-42.424	-7.826	f,i
$TiF_3(c) + HF = 0.5H_2 + TiF_4$	2.850	-77.870	-7.128	-52.459	10.924	f,i
$TiF_4(c) = TiF_4$	15.765	-54.534	-10.808	-0.285	-19.529	f,i
$TiO_2(anatase) + 4HF = 2H_2O + TiF_4$	4.002	-1.327	2.487	-5.767	-23.889	f,e
$TiO_2(rutile) + 4HF = 2H_2O + TiF_4$	4.495	-4.606	2.852	1.808	-25.493	f,r
$TiS(c) + 4HF = H_2 + H_2S + TiF_4$	-8.755	109.435	-0.353	-56.161	10.012	h
$TiS_2(c) + 4HF = 2H_2S + TiF_4$	-1.229	51.221	-0.808	-56.669	-6.196	f,h
$Ti_2O_3(c) + 8HF = H_2 + 3H_2O + 2TiF_4$	7.414	57.058	4.200	-4.661	-51.415	e
$Ti_3O_5(c) + 12HF = H_2 + 5H_2O + 3TiF_4$	-19.392	97.261	-4.368	-494.449	16.660	e
$Ti_4O_7(c) + 16HF = H_2 + 7H_2O + 4TiF_4$	-1.708	65.146	-0.450	-89.970	-45.021	e
$V(c) + 4HCl = 2H_2 + VCl_4$	-20.671	89.850	-6.129	-46.065	43.867	e
$VCl_2(c) + 2HCl = H_2 + VCl_4$	-3.158	-54.151	-5.366	-34.432	15.361	f,i
$VCl_3(c) + HCl = 0.5H_2 + VCl_4$	7.477	-77.275	-3.633	-14.382	-5.052	f,i

APPENDIX 2
(continued)

Solid Species (continued)

Reaction[c]	l_0	$l_1 \times 10^{-2}$	$l_2 \times 10^3$	$l_3 \times 10^{-3}$	$l_4 \times 10^1$	Ref.[d]
$VF_3(c) + 4HCl = 0.5H_2 + 3HF + VCl_4$	8.979	-169.198	-2.066	-0.065	-10.965	f,i
$VO(c) + 4HCl = H_2 + H_2O + VCl_4$	-9.735	-14.046	-5.109	-30.039	15.316	f,e
$VOSO_4(c) + 4H_2 + 4HCl = 5H_2O + H_2S + VCl_4$	31.870	27.184	-0.359	30.662	-83.602	f,j,u
$VOSO_4.H_2O(c) + 4H_2 + 4HCl = 6H_2O + H_2S + VCl_4$	0.965	6.751	-85.012	-40.659	63.955	f,u
$VOSO_4.3H_2O(c) + 4H_2 + 4HCl = 8H_2O + H_2S + VCl_4$	7.491	-58.817	-125.090	-42.672	103.212	f,u
$VOSO_4.5H_2O(c) + 4H_2 + 4HCl = 10H_2O + H_2S + VCl_4$	12.695	-116.962	-171.134	-36.070	148.509	f,u
$VOSO_4.6H_2O(c) + 4H_2 + 4HCl = 11H_2O + H_2S + VCl_4$	10.278	-142.139	-207.177	-31.207	191.136	f,u
$V_2O_3(karelianite) + 8HCl = H_2 + 3H_2O + 2VCl_4$	-9.651	-96.486	-6.711	-43.447	3.617	f,e
$V_2O_4(c) + 8HCl = 4H_2O + 2VCl_4$	-30.167	-42.312	-20.306	-395.705	72.275	f,e
$V_2O_5(shcherbinaite) + H_2 + 8HCl = 5H_2O + 2VCl_4$	1.994	-16.815	-6.971	-23.678	-20.479	f,e
$V_2S_3(c) + 8HCl = H_2 + 3H_2S + 2VCl_4$	-15.605	-72.458	-14.128	-38.209	29.645	f,h
$W(c) + 4H_2O = 3H_2 + H_2WO_4$	-25.894	-17.396	-5.495	-73.371	79.455	e
$WBr_5(c) + 4H_2O = 0.5H_2 + 5HBr + H_2WO_4$	9.127	-92.084	-26.952	-75.291	40.107	f,i
$WBr_6(c) + 4H_2O = 6HBr + H_2WO_4$	17.573	-91.297	-28.210	-73.245	27.812	f,i
$WCl_2(c) + 4H_2O = 2H_2 + 2HCl + H_2WO_4$	-10.827	-58.999	-8.797	-71.756	54.443	f,i
$WCl_4(c) + 4H_2O = H_2 + 4HCl + H_2WO_4$	4.097	-62.669	-15.878	-71.005	36.098	f,i
$WCl_5(c) + 4H_2O = 0.5H_2 + 5HCl + H_2WO_4$	8.480	-51.471	-30.797	-70.855	42.468	f,i
$WCl_6(c) + 4H_2O = 6HCl + H_2WO_4$	59.560	-55.951	26.062	-219.774	-128.623	f,i
$WO_2(c) + 2H_2O = H_2 + H_2WO_4$	-6.941	-80.915	-3.581	-39.705	32.878	f,e
$WO_3(c) + H_2O = H_2WO_4$	0.090	-89.526	-3.390	-35.375	14.700	f,e
$WS_2(tungstenite) + 4H_2O = H_2 + 2H_2S + H_2WO_4$	-5.504	-128.664	-0.389	-57.885	29.567	f,h
$Zn(c) + 2HCl = H_2 + ZnCl_2$	-4.892	45.095	-4.442	-5.000	15.332	f,e

Reaction						
$ZnBr_2(c) + 2HCl = 2HBr + ZnCl_2$	6.189	-90.256	-10.902	0.108	9.222	f,i
$ZnCl_2(c) = ZnCl_2$	11.621	-79.422	-5.176	7.823	-9.709	f,i
$ZnF_2(c) + 2HCl = 2HF + ZnCl_2$	4.745	-68.029	-12.420	-24.582	16.348	f,i
$ZnFe_2O_4(franklinite) + H_2 + 6HCl = 4H_2O + 2FeCl_2 + ZnCl_2$	29.638	-122.138	-5.612	22.169	-56.881	f,n
$ZnO(zincite) + 2HCl = H_2O + ZnCl_2$	5.770	-15.933	-1.073	11.865	-11.276	e
$ZnS(sphalerite) + 2HCl = H_2S + ZnCl_2$	6.631	-55.005	0.172	7.493	-14.344	f,h
$ZnS(wurtzite) + 2HCl = H_2S + ZnCl_2$	6.328	-49.798	0.032	3.328	-13.436	f,h
$ZnSO_4(zinkosite) + 4H_2 + 2HCl = 4H_2O + H_2S + ZnCl_2$	24.320	36.313	-21.109	72.083	-36.416	f,j,u
$ZnSO_4 \cdot H_2O(c) + 4H_2 + 2HCl = 5H_2O + H_2S + ZnCl_2$	12.801	2.126	-85.005	-2.714	42.867	f,u
$ZnSO_4 \cdot 6H_2O(bianchite) + 4H_2 + 2HCl = 10H_2O + H_2S + ZnCl_2$	-41.276	-102.305	-331.071	-130.955	403.272	f,j,u
$ZnSO_4 \cdot 7H_2O(goslarite) + 4H_2 + 2HCl = 11H_2O + H_2S + ZnCl_2$	43.387	-171.094	-198.314	76.698	122.427	f,j,u
$ZnO \cdot 2ZnSO_4(c) + 8H_2 + 6HCl = 9H_2O + 2H_2S + 3ZnCl_2$	85.833	63.640	6.487	168.841	-205.314	f,j,u

[a] Calculated at 1 atm pressure. [b] Valid from 298.15 to 1473.15 K. [c] These reactions define the derived species (left-most species) and are written in terms of component gas species (table 1). Species in this column include gases, liquids (liq), crystalline solids (c), amorphous solids (glass), and mineral species (listed by name). A mineral name followed by a slash means that the stoichiometry and the log K equation for that mineral has been devided by the number. [d] References in this column refer to the derived species. Sources of data for the component species are given in table 1. [e] Pankratz (1982). [f] Heat capacity of derived species does not extend to 2000 K. [g] Barin and Knacke (1973). [h] Pankratz, Mah, and Watson (1984). [i] Pankratz (1984). [j] Heat capacity eq (1) generated by regression of tabulated heat capacity data. [k] Pankratz, Stuve, and Gokcen (1984). [l] Chase and others (1978). [m] Stull and Prophet (1971). [n] Barin, Knackle, and Kubaschewski (1977). [o] Chase and others (1982). [p] Chase and others (1974). [q] Chase and others (1975). [r] Berman (1988). [s] Robie, Hemingway, and Fisher (1978). [t] Helgeson and others (1978). [u] DeKock (1982). [v] Enthalpy and entropy modified from Anovitz and others (1985) to be consistent with our data. [w] Heat capacity eq (2) from Berman and Brown (1985).

REFERENCES

Anovitz, L. M., Treiman, A. H., Essene, E. J., Hemingway, B. S., Westrum, E. F., Jr., Wall, V. J., Burriel, R., and Bohlen, S. R., 1985, The heat-capacity of ilmenite and phase equilibria in the system Fe-Ti-O: Geochimica et Cosmochimica Acta, v. 49, p. 2027–2040.

Barin, I., and Knacke, O., 1973, Thermochemical properties of inorganic substances: Berlin, Springer-Verlag, 921 p.

Barin, I., Knacke, O., and Kubaschewski, O., 1977, Thermochemical properties of inorganic substances (supplement): Berlin, Springer-Verlag, 861 p.

Berman, R. G., 1988, Internally-consistent thermodynamic data for minerals in the system $Na_2O-K_2O-CaO-MgO-FeO-Fe_2O_3-Al_2O_3-SiO_2-TiO_2-H_2O-CO_2$: Journal of Petrology, v. 29, p. 445–522.

Berman, R. G., and Brown, T. H., 1985, Heat capacity of minerals in the system $Na_2O-K_2O-CaO-MgO-FeO-Fe_2O_3-Al_2O_3-SiO_2-TiO_2-H_2O-CO_2$: representation, estimation, and high temperature extrapolation: Contributions to Mineralogy and Petrology, v. 89, p. 168–183.

Bernard, A., ms, 1985, Les mécanismes de condensation des gaz volcaniques: Ph.D. dissertation, University of Brussels, Belgium, 412 p. (in French)

Bernard, A., and Le Guern, F., 1986, Condensation of volatile elements in high-temperature gases of Mount St. Helens: Journal of Volcanology and Geothermal Research, v. 28, p. 91–105.

Bernard, A., Symonds, R. B., and Rose, W. I., Jr., 1990, Volatile transport and deposition of Mo, W and Re in high temperature magmatic fluids: Applied Geochemistry, v. 5, p. 317–326.

Casadevall, T., Rose, W., Gerlach, T., Greenland, L. P., Ewert J., Wunderman, R., and Symonds, R., 1983, Gas emissions and the eruptions of Mount St. Helens through 1982: Science, v. 221, p. 1383-1385.

Cashman, K. V., and Taggart, J. E., 1983, Petrologic monitoring of 1981 and 1982 eruptive products from Mount St. Helens: Science, v. 221, p. 1385-1387.

Chase, M. W., Jr., Curnutt, J. L., Downey, J. R., Jr., McDonald, R. A., Syverud, A. N., and Valenzuela, E. A., 1982, JANAF thermochemical tables, 1982 supplement: Journal of Physical and Chemical Reference Data, v. 11, p. 695-940.

Chase, M. W., Curnutt, J. L., Hu, A. T., Prophet, H., Syverud, A. N., and Walker, L. C., 1974, JANAF thermochemical tables, 1974 supplement: Journal of Physical and Chemical Reference Data, v. 3, p. 311–480.

Chase, M. W., Jr., Curnutt, J. L. McDonald, R. A., and Syverud, A. N., 1978, JANAF thermochemical tables, 1978 supplement: Journal of Physical and Chemical Reference Data, v. 7, p. 793–940.

Chase, M. W., Curnutt, J. L., Prophet, H., McDonald, R. A., and Syverud, A. N., 1975, JANAF thermochemical tables, 1975 supplement: Journal of Physical and Chemical Reference Data, v. 4, p. 1–175.

Chase, M. W., Jr., Davies, C. A. Downey, J. R., Jr., Frurip, D. J., McDonald, R. A., and Syverud, A. N., 1985, JANAF Thermochemical Tables, 3d Edition: Journal of Physical and Chemical Reference Data, v. 14, Supplement No. 1, 1856 p.

Cheynet, B., 1988a, Thermodata, On-line integrated information system for inorganic and metallurgical thermodynamics, *in* Cuthill, J. R., Gokoen, N. A., and Morral, J. E., editors, Computerized metallurgical databases: Warrendale, Pennsylvania, The Metallurgical Society, p. 28–40.

———— 1988b, Complex chemical equilibria calculations with the Thermodata system: *in* Thompson, W. T., Ajersch, F., and Eriksson, G., editors, Computer Software in Chemical and Extractive Metallurgy: Oxford, England, Pergamon Press, p. 31–44.

Christiansen, R. L., and Peterson, D. W., 1981, Chronology of the 1980 eruptive activity, *in* Lipman, P. W., and Mullineaux, D. R., editors, The 1980 Eruptions of Mount St. Helens, Washington: United States Geological Survey Professional Paper 1250, p. 17–30.

Chuan, R. L., Rose, W. I., Jr., and Woods, D. C., 1987, SEM characterization of small particles in eruption clouds, in Marshall, J. R., editor, Clastic Particles: scanning electron microscopy and shape analysis of sedimentary and volcanic clasts: New York, Van Norstrand Reinhold Company, Inc., p. 159–173.

DeKock, C. W., 1982, Thermodynamic properties of selected transition metal sulfates and their hydrates: United States Bureau of Mines Information Circular 8910, 45 p.

Delany, J. M., and Wolery, T. J., 1984, Fixed fugacity option for the EQ6 geochemical reaction path code: Lawrence Livermore National Laboratory, UCRL-53598, 20 p.

Denbigh, K., 1981, The Principles of Chemical Equilibrium, 4th edition: Cambridge, Cambridge University Press, 494 p.

Ellis, A. J., 1957, Chemical equilibrium in magmatic gases: American Journal of Science, v. 255, p. 416–431.

Gemmell, J. B., 1987, Geochemistry of metallic trace elements in fumarolic condensates from Nicaraguan and Costa Rican volcanoes: Journal of Volcanology and Geothermal Research, v. 33, p. 161–181.

Gerlach, T. M., 1979, Evaluation and restoration of the 1970 volcanic gas analyses from Mount Etna, Sicily: Journal of Volcanology and Geothermal Research, v. 6, p. 165–178.

———— 1980a, Evaluation of volcanic gas analyses from Kilauea Volcano: Journal of Volcanology and Geothermal Research, v. 7, p. 295–317.

———— 1980b, Investigations of volcanic gas analyses and magma outgassing from Earta'Ale lava lake, Afar, Ethiopia: Journal of Volcanology and Geothermal Research, v. 7, p. 415–441.

———— 1980c, Evaluation of volcanic gas analyses from Surtsey Volcano, Iceland, 1964–1967: Journal of Volcanology and Geothermal Research, v. 8, p. 191–198.

———— 1980d, Chemical characteristics of the volcanic gases from Nyiragongo lava lake and the generation of CH_4-rich fluid inclusions in alkaline rocks: Journal of Volcanology and Geothermal Research, v. 8, p. 177–189.

———— 1981, Restoration of new volcanic gas analyses from basalts of the Afar region: further evidence of CO_2-degassing trends: Journal of Volcanology and Geothermal Research, v. 10, p. 83–91.

Gerlach, T. M., and Casadevall, T. J., 1986a, Evaluation of gas data from high-temperature fumaroles at Mount St. Helens, 1980–1982: Journal of Volcanology and Geothermal Research, v. 28, p. 107–140.

———— 1986b, Fumarole emissions at Mount St. Helens Volcano, June 1980 to October, 1981: degassing of a magma-hydrothermal system: Journal of Volcanology and Geothermal Research, v. 28, p. 141–160.

Gerlach, T. M., and Nordlie, B. E., 1975, The C-O-H-S gaseous system, Part II: Temperature, atomic composition, and molecular equilibria in volcanic gases: American Journal of Science, v. 275, p. 377–394.

Getahun, A., Reed, M. H., and Symonds, R. B., 1992, Augustine volcano fumarole wall rock alteration: mineralogy, zoning, and numerical models of its formation process, *in* Kharaka, Y. K., and Maest, A. S., editors, Water-Rock Interaction—Proceedings of the 7th international symposium on water-rock interaction, Park City, Utah, 13–18 July, 1992: Rotterdam, Netherlands, A. A. Balkema Publishers, p. 1411–1414.

Giggenbach, W. F., 1975, A simple method for the collection and analysis of volcanic gas samples: Bulletin Volcanologique, v. 39, p. 132–145.

Giggenbach, W. F., and Matsuo, S., 1991, Evaluation of results from second and third IAVCEI field workshops on volcanic gases, Mt Usu, Japan, and While Island, New Zealand: Applied Geochemistry, v. 6, p. 125–141.

Govindaraju, K., 1984, 1984 compilation of working values and sample description for 170 international reference samples of mainly silicate rocks and minerals: Geostandards Newsletter, v. 8, special issue, 88 p.

Graeber, E. J., Gerlach, T. M., and Hlava, P. F., 1982, Metal transport and deposition in high temperature fumaroles at Mount St. Helens: EOS (Transactions of the American Geophysical Union) v. 63, p. 1143.

Graeber, E. J., Modreski, P. J., and Gerlach, T. M., 1979, Composition of gases collected during the 1977 East Rift eruption, Kilauea, Hawaii: Journal of Volcanology and Geothermal Research, v. 5, p. 337–344.

Grossman, L., and Larimer, J. W., 1974, Early chemical history of the solar system: Reviews of Geophysics and Space Physics, v. 12, p. 71–101.

Halliday, A. N., Fallick, A. E., Dickin, A. P., Mackenzie, A. B., Stephens, W. E., and Hildreth, W., 1983, The isotopic and chemical evolution of Mount St. Helens: Earth and Planetary Science Letters, v. 63, p. 241–256.

Heald, E. F., Naughton, J. J., and Barnes, I. L., Jr., 1963, The chemistry of volcanic gases. 2. Use of equilibrium calculations in the interpretation of volcanic gas samples: Journal of Geophysical Research, v. 68, p. 545–557.

Helgeson, H. C., Delaney, J. M., Nesbitt, H. W., and Bird, D. K., 1978, Summary and critique of the thermodynamic properties of rock-forming minerals: American Journal of Science, v. 278-A, 229 p.

Holloway, J. R., 1977, Fugacity and activity of molecular species in supercritical fluids, *in* Fraser, D. G., editor, Thermodynamics in Geology: Dordrecht, Holland, Reidel Publishing Co., p. 161–181.

Huff, V. N., Gordon, S., and Morrell, V. E., 1951, General method and thermodynamic tables for computation of equilibrium composition and temperature of chemical reactions: National Adv. Committee Aeronautics (NACA) Report 1037.

Keith, T. E. C., Casadevall, T. J., and Johnston, D. A., 1981, Fumarole encrustations: occurrence, mineralogy, and chemistry, *in* Lipman, P. W., and Mullineaux, D. R., editors, The 1980 Eruptions of Mount St. Helens, Washington: United States Geological Survey Professional Paper 1250, p. 239–250.

Kodosky, L. G., Motyka, R. J., and Symonds, R. B., 1991, Fumarolic emissions from Mount St. Augustine, Alaska: 1979–1984 degassing trends, volatile sources, and their possible role in eruptive style: Bulletin of Volcanology, v. 53, p. 381–394.

Krauskopf, K. B., 1957, The heavy metal content of magmatic vapor at 600°C: Economic Geology, v. 52, p. 786–807.

———— 1964, The possible role of volatile metal compounds in ore genesis: Economic Geology, v. 59, p. 22–45.

Lapham, D. M., Barnes, J. H., Downey, W. F., Jr., and Finkelman, R. B., 1980, Mineralogy associated with burning anthracite deposits of Eastern Pennsylvania: Pennsylvania Geological Survey Mineral Resources Report 78, 82 p.

Le Guern, F., ms, 1988, Ecoulements gazeux réactifs à hautes températures, mesures et modélisation: Ph.D. dissertation, University of Paris 7, 314 p. (in French).

Le Guern, F., and Bernard, A., 1982, A new method for sampling and analyzing volcanic sublimates—application to Merapi volcano, Java: Journal of Volcanology and Geothermal Research, v. 12, p. 133–146.

Le Guern, F., Gerlach, T. M., and Nohl, A., 1982, Field gas chromatograph analyses of gases from a glowing dome at Merapi volcano, Java, Indonesia, 1977, 1978, 1979: Journal of Volcanology and Geothermal Research, v. 14, p. 223–245.

Melson, W. G., and Hopson, C. A., 1981, Preeruption temperatures and oxygen fugacities in the 1980 eruption sequence, *in* Lipman, P. W., and Mullineaux, D. R., editors, The 1980 Eruptions of Mount St. Helens, Washington: United States Geological Survey Professional Paper 1250, p. 641–648.

Merzbacher, C., and Eggler, D. H., 1984, A magmatic geohygrometer: application to Mount St. Helens and other dacitic magmas: Geology, v. 12, p. 587–590.

Mojtahedi, W., 1989, Trace metals volatilisation in fluidised-bed combustion and gasification of coal: Combustion Science and Technology, v. 63, p. 209–227.

Muffler, L. J. P., Hendenquist, J. W., Kesler, S. E., and Izawa, E., 1992, Magmatic contributions to hydrothermal systems: EOS (Transactions of the American Geophysical Union), v. 73, p. 223–234.

Mullineaux, D. R., and Crandell, D. R., 1981, The eruptive history of Mount St. Helens, *in* Lipman, P. W., and Mullineaux, D. R., editors, The 1980 Eruptions of Mount St. Helens, Washington: United States Geological Survey Professional Paper 1250, p. 3–15.

Naughton, J. J., Lewis, V. A., Hammond, D., and Nishimoto, D., 1974, The chemistry of sublimates collected directly from lava fountains at Kilauea volcano, Hawaii: Geochimica et Cosmochimica Acta, v. 38, p. 1679–1690.

Pankratz, L. B., 1982, Thermodynamic properties of elements and oxides: United States Bureau of Mines Bulletin 672, 509 p.

———— 1984, Thermodynamic properties of halides: United States Bureau of Mines Bulletin 674, 826 p.

Pankratz, L. B., Mah, A. D., and Watson, S. W., 1987, Thermodynamic properties of sulfides: United States Bureau of Mines Bulletin 689, 427 p.

Pankratz, L. B., Stuve, J. M., and Gockcen, N. A., 1984, Thermodynamic data for mineral technology: United States Bureau of Mines Bulletin 677, 355 p.

Prausnitz, J. M., Anderson, T. F., Grens, E. A., Eckert C. A., and O'Connell, J. P., 1980, Computer Calculations for Multicomponent Vapor-Liquid Equilibria: Englewood Cliffs, New Jersey, Prentice Hall, Inc., 351 p.

Quisefit, J. P., 1988, Physico-chimie de l'aérosol volcanique. Modélisation thermochimique du refroidissement des émanations de haute température: Ph.D. dissertation, University of Paris 7, 258 p. (in French).

Quisefit, J. P., Toutain, J. P., Bergametti, G., Javoy, M., Cheynet, B. and Person, A., 1989, Evolution versus cooling of gaseous volcanic emissions from Momotombo Volcano, Nicaragua: Thermochemical model and observations: Geochimica et Cosmochimica Acta, v. 53, p. 2591–2608.

Reed, M. H., 1982, Calculation of multicomponent chemical equilibria and reaction processes in systems involving minerals, gases and an aqueous phase: Geochimica et Cosmochimica Acta, v. 46, p. 513–528.
———— 1992, Origin of diverse hydrothermal fluids by reaction of magmatic volatiles with wall rock: Geological Survey of Japan Report no. 279, p. 135–140.
Reed, M. H., and Spycher, N. F., 1984, Calculation of pH and mineral equilibria in hydrothermal waters with application to geothermometry and studies of boiling and dilution: Geochimica et Cosmochimica Acta, v. 48, p. 1479–1492.
Robie, R. A., Hemingway, B. S., and Fisher, J. R., 1978, Thermodynamic properties of minerals and related substances at 298.15 K and 1 bar (10^5 pascals) pressure and at higher temperatures: United States Geological Survey Bulletin 1452, 456 p.
Rose, W. I., Jr., 1987, Active pyroclastic processes studied with scanning electron microscopy, *in* Marshall, J. R., editor, Clastic Particles: scanning electron microscopy and shape analysis of sedimentary and volcanic clasts: New York, Van Norstrand Reinhold Company, Inc., p. 136–158.
Rose, W. I., Chuan, R. L., and Woods, D. C., 1982, Small particles in plumes of Mount St. Helens: Journal of Geophysical Research, v. 87, p. 4956–4962.
Rose, W. I., Wunderman, R. L., Hoffman, M. F., and Gale, L., 1983, A volcanologist's review of atmospheric hazards of volcanic activity: Fuego and Mount St. Helens: Journal of Volcanology and Geothermal Research, v. 17, p. 133–157.
Rutherford, M. J., Sigurdsson, H., Carey, S., and Davis, A., 1985, The May 18, 1980, eruption of Mount St. Helens 1. Melt composition and experimental phase equilibria: Journal of Geophysical Research, v. 90, p. 2929–2947.
Saxena, S. K., and Eriksson, G., 1983, High temperature phase equilibria in a solar-composition gas: Geochimica et Cosmochimica Acta, v. 47, p. 1865–1874.
Scheidegger, K. F., Federman, A. N., and Tallman, A. M., 1982, Compositional heterogeneity of tephras from the 1980 eruptions of Mount St. Helens: Journal of Geophysical Research, v. 87, p. 10861–10881.
Spycher, N. F., and Reed, M. H., 1988, Fugacity coefficients of H_2, CO_2, CH_4, H_2O and of H_2O-CO_2-CH_4 mixtures: A virial equation treatment for moderate pressures and temperatures applicable to calculations of hydrothermal boiling: Geochimica et Cosmochimica Acta, v. 52, p. 739–749.
———— 1989, Evolution of a Broadlands-type epithermal ore fluid along alternative P-T paths: implications for the transport and deposition of base, precious, and volatile metals: Economic Geology, v. 84, p. 328–359.
Stoiber, R. E, and Rose, W. I., Jr., 1974, Fumarolic incrustations at active Central American volcanoes: Geochimica et Cosmochimica Acta, v. 38, p. 495–516.
Stull, D. R., and Prophet, H., 1971, JANAF thermochemical tables, 2d edition: National Bureau of Standards Reference Data Series, NBS-37, 1141 p.
Swanson, D. A., and Holcomb, R. T., 1990, Regularities in growth of the Mount St. Helens dacite dome, 1980–1986, in Fink, J. H., editor, Lava flows and domes: New York, Springer-Verlag, p. 3–24.
Symonds, R. B., 1993, Scanning electron microscope observations of sublimates from Merapi volcano, Indonesia: Geochemical Journal (accepted).
Symonds, R. B., Reed, M. H., and Rose, W. I., 1992, Origin, speciation, and fluxes of trace-element gases at Augustine volcano, Alaska: insights into magma degassing and fumarolic processes: Geochimica et Cosmochimica Acta, v. 56, p. 633–657.
Symonds, R. B., Rose, W. I., Gerlach, T. M., Briggs, P. H., and Harmon, R. S., 1990, Evaluation of gases, condensates, and SO_2 emissions from Augustine volcano, Alaska: the degassing of a Cl-rich volcanic system: Bulletin of Volcanology, v. 52, p. 355–374.
Symonds, R. B., Rose, W. I., and Reed, M. H., 1988, Contribution of Cl- and F-bearing gases to the atmosphere by volcanoes: Nature, v. 334, p. 415–418.
Symonds, R. B., Rose, W. I., Reed, M. H., Lichte, F. E., and Finnegan, D. L., 1987, Volatilization, transport and sublimation of metallic and non-metallic elements in high temperature gases at Merapi Volcano, Indonesia: Geochimica et Cosmochimica Acta, v. 51, p. 2083–2101.
Thomas, E., Varekamp, J. C., and Buseck, P. R., 1982, Zinc enrichment in the phreatic ashes of Mt. St. Helens, April 1980: Journal of Volcanology and Geothermal Research, v. 12, p. 339–350.
Toutain, J. P., ms, 1987, Contribution à l'études des sublimés volcaniques. Minéralogie, géochimie, thermodynamique. Exemples du Momotombo, du Piton de la Fournaise et du Poas: Ph.D. dissertation, University of Paris 6, 190 p. (in French).
Van Zeggeren, F., and Storey, S. H., 1970, The Computation of Chemical Equilibria: Cambridge, England, Cambridge University Press, 176 p.

Varekamp, J. C., Thomas, E., Germani, M., and Buseck, P. R., 1986, Particle geochemistry of volcanic plumes of Etna and Mount St. Helens: Journal of Geophysical Research, v. 91, p. 12233–12248.

Vie Le Sage, R., 1983, Chemistry of the volcanic aerosols, *in* Tazieff, H., and Sabroux, J. C., editors, Forecasting Volcanic Events: Amsterdam, Elsevier, p. 445–474.

Voight, B., 1981, Time scale for the first moments of the May 18 eruption, *in* Lipman, P. W., and Mullineaux, D. R., editors, The 1980 Eruptions of Mount St. Helens, Washington: United States Geological Survey Professional Paper 1250, p. 69–86.

Wolery, T. J., 1979, Calculation of chemical equilibrium between aqueous solution and minerals: The EQ3/6 software package: Lawrence Livermore National Laboratory, UCRL-52658, 41 p.

Zeleznik, F. J., and Gordon, S., 1960, An analytical investigation of the general methods of calculating chemical equilibrium compositions: NASA Technical Note D-473.